FUNCTIONAL IMPACT OF OBESITY OR INTERMITTENT FEEDING ON INTESTINAL STEM CELLS

Amanda Taren Mah

A dissertation submitted to the faculty at the University of North Carolina at Chapel Hill in partial fulfillment of the requirements for the degree of Doctor of Philosophy in the Department of Nutrition in the Gillings School of Global Public Health.

Chapel Hill
2015

Approved by:

P. Kay Lund

Scott Magness

Liza Makowski

Daniel Pomp

Praveen Sethupathy

ABSTRACT

Amanda Taren Mah: Functional impact of obesity or intermittent feeding on intestinal stem cells
(Under the direction of P. Kay Lund)

Intestinal stem cells (ISCs) and progenitors constantly renew the intestinal epithelium. Effects of obesity or intermittent feeding specifically on ISCs versus progenitors are not defined. This dissertation used Sox9-EGFP reporter mice to test the hypothesis that obesity or intermittent feeding affects proliferation, numbers or intrinsic function of ISCs. Sox9-EGFP mice permit specific evaluation of ISCs or progenitors by histology or flow cytometry and intrinsic function in culture. High fat diet feeding induced obesity and hyperinsulinemia. ISC numbers and proliferation were selectively increased in obese mice. However, ISCs from obese mice exhibited impaired intrinsic function based on reduced ability to survive and generate enteroids *in vitro*. Excess insulin or IGF1 corrected this *in vitro* defect indicating that ISCs from obese mice develop acquired dependence on elevated insulin or IGF1 for survival or proliferation.

Sox9-EGFP mice were subjected to 20 weeks of an intermittent fasting regimen involving alternating days of *ad libitum* access to food or fasting (ADF). ADF reportedly produces similar benefits to metabolism or health as calorie restriction. Total food intake and activity did not differ between ADF and *ad libitum* fed controls. Despite this, ADF mice did not gain body weight and displayed significantly lower fat mass and fasting plasma triglycerides. ADF did not alter ISC number, but affected numbers of intestinal progenitors. After a fast cycle, ADF animals displayed increased progenitors but decreased proliferation, relative to short-term fasted controls. This effect was reversed in ADF animals following a feed cycle suggesting that ADF leads to fasting-induced increases in progenitors that can be rapidly mobilized during feeding. After a fast cycle, ADF animals displayed decreased colonic epithelial cell proliferation associated with increased expression of an anti-proliferative insulin receptor isoform B implicated in protection against colon tumorigenesis.

In summary, obesity and hyperinsulinemia promote ISC expansion and hyperproliferation but impaired ISC function, effects that may be relevant to obesity-associated intestinal dysfunction or tumorigenesis. ADF selectively affects small intestinal progenitors and not ISCs, leads to reduced proliferation of colonic epithelium, and promotes an insulin receptor isoform that may decrease cancer risk.

To my family who are my biggest fans, thank you for your unconditional love and support throughout this journey, it could not have been possible without you.

ACKNOWLEDGEMENTS

First, I would like to thank my mentor Dr. P. Kay Lund. She has provided me with the knowledge, tools and confidence to be a great scientist by giving me independence when I wanted it and advice when I needed it. She constantly challenges and encourages me to think innovatively. She is an incredible mentor and brilliant scientist and it has been an honor to work with and learn from her.

Thank you to past and present members of the Lund lab. First, I would like to thank Laurianne for being my go-to person in the lab for many years and instrumental in all of my projects. She has devoted countless hours teaching me scientific techniques, explaining everything from flow cytometry to cell culture, and answering any questions I had, no matter how big or small. Her love for science is infectious and I know I can always go to her for encouragement, whether it is after a failed experiment or negative results or whether she is in NC or France. She has taught me to think creatively and to aim high when it comes to science, to be bold in thought and fearless at the bench. Thank you to Shengli for always cheering me on and for helping me, whether it was teaching me my first RNA extraction, or about inflammation and fibrosis, or chatting about nutrition. To Emily, for being my companion in everything tissue and crypt culture, for checking my math, and for bringing my favorite donuts even after ruining your sacs. To Jim, thank you for providing guidance on anything tissue culture related and for all the yearly Girl Scout cookies. To Eric, it has been fun sharing a cubicle and a sac bench with you. Thank you for always placing last minute orders, making reagents, opening the autoclave door and getting liquid nitrogen for me. Of course, thank you for your songwriting abilities, it has made long days shorter and tiring days more fun. Josh, thank you not only for keeping the lab running smoothly but also for keeping me grounded and always making sure I take time to relax. To Sarah, thank you for being a great lab mate and friend, for making sure there were always sweets in the lab, for the brainstorming and Q&A sessions we had between the walls, teaching me about genetics and statistics, editing my papers, weighing mice and changing media. To Elle, you started off running and have been instrumental in being my second pair of hands without any complaint. Thank you so much for always offering your help, for coming in even after a long day of classes and on the weekends, for adopting my mice as your own, and for teaching me about microbes. To Agostina, I have been very lucky and fortunate to have a friend like you every step of the way,

from writing our proposals, to submitting our papers at the same time, and writing and defending together. Thank you for your help in the lab and your friendship outside the lab. Thank you for being my human calculator, for carrying the bag of diet to and from the mouse room for me, for helping me with mouse sacs, epithelial isolations, protein extractions and everything in between. Thank you for always letting me bounce ideas off of you and for taking much needed coffee breaks with me. Thank you to all the undergraduates who have come through the lab, especially Hannah and Jenny for your contributions to my projects, and to Adeola for always offering a helping hand with genotyping and any last minute experiments.

Finally, I would like to acknowledge Kirk McNaughton and Ashley Ezzell at the Cell Biology and Physiology Histology Research Core and Carolyn Suitt at the UNC Center for Gastrointestinal Biology and Disease (CGIBD) Histology Care for their work and guidance; Barry Udis and the UNC Flow Cytometry Core Facility for their assistance in all sorting and flow experiments; Qing Shi and Kunjie Hua at the Nutrition Obesity Research Core and Carlton Anderson at the CGIBD Advanced Analytics Core for performing ELISAs and Fluidigm Biomark experiments and Neal Kramarcy and Michael Chua at the Michael Hooker Microscopy Facility for their help with confocal microscopy. Thank you to my professors in the Department of Nutrition for teaching and challenging me along the way, to Joanne Lee for all your administrative help; the UNC Intestinal Stem Cell Group for useful discussions; and my committee members for their input and guidance throughout my PhD career.

PREFACE

Chapter 2 of this work was published in *Endocrinology* in 2014. Authors contributed to the work in the following manner. A. T. Mah designed, conducted and analyzed majority of experiments, wrote manuscript, L. Van Landeghem designed, conducted, analyzed and contributed to writing manuscript, H. E. Gavin conducted and analyzed morphological measurements, S. T. Magness provided input on project and experimental design and oversaw high-throughput gene expression experiments, P. K. Lund oversaw studies, provided intellectual input and participated in all aspects of analyzing data and preparation of manuscript.

Chapter 3 of this work is in preparation for submission. The following authors contributed to this work: Amanda T. Mah, Laurianne Van Landeghem, R. Eric Blue, Elaine M. Glenny, Jennifer T. Wajahn, M. Agostina Santoro, and P. Kay Lund. Specific author contributions to this work are as described. A. T. Mah designed, conducted and analyzed majority of experiments and wrote manuscript. L. Van Landeghem designed and conducted flow cytometry experiments. R. E. Blue assisted with tissue harvest and epithelial isolations. E. M. Glenny performed gene expression experiments and monitored mouse feedings. J.T Wajahn performed morphological measurements, M. A. Santoro performed epithelial isolations and assisted with mouse feedings. P. K. Lund oversaw all studies and analyses and contributed to the writing of the manuscript.

All work in this dissertation was supported by the following grants: 2-T32-DK07686 (ATM), R01-DK040247–19 (PKL), R01-AG041198-01A1 (PKL), P30-CA06086 (UNC Flow Cytometry Core Facility), P30-DK034987 (CGIBD) and P30-DK056350 (NORC).

TABLE OF CONTENTS

LIST OF TABLES

LIST OF FIGURES

LIST OF ABBREVIATIONS

2-MG	sn-2-monoglyceride
ADF	Alternate day fasting
ALPI	Alkaline phosphatase, intestinal
ANOVA	Analysis of variance
AOM	Azoxymethane
APC	Adenomatosis polyposis coli
ATOH1/MATH1	Atonal homolog 1
BAC	Bacterial artificial chromosome
BMI	Body mass index
BMI1	Bmi1 polycomb ring finger oncogene
BMP	Bone morphogenetic protein
BMPR1a	Bone morphogenetic protein receptor, type 1A
BMPR2	Bone morphogenetic protein receptor, type II
BRDU	5-Bromo-2´-Deoxyuridine
CAZymes	Carbohydrate active enzymes
CBC	Crypt base columnar
CCK	Cholecystokinin
CE	Cholesterol ester
CKI	Casein kinase I
CR	Calorie restriction
CRC	Colorectal cancer
CSC	Colon stem cell
CSL	CBF-1/RBP-Jκ, Su(H), Lag-1
DAG	Diacylglycerol
DAPI	4', 6-diamidino-2-phenylindole
DIO	Diet-induced obesity
DLL	Delta-like ligand

DSS	Dextran sodium sulfate
EDU	5-Ethynyl-2′-deoxyuridine
EEC	Enteroendocrine cell
EGF	Epidermal growth factor
EGFP	Enhanced green fluorescent protein
ELISA	Enzyme-linked immunosorbent assay
ER	Endoplasmic reticulum
FACS	Fluorescence activated cell sorting
FFA	Free fatty acid
FZD	Frizzled homolog
GFI1	Growth factor independent 1
GFP	Green fluorescent protein
GH	Growth hormone
GIP	Glucose-dependent insulinotropic peptide
GLP-1	Glucagon-like peptide 1
GLP-2	Glucagon-like peptide 2
GSK3β	Glycogen synthase kinase 3 beta
H&E	Hematoxylin & eosin
HBSS	Hank's balanced salt solution
HES	Hairy and enhancer of split
HFD	High fat diet
HOPX	HOP homeobox
IACUC	Institutional Animal Care and Use Committee
IBD	Inflammatory bowel disease
IGF1	Insulin-like growth factor 1
IGF1R	Insulin-like growth factor 1 receptor
IGF2	Insulin-like growth factor 2
IGFBP	Insulin-like growth factor binding protein

IL6	Interleukin-6
IR-A	Insulin receptor isoform-A
IR-B	Insulin receptor isoform-B
IR/Insr	Insulin receptor
IRS-1	Insulin receptor substrate 1
IRS-2	Insulin receptor substrate 2
ISC	Intestinal stem cell
LCT	Lactase
LGR5	Leucine rich repeat containing G protein coupled receptor 5
LPS	Lipopolysaccharide
LRC	Label retaining cell
LRIG1	Leucine-rich repeats and immunoglobulin-like domains 1
LRP	Low density lipoprotein receptor-related protein
LYZ	Lysozyme
MAPK	Mitogen activated protein kinase
MRI	Magnetic resonance imaging
MTERT	Mouse telomerase reverse transcriptase
MTTP	Microsomal triglyceride transport protein
MUC2	Mucin-2
NFκB	Nuclear factor kappa B
NGN3	Neurogenin 3
NICD	Notch intracellular cytoplasmic domain
OCT	Optimal cutting temperature medium
OLFM4	Olfactomedin 4
PBS	Phosphate buffered saline
PFA	Paraformaldehyde
PI3K	Phosphatidylinositol 3-kinase
QRTPCR	Quantitative real-time polymerase chain reaction

RER	Respiratory exchange ratio
RT-PCR	Reverse transcription polymerase chain reaction
SCFA	Short chain fatty acid
SEM	Standard error of the mean
SIM	Sucrase isomaltase
SOCS	Suppressor of cytokine signaling
TG	Triglyceride
TGFβ	Transforming growth factor, beta
TLR	Toll-like receptor
TNFα	Tumor necrosis factor alpha
TPN	Total parenteral nutrition
TRF	Time restricted feeding
WNT	Wingless-type MMTV integration site family member

CHAPTER 1: AN INTRODUCTION TO THE INTESTINE, INTESTINAL STEM CELLS, OBESITY, HYPERINSULINEMIA, INTERMITTENT FEEDING, AND NUTRIENT DIGESTION AND ABSORPTION

Structure and function of the intestine

The gastrointestinal tract functions to digest and absorb incoming nutrients and to act as a barrier blocking harmful toxins, commensal bacteria or pathogens present in the lumen from entering the bloodstream. Anatomically, the gastrointestinal tract is divided into the esophagus, stomach, small intestine and colon. This dissertation focuses on the small intestine and colon, as these are the major sites of nutrient and fluid absorption. Figure 1.1 shows histology of the intestine to illustrate the mucosa (epithelium, lamina propria and muscularis mucosa) and underlying submucosa and muscle layers (circular and longitudinal muscle). Neuronal plexi lie between the submucosal and muscle layer (Meissner's plexus) or between the inner circular and outer longitudinal muscle layers (Myenteric plexus). This dissertation focuses on the intestinal epithelium, the innermost lumenal monolayer of epithelial cells lining both the small intestine and colon, responsible for mediating nutrient and fluid absorption and barrier function.

The intestinal epithelium

The small intestine comprises three regions, from proximal to distal, the duodenum, the jejunum and the ileum. The jejunum makes up 50% of the small intestine and is the main site for nutrient absorption. The intestinal epithelium lines the innermost surface of the intestine facing the lumen and is the most rapidly renewing tissue in the body, renewing itself every 3-7 days depending on region and species (1). The epithelium is organized into two zones: crypts of Lieberkühn, which house the proliferative cells and a small number of differentiated cells and villi, which contain differentiated cell types (Figure 1.2). Crypts are invaginations into the lamina propria that contain the proliferative stem and progenitors cells. Intestinal stem cells (ISCs) divide to renew themselves and give rise to more rapidly dividing progenitors, or transit-amplifying cells. Progenitors undergo additional divisions while migrating out of the crypt before they differentiate into one of four specialized cell types. Multiple crypts feed onto a villus, which is a finger-like projection that protrudes into the lumen and dramatically increases the surface area of the epithelium. Villi contain three of the four differentiated cell lineages, the absorptive enterocyte and secretory

goblet and enteroendocrine cells (EECs). Once on the villus, the differentiated cells continue towards the villus tip where they are sloughed off in a process called anoikis. A fourth differentiated cell type, the Paneth cell, migrates down to the base of the crypt where they are intercalated between ISCs. (Figure 1.2b)

The colonic epithelium has crypts but no villi (Figure 1.2). Proliferative cells reside in the colon crypt, close to the crypt base, but not quite as uniform in location as in small intestine. As cells migrate up the colon crypt, they differentiate into colonocytes, goblet or EEC within the crypt and at the crypt surface so that surface epithelium at the crypt opening contains only differentiated cells (Figure 1.2b).

Cell types of the intestinal epithelium can be distinguished by their enrichment of specific mRNAs or encoded proteins, which is summarized in Table 1.1. The cell types and markers are discussed in further detail below.

Intestinal stem cells (ISCs)

In the small intestine, ISCs reside at or near the base of the crypt, self-renew and give rise to progenitors capable of producing all intestinal epithelial cell lineages. ISCs are responsible for continuous renewal of the epithelium. Historically, the location of ISCs in the small intestine has been debated between two schools of thought: the classic model and the stem cell zone model. The classic model proposed that ISCs reside at the +4 position of the crypt (counting up from the crypt base), identified by Potten and colleagues based on the ability of cells at this position to retain DNA label, which indicated they were slowly cycling (2), while Paneth cells and Paneth cell progenitors were thought to occupy positions 1-3 below them. The stem cell zone model states that ISCs reside at the crypt base sandwiched between Paneth cells, and are distinctly slender in shape, often referred to as crypt base columnar (CBC) cells (1). Current views on the location of ISCs have evolved since then to propose that two ISC populations exist based on location and cycling kinetics; 1) the actively cycling CBC ISCs located at the base of the crypt in between Paneth cells and 2) reserve ISCs located at the +4 position.

Until recently it was difficult to study ISCs *in vivo* or directly study ISCs due to a lack of ISC biomarkers. However in the past decade, landmark studies have identified and validated biomarkers of actively cycling ISCs and slowly cycling reserve ISCs. *Lgr5* was first identified as a marker of actively cycling ISCs equivalent to CBC cells by Barker et al. in 2007 (3). This landmark paper used a method termed lineage tracing to validate *Lgr5* as an ISC biomarker. Lineage tracing involves using inducible Cre to irreversibly mark all cells that express a putative ISC marker (described in later sections). Since then, other ISC biomarkers have been identified by the same method such

as *Olfm4* (4). Lineage tracing has also identified biomarkers of the +4 reserve ISC. These biomarkers, which lineage traced, include *Bmi1* (5), *Hopx* (6), *mTert* (7) and *Lrig1* (8). Studies in markers of the reserve ISC population appear to mark different cells by position, indicating there are different types of reserve ISC enriched for specific markers. There still exists debate as to whether the expression of identified markers of reserve ISC is restricted to those cells. Transcriptomic and proteomic profiling of *Lgr5*$^{+}$ cells by Munoz et al. revealed expression of markers of +4 reserve ISCs in the *Lgr5*$^{+}$ population, causing them to conclude that markers of the +4 reserve ISC population are not exclusively expressed in those cells (9). However recent studies have shown that both populations are distinctly different in function. Studies ablating *Lgr5*$^{+}$ cells through genetic disruption or radiation showed that *Bmi1*$^{+}$ cells gave rise to *Lgr5*$^{+}$ cells to maintain intestinal homeostasis under these conditions (10,11), which indicated for the first time that the two populations are interchangeable when necessary. While the ISC field is still changing, one current view is that the actively cycling CBC ISCs are responsible for normal epithelial renewal while the more slowly cycling reserve ISCs are activated during injury to generate CBC ISC and renew crypts (10-13).

Currently, there is less known about colon stem cells (CSCs), as they have not been as extensively characterized compared to ISCs of the small intestine. Similar to that in the small intestine, *Lgr5* and *Lrig1* have been shown to be markers of CSCs residing at the crypt base (3,8). However there is some debate about whether CSCs differ or differ in location in proximal versus distal colon.

The advancements in ISC biomarker discovery have now provided tools and techniques to study ISC biology during homeostasis as well as during adaptive responses to obesity or intermittent feeding. This dissertation explores the effect of obesity or intermittent feeding directly on ISC, which was not possible before.

Signaling networks required for ISC maintenance comprise the ISC niche and control cell fate specification

In 1978, Ray Schofield first described the concept of the "stem cell niche" as an environment where stem cells and other cells interact to regulate stem cell behavior (14). In the intestine, the ISC niche is composed of cells surrounding the ISCs at the crypt base, including neighboring Paneth cells and underlying mesenchymal cells termed subepithelial myofibroblasts. Factors secreted from these cells act on ISCs to maintain ISC behavior through a variety of signaling pathways. Key signaling pathways present or inhibited at the crypt base (Notch, Wnt and Bmp) comprise the ISC niche and are responsible for ISC maintenance and proliferation (Figure 1.3). The Wnt and Notch pathway also dictate lineage allocation of intestinal progenitors where the Notch pathway promotes the absorptive lineage while the Wnt pathway promotes the secretory lineage (Figure 1.4).

Notch pathway

The Notch pathway consists of five Notch ligands (Dll1, 3, 4, Jagged-1, 2) and four Notch receptors (Notch1-4). In the intestine, *Notch1, Notch2, Dll1, Dll4* and *Jagged-1* are expressed in epithelial cells of the crypt, while *Notch3* and *Notch4* are expressed in the surrounding endothelial and mesenchymal cells (15-17). Notch signaling occurs between adjacent interacting cells so that membrane bound ligands of one cell bind to membrane bound receptors on a neighboring cell (Figure 1.5a). Interaction between ligand and receptor results in cleavage within the transmembrane domain of the receptor by γ-secretase enzymes releasing the Notch intracellular cytoplasmic domain (NICD). NICD translocates to the nucleus and binds to and activates the DNA-binding transcription factor CSL (CBF-1/RBP-Jκ, Su(H), Lag-1). Binding of the NICD-CSL complex and recruited transcriptional co-activators promotes transcription of Notch target genes (Figure 1.5a).

In the intestine, the Notch pathway plays roles in ISC maintenance, proliferation and cell fate determination. Disruption of Notch signaling through genetic ablation or pharmacological inhibitors led to the loss of proliferative cells in the crypts, which illustrated the role of Notch in maintaining ISCs and proliferative crypt compartments in the intestine (18,19). Conversely Notch signaling is implicated in colorectal cancer (CRC) as expression of Notch ligands, receptors and downstream targets are oftentimes up-regulated in tumors (20).

In addition with loss of ISC maintenance and proliferation, disruption of the Notch pathway resulted in conversion of epithelial cells into goblet and EECs (18,19,21-23) indicating a role for Notch in regulating lineage specification (Figure 1.4). A key transcriptional target of Notch signaling is *Hes1*. Embryos lacking *Hes1* developed excessive secretory cells at the expense of the absorptive cell lineage (24,25). It has been shown recently that other isoforms of Hes, including *Hes3* and *Hes5* are able to compensate for loss of *Hes1* and loss of all three isoforms lead to forced differentiation to a secretory cell fate (26). Conversely, gain of function experiments showed that ectopic expression of Notch favors the absorptive cell lineage (27). Along with promoting the absorptive lineage, *Hes1* simultaneously represses the secretory lineages by repressing the transcriptional activator *Atoh1*.

Wnt pathway

The Wnt pathway is one of the more commonly discussed and well-studied pathways in the intestinal epithelium. The canonical Wnt pathway requires interaction between multiple Wnt ligands and their receptors. Wnt ligands include mesenchyme derived Wnt2b and 5a and Paneth cell derived Wnt3b, 6 and 9b (Figure 1.3). Receptors include Frizzled (Fzd5-7) or low-density lipoprotein receptor-related protein (LRP5-6) receptors and are expressed

on crypt epithelial cells (28,29). Activation of Wnt signaling leads to a block on β-catenin degradation by a complex consisting of axin, adenomatous polyposis coli (APC), casein kinase I (CKI) and glycogen synthase kinase 3β (GSK3β), known as a destruction complex. Stabilized β-catenin then travels to the nucleus where it can act with the T-cell factor (TCF) family of transcription factors to turn on expression of Wnt target genes (Figure 1.5b). The Wnt pathway is involved in cell proliferation, cell differentiation and maintenance of ISCs.

Wnt signals occur in a gradient with the most concentrated area found at the crypt base where Wnt producing mesenchymal and Paneth cells reside (30) (Figure 1.3). Wnt signaling is essential for the maintenance of ISCs. Deletion of *Tcf7l2* gene (encodes TCF4 protein) resulted in the loss of ISCs with an epithelium consisting of differentiated villus cells (31) and genetic deletion of β-catenin led in crypt ablation (32). Inhibition and overexpression studies have shown the Wnt pathway in regulating proliferation. Overexpression of Wnt inhibitor *Dickkopf-1* blocked cell proliferation (33,34) while overexpression of Wnt agonist *R-spondin1* lead to hyperproliferation (35). Wnts regulate maintenance and proliferation of CBC ISC but have also been shown to act on Paneth cells to promote maturation (29). Due to its role in cell proliferation, Wnt signaling is implicated in a wide range of cancers, especially sporadic CRC (36). Inactivating mutations in *APC* account for 85% of sporadic CRC cases and leads to stabilization and nuclear translocation of β-catenin, which results in constitutively active Wnt signaling (36,37).

Similar to the Notch pathway, in addition to ISC maintenance, Wnt signaling also plays a role in cell differentiation. Wnt target gene *Atoh1* (also referred to as *Math1*) is a transcription factor that directs intestinal progenitors to the secretory lineage (Figure 1.4). Impaired Wnt signaling decreased $Atoh1^{+}$ progenitors and resulted in intestines containing predominantly absorptive enterocytes (31,32,34). Animals with intestine specific deletion of *Atoh1* displayed increased absorptive enterocytes at the expense of secretory cell lineages (38,39) while intestine specific *Atoh1* overexpression promoted secretory cell fate (40). Transcription factors regulated by *Atoh1* further direct cells toward a specific secretory cell type. *Gfi1* is downstream *Atoh1* as $Atoh1^{-/-}$ intestines lacked of *Gfi1* expression. *Gfi1* controls Paneth and goblet cell fate as $Gfi1^{-/-}$ animals do not contain Paneth cells, reduced goblet cell number, but enhanced number of EECs (41). *Ngn3*, another transcription factor downstream *Atoh1*, is required for EEC specification as $Ngn3^{-/-}$ animals did not develop EEC (42) (Figure 1.4).

Bmp pathway

Bone morphogenetic protein (BMP) signaling negatively regulates the pro-proliferative actions of Wnt signaling (43). BMPs are members of the transforming growth factor beta (TGF-β) superfamily that act via BMP receptors. *Bmp2* and *Bmp4* ligands are expressed in a gradient along the crypt/villus axis with high levels at the villus tips in the intervillus mesenchyme and decreasing levels traveling to the crypt base. Other members of the Bmp pathway like Bmp receptors *Bmpr1a* and *Bmpr2* and phosphorylated SMAD proteins are found in the villus compartment (43). *Noggin* and *Gremlin-1*, inhibitors of Bmp signaling, are expressed at the crypt base in order to keep Bmp signaling low and maintain high levels of Wnt signaling (Figure 1.3). Bmp signaling leads to phosphorylation and activation of the Smad family of transcription factors (Figure 1.5c). Bmp pathway inhibition by overexpression of *Noggin* (44) or deletion of *Bmpr1a* (43) lead to ectopic crypt or polyp formation, respectively, indicating blocking the negatively regulating Bmp pathway promotes intestinal proliferation, presumably due to uncontrolled Wnt activation.

Differentiated cells of the intestinal epithelium

Absorptive enterocytes

Absorptive enterocytes comprise over 90% of the intestinal epithelial cell population. They are highly specialized, polarized cells with an apical side in contact with the lumen and a basolateral side in contact with the bloodstream. The apical membrane contains a brush border enriched with specific brush border enzymes that are responsible for the final steps of digestion of some nutrients (i.e. disaccharides and peptides) and for absorption of nutrients and transport through the enterocyte into the circulation (blood/lymphatics). For this reason, brush border enzymes such as alkaline phosphatase (*Alpi*), sucrose isomaltase (*Sim*) and lactase (*Lct*) are useful markers of enterocytes (Table 1.1).

Goblet cells

Goblet cells, one type of secretory cell, secrete mucins and trefoil factors that act to protect the intestinal epithelium from physical and chemical stress caused by contents moving through the intestinal lumen. Goblet cells are present in both the crypt and villus compartments and the number of goblet cells increases in a proximal to distal gradient so that the smallest and largest percentage of goblet cells is found in the duodenum and distal colon, respectively. The most commonly secreted mucin in the intestine is mucin-2 (*Muc2*) and is often used as a marker of goblet cells (Table 1.1). Mucins and other secretory products of goblet cells form a layer of mucous that coats the

intestinal epithelium. Genetic deletion of mucins or genes involved in producing mucins resulted in increased bacterial adhesion, inflammatory cytokines and colitis (45,46). This suggested a role for goblet cells in protecting the host against lumenal contents such as microbes.

Paneth cells

Paneth cells, named after Josef Paneth, are situated in between CBC ISCs. Paneth cells contain large granules making them histologically distinct cells. They secrete many peptides that are vital to intestinal epithelial homeostasis including antimicrobial peptides and proteins that comprise the ISC niche. Their secreted antimicrobial peptides such as lysozyme and defensins (termed cryptidins in mice) mediate two main functions: innate immunity to protect the host from pathogens and to modulate or shape the intestinal microbiota (47). Mice with compromised Paneth cell function or genetic deletion of Paneth cells experienced bacterial translocation (48,49) and altered microbial communities (50). Paneth cells can be readily visualized by hematoxylin and eosin (H&E) staining, but its secretions such as lysozyme (*Lyz*) and defensins/cryptidins (such as *Defa1*) are used as markers for identification (Table 1.1).

Enteroendocrine cells (EECs)

EECs are hormone-secreting cells present in both the crypt and villus of the small intestinal epithelium and colonic crypts. In the small intestine, EECs comprise ~1% of the total epithelial population. Although small in number, there are up to 15 different types of EECs that differ in location and hormone(s) secreted (51). Hormones secreted by EECs regulate intestinal motility, bicarbonate release, enzyme secretion, appetite, insulin release and nutrient uptake (52).

Defining ISC biomarkers: *in vivo* and *in vitro* methods to evaluate stemness

Label retention

Label retention is used to identify slowly cycling cells and was used by Potten and colleagues to identify the +4 reserve ISC (2). DNA analogues such as 5-bromo-2'-deoxyuridine (BrdU) or tritiated thymidine are administered to animals and incorporate into the DNA of cells undergoing the S-phase of the cell cycle thereby marking all proliferating cells. Following administration, a washout period starts where the actively proliferating cells will divide and dilute out the label. Cells that do not actively divide or are slowly dividing will retain the label and referred to as label retaining cells (LRCs) (Figure 1.6a).

In vivo lineage tracing

Lineage tracing is a method to identify progeny of single cells and is now considered a gold standard for defining ISC biomarkers. Lineage tracing requires a conditional knock-in mouse in order to control and visualize progeny of putative ISCs. Using the Cre-lox system, a CreERT2 element is inserted downstream the promoter of the gene of interest and crossed with a reporter mouse containing a transcriptional stop sequence flanked by loxP sites upstream the reporter. Upon tamoxifen administration, Cre recombinase will remove the transcriptional stop and turn on the reporter gene in cells expressing Cre, permanently marking cells expressing the gene of interest. Progeny will inherit the reporter expression and can be visualized at different time points. Since ISCs give rise to all cells of the intestinal epithelium, lineage tracing of true ISC biomarkers result in all cells expressing the reporter and is characteristically seen as ribbons of positive cells (Figure 1.6b).

In vitro enteroid formation

Until recently, studying the intestinal epithelium, including ISCs, *ex vivo* proved difficult due to the lack of survival in traditional *in vitro* culture methods. ISC function is assessed by stemness assays. Stemness is defined as the ability of a cell to self-renew and can give rise to all cell populations within that particular tissue (multipotency). The Clevers group used the knowledge of the signaling pathways enriched in the ISC niche to develop a novel and elegant *in vitro* culture system that promotes ISC survival and tests ISC intrinsic function in the absence of niche cells (53). In this model, ISCs are grown in a three-dimensional Matrigel system where the Matrigel acts as the extracellular matrix and is supplemented with niche factors identified to promote and maintain ISC survival and function including EGF, Noggin, and Wnt agonist R-spondin1. This system allows ISCs to survive and grow into structures termed enterospheres and then enteroids that contain a lumen and crypt buds containing ISCs and all differentiated lineages (54) (Figure 1.7). The ability to use this system to culture ISCs *in vitro* has allowed researchers to better understand regulation of ISC function through genetic manipulation or pharmacological treatment, that may otherwise be complicated or confounded by other factors *in vivo*. It is noted that although individual ISCs can survive and yield enteroids in this system, the efficiency is low such that typically 10,000 cells yield on average 15-20 enteroids for an efficiency of 0.15-0.2%. This efficiency has been used by us and others to quantify the impact of physiological perturbations on stemness or intrinsic function of ISCs.

Generating ISC reporter mouse models to study ISC in vivo

Putative ISC biomarkers were validated using methods described above to demonstrate stemness and multipotency, through the use of genetically engineered mouse models expressing reporter genes driven by the promoter for the gene of interest. There are different ways to engineer mice expressing a fluorescent marker or other reporters that mark gene expression; these include transgenic or a knock-in mouse models.

Transgenic mice have a segment of DNA introduced into the genome that is normally not present. For larger segments, DNA must be packaged into a vector such as a bacterial artificial chromosome (BAC). Large DNA sequences (up to 300kb) can be inserted into a BAC vector. This is then injected into oocytes, where it randomly integrates into the genome, resulting in embryos that carry the recombinant gene. Since the DNA integrates randomly, the transgene may or may not fully recapitulate the endogenous protein of interest.

Knock-in mice avoid the problem of random integration that occurs in transgenic mouse models. To generate knock-in mice, cells expressing a targeting vector containing the transgene are introduced into a mouse embryo and implanted into a surrogate female mouse. Knock-in reporter models are targeted downstream of the promoter for the gene of interest, therefore reporter expression is found in cells expressing that gene. For example, in *Bmi1-EGFP* reporter mice, the *Bmi1* promoter is driving EGFP expression, therefore only cells expressing *Bmi1* will express EGFP. In conditional knock-in animals, permanently turning on expression of the transgene can be controlled and therefore used to perform lineage tracing experiments as described above.

ISC reporter mouse models

The majority of ISC reporter mice are knock-in animals and some contain a conditional CreERT2 element required to perform lineage-tracing experiments. Table 1.2 summarizes key ISC biomarkers and reporter animals generated to study ISC. The different reporter models have gained more attention recently due to single-cell analyses in various reporter models assessing the heterogeneity in the cell populations being marked. Briefly, Li et al compared different knock-in reporter animals and found that reporter or inducible reporter animals of the same gene (i.e. *Bmi1-EGFP* and *Bmi1-CreERT2*) marked different cells, indicating the reporter animal used is an important factor when pursuing ISC studies (55).

The Sox9-EGFP mouse model is a BAC transgenic model that is described in more detail below. In the intestine, Sox9-EGFP follows endogenous Sox9 protein expression, except that Sox9-positive Paneth cells are Sox9-EGFP Negative (56).

Sox9-EGFP mouse model

Currently no single ISC reporter is ideal as none of the models described above is validated as marking both CBC ISCs and +4 reserve ISCs, and there is evidence for interconversion between the two ISC subtypes (10,11). The Sox9-EGFP model has some potential advantages in this regard. In the Sox9-EGFP mouse model, a BAC transgene containing a large amount of flanking gene regulatory elements of the *Sox9* gene drives expression of EGFP. In the intestines of Sox9-EGFP mice, distinct levels of Sox9-EGFP mark different intestinal epithelial cell types (56,57). Figure 1.8a depicts the cell types corresponding to Sox9-EGFP expression levels in the small intestine. High level expression (Sox9-EGFP High) mark cells dramatically enriched for expression of all known gastrointestinal hormones and known markers of EECs and these same cells are enriched for markers of the +4 reserve ISCs (13,56,57). This suggests that this population of cells contain both EECs and +4 reserve ISCs. Direct evidence that Sox9-EGFP High cells contain +4 reserve ISCs stems from findings that they exhibit functional characteristics of ISC *in vitro* but only after activation by radiation induced epithelial damage (13). Low Sox9-EGFP levels (Sox9-EGFP Low) correspond to the actively cycling CBC ISC. The evidence for this was high-level expression of *Lgr5*, the first validated ISC biomarker, observed in this population and the ability of Sox9-EGFP Low cells (and no other Sox9-EGFP population) from "normal" small intestine to generate enteroids containing all differentiated lineages *in vitro* (56,57). Sox9-EGFP Sublow cells mark the rapidly dividing progenitor population while cells negative for Sox9-EGFP correspond to Paneth cells, goblet cells and enterocytes (13,56,57).

Our group performed transcriptomic analyses of each of these populations by gene microarray, which provided strong evidence that different Sox9-EGFP levels mark different intestinal epithelial cells. Sox9-EGFP Low cells were enriched for many genes enriched in *Lgr5* expressing ISC (58). Sox9-EGFP Sublow cells were enriched for genes involved in cell cycle progression and Sox9-EGFP Negative cells were enriched for genes encoding mucins (goblet cells), antimicrobial peptides (Paneth cells) and brush border enzymes (enterocytes). Sox9-EGFP High cells were enriched for EEC hormones and markers. However it revealed Sox9-EGFP High cells were also enriched for markers of reserve ISC such as *Bmi1* and *Hopx* (13). *In vitro* culture of Sox9-EGFP High cells during peak regeneration following abdominal radiation revealed Sox9-EGFP High cells can form enteroids which indicated a subset of Sox9-EGFP High cells were radiation activatable to acquire ISC-like functions (13). These findings were highlighted in a subsequent paper from Buczacki et al where they used a complex genetic mouse model capable of marking LRCs without the use of a thymidine analog thereby marking the slowly cycling reserve

ISC population. The LRCs in this model expressed transcripts associated with Paneth cells, EECs and ISCs and were able to form enteroids following radiation. They concluded secretory precursors are able to acquire ISC-like characteristics when activated by radiation (12).

ISC mouse models using fluorescent reporter expression such as EGFP are valuable tools to assess and use ISC for downstream applications. In the Sox9-EGFP reporter mouse, we are able to use EGFP intensity to visualize Sox9-EGFP Low and High cells by immunofluorescence, quantify all four populations of cells, including ISC, by flow cytometry and isolate all populations by fluorescence activated cell sorting (FACS) (Figure 1.8b-c). Isolated cells can then be used to assess gene expression changes or cultured *in vitro* to study intrinsic function. One limitation of the Sox9-EGFP model is the inability to perform lineage tracing because *Sox9* is expressed in other cells at different levels. Despite this, we are able to use the Sox9-EGFP reporter mouse to evaluate the effects of obesity and intermittent feeding directly on ISC and other intestinal epithelial cell populations.

Obesity, hyperinsulinemia and insulin resistance

Obesity is defined as a body mass index (BMI) > 30kg/m^2. Although rates of obesity have started to level off in the United States, prevalence remains high with about 35% of the adult population considered obese (59). Causes of obesity are highly complex, involving interactions between genetics, environment and multiple organs. Evolutionarily, humans store nutrients as fat and utilize their fat stores for energy production in times of nutrient restriction. However, in the past decades, the increase in calorie-dense foods combined with decreased physical activity has lead to increased obesity rates. Obesity is associated with increased fat accumulation and enlargement of multiple fat depots and results in or increases risk of a host of metabolic disorders. Increased prevalence of obesity has been associated with increases in insulin resistance and type 2 diabetes (59,60). Insulin resistance is marked by high levels of insulin (hyperinsulinemia) relative to glucose levels and is due to reduced ability of insulin-sensitive tissues to respond to insulin. Pancreatic β cells therefore produce more insulin to maintain normal blood glucose levels. However if insulin resistance is not remedied, over time, β cells start to fail leading to the inability to produce insulin and subsequent inability to control plasma glucose and the development of type 2 diabetes occurs.

Insulin is an anabolic hormone that is released in response to food intake to lower blood glucose and promote glycogen, TG and protein synthesis. Insulin can also promote cell growth. The metabolic and growth effects of insulin are mediated by insulin binding to insulin receptor (IR). Insulin binds to and activates IR leading to phosphorylation of insulin receptor substrates (IRS; most common are IRS-1 and IRS-2). Tyrosine phosphorylation

of IRS proteins promotes downstream activation of phosphoinositide-3-kinase (PI3K) or mitogen-activated protein kinase (MAPK) pathways. Signaling through PI3K activates AKT/PKB to regulate the metabolic effects of insulin signaling such as promoting glucose uptake by GLUT4 translocation to the plasma membrane, glycogen and protein synthesis and suppressing gluconeogenesis. Signaling through MAPK is involved in transcriptional regulation of genes involved in promoting cell growth (Figure 1.9).

There are a number of mechanisms linking obesity and hyperinsulinemia to insulin resistance and type 2 diabetes, many involving disruptions in the insulin-signaling pathway (Figure 1.9). Inflammatory cytokines and factors that promote inflammatory cytokine production are implicated in impaired insulin signaling (61-63).

During obesity, there is increased macrophage infiltration in adipose tissue, increased plasma endotoxins such as lipopolysaccharides (LPS) and increased FFA and FFA metabolites such as diacylglycerol (DAG), and all increase production of pro-inflammatory cytokines (62). Inflammatory pathways activated by pro-inflammatory cytokines promote serine phosphorylation of IRS-1 rendering it inactive. Pro-inflammatory cytokines can also induce expression of suppressors of cytokine signaling (SOCS) proteins. SOCS3 can interfere with insulin signaling by binding to and preventing IRS-1 from docking onto IR (64) (Figure 1.9). Interestingly, the lipogenic functions of insulin are preserved despite defective insulin-stimulated glucose clearance, so that hepatic and muscle lipogenesis increases leading to increased ectopic TG storage.

Obesity and the intestine

The effect of obesity has been commonly studied in metabolic and insulin-sensitive tissues such as liver, adipose tissue and skeletal muscle. There is increasing attention on the role of the intestine in obesity due to its role in nutrient absorption and barrier function, as well as increased interest in the intestinal microbiome.

Obesity and nutrient absorption

The intestine functions to digest and absorb ingested food. More detailed descriptions of macronutrient digestion and absorption can be found in later sections. Despite its functions, not much is known about the effect of obesity on nutrient absorption. Transcriptomic analysis on different regions of the small intestine revealed differential effects of high fat diet (HFD) on gene expression in different regions. Compared to the duodenum and ileum, the jejunum exhibited the highest number of differentially regulated genes, which is expected, as it is the major site of lipid absorption (65). Gene networks reported to be regulated by HFD in the small intestine included lipid metabolism, cell cycle and inflammation (65). Gene expression analysis of transcription factors involved in cell

fate determination revealed obesity modulates expression of transcription factors associated with decreased secretory lineage allocation and increased absorptive cells (66). A limitation of these studies was that gene expression was analyzed in the total epithelium, which is composed of >90% absorptive enterocytes. Thus genes or transcription factors expressed in enterocytes could be over-represented and any diet-associated change in relative enterocyte mass could indirectly impact levels of mRNAs expressed in enterocytes or less abundant cell types. This dissertation addresses this limitation by using the Sox9-EGFP mouse model to more directly evaluate the effect of HFD-induced obesity on specific cell types.

Obesity and intestinal hormones

EECs secrete hormones that regulate appetite and satiety and are a heterogeneous population, meaning different cells secrete different hormones. Up to 15 hormones exist and act to increase insulin production and regulate appetite and intestinal growth. Their complexity is too great to give a comprehensive overview of each hormone however key hormones are addressed. Glucagon like peptide 1 (GLP-1) and glucose-dependent insulinotropic peptide (GIP) are incretins that promote insulin synthesis and secretion by pancreatic β-cells. Cholecystokinin (CCK) is a hormone released in response to food intake that mediates digestion and satiation. Glucagon like peptide 2 (GLP-2) is another EEC hormone generated from the same mRNA as GLP-1, however GLP-2 functions in intestinal growth via insulin-like growth factor 1 (IGF1). Studies in animals have shown that obesity decreased plasma levels of GLP-1 and CCK (67-69) and increased plasma levels of GLP-2 (70). Changes in EEC hormones during obesity is further highlighted in studies that have shown hormonal levels can change following gastric bypass surgery or weight loss (71,72). Modulating intestinal hormone levels through exogenous administration is currently being tested as potential treatments for obesity.

Obesity and intestinal permeability

Obese mice display increased intestinal permeability as measured by the ability of non-digestable fluorescent probes administered orally to appear in the bloodstream (73) and decreased intestinal expression of tight junction proteins (74). Increased permeability permits entry of toxins or bacterial products such as LPS, a structural component of gram-negative bacteria, into the bloodstream. Animals fed HFD for 4 weeks displayed elevated plasma LPS, prior to the onset of frank obesity (61), which indicated that increased intestinal permeability preceded HFD induced body weight gain. Elevated levels of LPS in the bloodstream due to HFD have been termed metabolic endotoxemia (61). The consequences of metabolic endotoxemia include increased inflammation in adipose tissue,

increased liver TG and hepatic insulin resistance (61). Some studies suggest however that LPS is not required for development of HFD-induced glucose intolerance (75). It is unknown whether the loss of barrier function in obesity is due to improper intestinal epithelial renewal carried out by ISC. Exploring the effects of obesity directly on ISC will to link obesity to ISC function, renewal and intestinal permeability.

Obesity and intestinal inflammation

Obesity is characterized by a state of low-grade inflammation. Our lab demonstrated that intestinal inflammation occurs prior to HFD induced increases in body weight or plasma insulin levels. In the intestine, mRNA levels of the pro-inflammatory cytokine *Tnfα* was up-regulated in the ileum of animals fed HFD for 6 weeks, preceding significant changes in body weight. The degree of TNFα mRNA increase was positively correlated with weight gain, fat mass, plasma insulin and plasma glucose levels (76). Furthermore, HFD-induced intestinal inflammation, measured by NFkB activation, was detected in a variety of cell types in the intestine, including intestinal epithelial cells, immune cells and endothelial cells, indicating that multiple cell types are able to contribute to HFD-induced inflammation (76). Additionally, mesenteric fat surrounding the intestine of obese animals displayed increased expression of inflammatory cytokines and macrophage infiltration (77). Studies in humans have been less conclusive with contradicting reports of differences in fecal inflammatory markers between lean and obese patients (78-81). Increased inflammation can be linked to changes in intestinal function including altered or reduced barrier integrity and may modulate the intestinal microbiota.

Obesity and intestinal microbiota

The intestinal microbiota consists of trillions of microorganisms that interact collectively to impact host health by regulating various functions including immunity/host defense and harvesting energy from ingested food. The genome of these organisms is termed the microbiome. Microbiota and their associated microbiome can change in response to a number of factors including environment (i.e. antibiotics) or nutrition (i.e. obesity) and in pathophysiological states (i.e. inflammatory bowel disease (IBD)). It is now widely accepted that the intestinal microbiota is altered in obesity. However the extent to which the altered microbiota is the cause or consequence of obesity is yet to be fully elucidated. In both genetic and diet-induced mouse models of obesity (82-85) and in obese and lean humans (85), the microbial communities shift to favor increased abundance of Firmicutes while decreasing Bacteroidetes. This effect can be reversed after weight loss or surgical treatment of obesity (86,87). It has also been shown that HFD alone, in the absence of obesity can alter microbial composition (88). Germ free mice, mice devoid

of any microbes and maintained in a sterile environment, are protected from diet-induced obesity (DIO) (76,89), providing evidence that microbes are required for HFD-induced increases in fat mass at least in mouse models tested. Current research is now focusing on understanding how specific bacterial subtypes or species contribute to obesity and associated metabolic consequences. *Akkermansia mucinphilia*, a mucin degrading bacteria, has gained increased attention in the past few years and is inversely correlated to body weight in mice and humans (90,91). *A. mucinphilia* increases with metformin treatment (92), a drug used to improve insulin sensitivity in type 2 diabetes. Everard et al demonstrated that *A. mucinphilia* administration via prebiotics or oral gavage reversed obesity associated increases in fat mass, adipose tissue inflammation and fasting hyperglycemia (90). Together, these studies provide evidence for the role of the intestinal microbiota or specific bacterial species in obesity associated pathologies. One potential confounder in studies of DIO is a potential influence of low fiber intake or levels in obesogenic diets. Fiber is a non-digestable carbohydrate that is metabolized to short chain fatty acids (SFCA) such as butyrate by the microbiota. Butyrate has been shown to be anti-tumorigenic in the colon (93,94). Current views are that fiber is protective, particularly in the pathogenesis of intestinal inflammation and CRC (94,95). Our studies of mice with DIO aimed to test if existing obesity and hyperinsulinemia, indicative of insulin resistance, affected ISCs. Our studies did not address the impact of microbiota or fiber, but these are interesting future directions.

Obesity and changes in intestinal epithelial morphology

Surprisingly, there are a limited number of studies exploring the effect of obesity on intestinal epithelial morphology. In animal models, obesity increased villus height associated with increased villus cell number and crypt cell proliferation (70,96,97), presumably as an adaptation to increase intestinal absorptive capacity. However there is no direct evidence on the effect of obesity on ISCs, the cells responsible for repopulating the epithelium, which is important since improper epithelial renewal may lead to intestinal dysfunction. The Sox9-EGFP reporter model allows for interrogation of the effects of DIO on ISCs to provide direct evidence for the role of ISCs in DIO associated increases in villus height observed in previous studies.

Alternate day fasting and intermittent feeding diets

Alternate day fasting (ADF), a type of intermittent feeding diet, involves alternating days of food restriction and free access to food. ADF is being studied as an alternative to daily calorie restriction (CR). Another intermittent feeding diet called modified ADF or intermittent CR involves a reduction in calorie intake rather than 100% food restriction on alternating or a subset of days. A similar diet called the 5:2 diet, because it involves two non-

consecutive days of CR and five days of *ad libitum* eating a week, is gaining popularity among humans. The overall principle of these diets is complete (true ADF) or partial CR (modified ADF) on a subset of days during the week, rather than consistent restriction of calorie intake everyday. The popularity of this type of diet stems from the difficulty to adhere to constant CR (98,99), which is defined as 20-40% restriction of calories without malnutrition every day (100,101). The reported beneficial effects of CR require sustained and long-term adherence to the diet, which many humans cannot achieve. Rodent and human studies of ADF or intermittent feeding have increased in the past few years and indicate benefits in weight loss, improved metabolism, and factors involved in cardiovascular disease and cancer risk, although with some variability across studies or between rodents and humans. Table 1.3 and Table 1.4 summarize findings from select ADF studies in animals (Table 1.3) and humans (Table 1.4) on body weight and fasting glucose, insulin and insulin-like growth factor 1 (IGF1) levels. Studies in animals have yielded mixed results regarding the effect of ADF to reduce body weight, but metabolic benefits of ADF occur in the absence of weight loss (102-107). Several human trials in ADF or intermittent feeding have shown reductions in body weight in overweight/obese subjects. Overweight subjects that completed a 3-week ADF intervention decreased their body weight by 3% (108), while an 8-week study of modified ADF where subjects were 80% CR every other day lost 8% of their body weight (109). ADF has been shown to decrease fasting glucose and insulin levels in animals, similar to that seen in CR (Table 1.3) (102,107). Human studies have produced mixed results on improving fasting glucose and insulin in normal weight subjects however ADF appears to be more effective at lowering fasting plasma glucose and insulin levels in overweight and obese subjects (Table 1.4) (103,108,110-114).

Along with its effects on body weight and metabolic parameters, there is evidence that ADF potentially has anti-tumorigenic effects. Animal studies coupling dietary restriction and a carcinogen/mutagen or tumor cell xenografts revealed that intermittent feeding (including ADF) increased survival and decreased tumor number and size (115,116). It has been speculated that the beneficial effects of intermittent feeding on tumorigenesis is due to decreased proliferation. Varady et al. reported that ADF decreased proliferation of T-cells and prostate cells and this was associated with decreased levels of circulating IGF1 (105). ADF has also been shown to decrease proliferation rates of mammary epithelial cells and keratinocytes (117). Taken together, these findings suggest that ADF may confer a protective effect on tumorigenesis by decreasing cell proliferation

Recent publications on time restricted feeding (TRF) in mice have shown similar outcomes on body weight and metabolic parameters as described above (118-120). Similar to ADF, TRF is limiting access to food to a specific

time each day. In these studies, mice were allowed access to food only for 8-hours during the dark cycle, which is the normal nocturnal feeding period for a mouse. TRF using HFD produces similar outcomes as standard chow when measuring metabolic parameters such as body weight, body composition, insulin, leptin and cholesterol indicating the diet timing may be more important than diet composition. Mice subjected to longer term TRF displayed similar benefits (119). The effects of TRF were associated with changes in the intestinal microbiota including decreases in Lactobacillus and Lactococcus, both of which have been associated with increased body fat and obesity associated metabolic disruptions (120).

Although more research needs to be completed in this area, it appears that ADF or other intermittent or restricting feeding regimens may be beneficial in promoting weight loss and reduced fat, improved glucose and insulin homeostasis and reduced cell proliferation associated with changes in the gut microbiome. Although ADF alters the intestinal microbiota, its impact on the intestinal epithelium or ISCs has not been addressed. A recent study by Yilmaz et al. reported long-term CR increases ISC number, ISC proliferation and decreased progenitor proliferation (121). Based on these findings and the similarities between CR and ADF, our current study tested the hypothesis that ADF and associated changes in insulin levels will impact ISC and progenitors associated with changes in intestinal growth using the Sox9-EGFP reporter mouse model.

Overview of the insulin and IGF system

The insulin/IGF system is composed of multiple signaling ligands and receptors that mediate different actions including growth, apoptosis and metabolism in various tissues throughout the body. This section will describe the ligands and receptors that make up the insulin/IGF system and their effects on the body, including known effects on the intestine.

Ligands and receptors of the insulin/IGF system

The insulin/IGF system is composed of three ligands (insulin, IGF1 and IGF2) with differing affinities to bind two receptors (IR or IGF1 receptor (IGF1R)). IGF1 and IGF2 are produced at very high levels in the liver but both are produced in other, if not all non-hepatic tissues. In the liver, IGFs are expressed at high levels in hepatocytes, while IGFs are produced by mesenchymal cells in other tissues, including the intestine (122-128). Insulin is produced by the β-cells of the pancreas. Insulin and IGFs bind their own receptors preferentially, however at high levels insulin and IGFs can bind to either IR or IGF1R to initiate downstream signaling pathways.

Both IR and IGF1R consist of an extracellular ligand binding α-subunit and a transmembrane tyrosine kinase β-subunit joined by disulfide bonds (Figure 1.10a). IR and IGF1R are highly homologous and differences are mainly located in their extracellular domain indicating functional differences lie in their ligand binding affinities. IGF1R is expressed in a wide variety of tissues to mediate the growth and anti-apoptotic effects of IGFs (129). IR exists in two functionally distinct isoforms, IR isoform A (IR-A) and IR isoform B (IR-B). Production of the two IR isoforms occurs through alternative splicing of IR pre-mRNA to promote the exclusion (IR-A) or inclusion (IR-B) of exon 11. Current views are that classical metabolic effects of insulin occur through IR-B signaling while IR-A mediates the growth effects of insulin (Figure 1.10b). IR is expressed in metabolically active, insulin-target tissues at high levels such as adipose tissue, liver and skeletal muscle and expression ratio favors IR-B. Lower, but detectable expression of IR exists in many tissues that are not considered targets of insulin action such as the brain and pancreas (130).

Insulin and IGFs bind their own receptors preferentially but do cross-react with each other's receptors at differing affinities. Insulin can bind both IR-A and IR-B. IGF1 and IGF2 can bind the IGF1R, however IGF2 can bind IR-A, providing dual sources for growth signaling through IR-A (Figure 1.10b).

Metabolic actions of insulin

The common actions associated with insulin are its effects on metabolism and is summarized in Table 1.5. Insulin is an anabolic hormone that is produced by β-cells of the pancreas in response to nutrient intake and its metabolic activities include regulation of glucose, lipid and protein metabolism.

Following ingestion of a meal, insulin levels increase and act to lower blood glucose by promoting glucose uptake and glycolysis in adipose tissue and skeletal muscle, hepatic glycogen synthesis and inhibiting hepatic glycogenolysis and gluconeogenesis. Inhibition of glycogen breakdown and gluconeogenesis occurs directly by inhibition of key regulatory enzymes in both processes as well as indirectly by decreasing gluconeogenic precursors. Insulin mediated glucose uptake occurs through translocation of glucose transporter GLUT4 to the plasma membrane of insulin-responsive tissues. GLUT4 facilitates glucose entry into adipose tissue and skeletal muscle where glucose can undergo glycolysis to produce ATP or glycogen synthesis. Insulin also positively regulates activity of key glycolytic and glycogen synthesis enzymes.

In addition to glucose metabolism, insulin also regulates lipid and protein metabolism. Insulin promotes TG synthesis and storage in adipose tissue during the fed state by generating of FFA and glycerol 3-phosphate. Glucose

that is transported into fat cells by GLUT4 undergoes glycolysis to generate glycerol-3-phosphate, the glycerol backbone required to produce TG. Insulin mediated stimulation of lipoprotein lipase in adipose tissue allows for the breakdown of TG from circulating chylomicrons into FFA. TG are formed through a series of enzymatic reactions between FFA and glycerol-3-phosphate and stored in adipose tissue. Along with promoting TG synthesis, insulin inhibits lipid breakdown by inhibiting hormone sensitive lipase, the enzyme required for lipolysis. Insulin increases protein synthesis and inhibits proteolysis by promoting transport of amino acids into tissue such as hepatocytes and skeletal muscle. Because of decreased gluconeogenesis, amino acids can be used to synthesize protein.

Insulin and IR in intestinal growth and cancer

In addition to its effects on metabolism, insulin can also regulate growth, including intestinal growth. Studies in intestinal resection, where 75% of the small intestine is removed, animals that received oral insulin after surgery demonstrated increased intestinal regeneration as measured by increased villus height and proliferation and decreased apoptosis associated with increased expression of IR (131-133). *In vitro* studies have shown that insulin treatment increases proliferation of Caco2 cells (133).

Due to its role in cell proliferation, there is increasing evidence for the role insulin and IR in cancer. Many epidemiological studies linking IR to intestinal cancers stem from the relationship that type 2 diabetics are at an elevated risk for developing CRC (134,135). In normal mucosa of humans, elevated plasma insulin and decreased apoptosis are associated with increased adenoma risk (136). Animals injected with azoxymethane (AOM), a carcinogen known to initiate colon tumors, and later given insulin injections developed a greater number of and larger tumors (137).

IR-A has been implicated as the IR isoform associated with cancer because of its role in growth and ability to bind insulin and IGF2. IR-A expression is dominant in a number of cancers including breast, lung and colon (138). Aberrant IR-A expression is observed in thyroid and breast cancer cells (130). Our lab has explored IR isoform expression in intestinal cancers. Andres et al. showed that in a panel of CRC cell lines, IR isoform expression in Caco2 cells was about equal, with similar levels of both IR-A and IR-B. In more aggressively growing CRC cell lines, IR-B was very low or absent and IR-A expression predominated (139). Forced IR-B expression in Caco2 cells and SW480 cells, a more aggressive CRC cell line, was able to decrease cell proliferation (139). Additionally, we have shown that jejunal and colonic tumors from $Apc^{Min/+}$ mice expressed predominantly IR-A, consistent with elevated IR-A expression in tumors of other tissues (139). Our group has recently shown that

increased IR-A:IR-B ratios in the normal human rectal mucosa of patients with elevated plasma insulin predicted intestinal adenoma risk, which indicated levels of IR-A in normal tissue may also be important in assessing cancer risk (140). Although insulin does have effects on growth, IR-A also has an affinity for IGF2, which also has mitogenic properties (discussed in later sections). Therefore it is likely that insulin and IGF2 may both contribute to IR-A signaling in cancer.

Role of insulin and IR isoforms in the intestine

The intestinal epithelium expresses IR and can respond to circulating insulin. Despite this, little attention has been given to the effect of insulin and the function of IR on the intestinal epithelium. Using the Sox9-EGFP mouse model, our lab has shown that IR-A is expression is greatest in proliferative ISCs (Sox9-EGFP Low) and progenitors (Sox9-EGFP Sublow), differentiated cells (Sox9-EGFP Negative) express primarily IR-B and Sox9-EGFP High cells, which are composed of reserve ISCs and differentiated EECs express equal levels, consistent with the functions of the two isoforms (139) (Figure 1.11a). These data suggested IR isoforms are expressed in a gradient where IR-A is highest at the crypts where proliferative stem and progenitors reside and expression decreases up the crypt/villus axis, while the greatest IR-B expression is observed in differentiated enterocytes on the villi and expression decreases down the crypt/villus axis (Figure 1.11c).

However it is unknown how IR isoforms are altered in specific intestinal epithelial cell types during obesity and ADF. Using the Sox9-EGFP reporter mouse, we are able to address this key question by isolating Sox9-EGFP populations and assessing IR isoform expression.

Effect of IGFs on intestinal growth

IGF1 is an anti-apoptotic, pro-proliferative growth factor in many tissues, including the intestine. Animal studies mimicking overproduction of IGF1 have provided evidence for its growth promoting effects on the small intestine. IGF1 administration prevented mucosal hypoplasia due to total parenteral nutrition (TPN) and promoted epithelial growth in response following intestinal resection by increasing crypt cell proliferation and inhibiting apoptosis (141-144). IGF1 pre-treatment of rat intestinal epithelial cells attenuated apoptosis induced by reactive oxygen species (145). Studies from our lab have shown that transgene mediated IGF1 overexpression potently promoted growth of the intestinal epithelium in both small intestine and colon (146,147). IGF1 increased proliferation and reduced apoptosis in crypts following radiation (148). Consistent with its pro-proliferative and anti-apoptotic functions, data from our lab revealed *Igf1r* mRNA is expressed in a gradient with highest expression in the

proliferative crypt cells. Using the Sox9-EGFP reporter mouse, we show *Igf1r* expression was highest in Sox9-EGFP Low ISCs, providing direct evidence that ISCs express *Igf1r* and indicating ISC may be particularly sensitive or responsive to IGFs and insulin (Figure 1.11b). These data also show that *Igf1r* is expressed in a gradient (similar to IR-A) where ISCs express the highest levels of *Igf1r* and expression decreases up the crypt/villus axis, where differentiated cell types express low *Igf1r* mRNA (Figure 1.11c). Recent studies from our lab using the Sox9-EGFP reporter model revealed that IGF1 selectively increased the number of actively cycling Sox9-EGFP Low ISCs in uninjured intestine and during crypt regeneration. Expansion of Sox9-EGFP Low ISCs was associated with regulation of distinct gene networks by IGF1 in Sox9-EGFP Low ISCs versus Sox9-EGFP High cells (Van Landeghem et al, *In revision*).

IGF1 can also mediate the effects of growth hormone (GH) and GLP-2, two hormones approved or under clinical trial as enterotrophic therapies (122). GH overexpressing transgenic mice display increased circulating levels of IGF1, increased small intestinal length and increased mucosal mass, although growth effects are not as dramatic as in IGF1 overexpressing transgenic models. GLP-2 induces intestinal growth by promoting local IGF1 expression (149) in intestinal subepithelial myofibroblasts (125). IGF1R is required for GLP-2 mediated intestinal epithelial growth during refeeding after a fast (150).

IGF2 levels are high during fetal growth and development and IGF2 knockout fetuses are smaller (130). Current views are that IGF2 mediates growth during development through interactions with IGF1R and IR-A.

IGFs and IGF1R in intestinal cancer

Elevated levels of IGF1, IGF2 and IGF1R are associated with cancer. Evidence from numerous epidemiological studies indicates an association between excessive IGF1 and intestinal cancers. Patients with acromegaly, a disorder characterized by overproduction of GH and IGF1, are at increased risk for developing CRC (151-153). The Physicians Health Study and the Nurses Health Study both found patients in the top quintile (Physicians Health Study) or tertile (Nurses Health Study) of circulating IGF1 levels were at >2 fold increased risk for developing CRC compared to those in the lowest group (154,155). IGF1 treatment of CRC cell lines promoted proliferation and inhibited apoptosis (129) while reducing IGF1 levels by pharmacological inhibitors blocked growth of colon tumors (156). Additionally, loss of heterozygosity for IGF2, which allows both alleles to be expressed, thereby increasing IGF2 levels, is linked to CRC (157-159). It is widely known that IGF1R expression is

common in cancer cell lines and human cancers (129) therefore IGF1R antagonists are prime targets for cancer therapies and are currently being tested (160).

Nutritional regulation of insulin and IGF1

Elevated levels of insulin and IGF1 are seen in obesity while decreased levels are observed during CR, indicating both can be regulated by nutritional status (161-164). Hyperinsulinemia also decreases the production of IGF binding proteins (IGFBPs) that normally bind and sequester IGFs making them unavailable to signal through their receptors. Decreased IGFBPs lead to an increase in bioavailable IGF1, further increasing IGF1 levels. Insulin and IGF1 levels are common mechanisms linking obesity associated increased cancer risk (165,166). Animal studies have shown that IGF1 administration reverses the anti-tumorigenic effect of diet restriction (167). However the effect of obesity and associated hyperinsulinemia and IGF1 on the intestinal epithelium and more directly on ISC has largely been ignored. The Sox9-EGFP reporter mouse allows us to explore expression of *Igf1r*, IR-A and IR-B in ISCs and other intestinal epithelial cell types during obesity and ADF to assess whether they can alter the expression in these receptors in ISC.

Nutrition and the intestinal epithelium

Lipid digestion and absorption

Lipid digestion begins in the upper small intestine and lipid digestion and absorption are typically completed by the time fecal material enters the colon. Pancreatic lipases digest TG to yield two FFA and one sn-2-monoglyceride (2-MG). Bile is essential for efficient lipid digestion and absorption. Bile emulsifies lipids into small droplets to ensure access and efficacy of lipases. Bile salts also ensure solubility of products of lipid digestion by forming micelles, which have hydrophilic regions on the outside interfacing with the aqueous portion of lumenal contents and inner hydrophobic regions where lipids reside. These structures termed mixed micelles contain FFA, 2-MG and other components such as bile salts and cholesterol. Mixed micelles then travel through a layer of mucous and an unstirred water later in order to reach the apical membrane of absorptive enterocytes on villi of the intestinal epithelium. FFA are thought to leave the micelle and enter the enterocyte by passive diffusion or via FFA transporters. Short (<6 carbons) and medium (6-12 carbons) chain fatty acids are absorbed by passive diffusion into the bloodstream. Longer chain fatty acids (>12 carbons) appear to enter via transporters, such as CD36. Mice with deletion of *Cd36* still display complete lipid absorption indicating that other transporter(s) likely aid in FFA absorption (168) (Figure 1.12a). Following entry into enterocytes, FFA and 2-MG are re-esterified to TG and

repackaged with phospholipids, fat soluble vitamins and cholesterol esters (CE) in the endoplasmic reticulum (ER). They associate with apolipoproteins and load onto nascent chylomicrons to form mature chylomicrons in the Golgi apparatus. CD36 null animals do display lipid accumulation in the intestine, indicating a role for CD36 in chylomicron production and secretion (169). Chylomicrons travel to the basolateral membrane of the enterocyte and are released into the lymphatics (Figure 1.12b). Chylomicrons interact with lipoprotein lipase that is present on endothelial cells that line capillaries to break down TG into glycerol and FFA for entry into adipose tissue and skeletal muscle. These lipids can be used for ATP production by the process of β-oxidation or re-esterified into TG for storage. In obese states, ectopic fat accumulation can occur in non-adipose tissue such as the liver, thereby compromising proper function. Elevated insulin can promote hepatic fat accumulation, which is an unwanted consequence of obesity and associated hyperinsulinemia.

Carbohydrate digestion and absorption

About 50% of the carbohydrates ingested are in the form a starch. Starch is a polysaccharide that must be enzymatically digested prior to absorption by the intestine. Digestion begins in the mouth where salivary amylases initiate starch breakdown. This continues as food travels down to the intestine where pancreatic α amylase yields oligosaccharides. Brush border oligosaccharidases and disaccharidases further break down oligosaccharaides to generate the monosaccharides: glucose, galactose and fructose. Transporters exist on the apical membrane of enterocytes to facilitate monosaccharide absorption. The sodium-linked glucose transporter (SGLT1) facilitates glucose and galactose uptake while GLUT5 is responsible for fructose entry into the enterocyte. GLUT2, located on the basolateral membrane, facilitates transport of all three monosaccharides out of the enterocyte into the interstitial space and then the bloodstream (Figure 1.13). Glucose can then be used by peripheral tissues to generate ATP for energy or can be stored as glycogen in the liver or other tissues including kidney and skeletal muscle. In the case of high carbohydrate intake, excess glucose is converted to acetyl-CoA and used to synthesize lipids and stored as fat.

Protein digestion and absorption

Enzymatic digestion of proteins into amino acids begins in the stomach by gastric proteases, particularly pepsin, and continues in the small intestine via pancreatic proteases. The brush border of enterocytes contains oligopeptidases or dipeptidases, which digest peptides into amino acids. Similar to glucose, amino acids are transported into enterocytes by a family of sodium-linked amino acid transporters. Additionally, oligopeptides are also capable of being absorbed by enterocytes and moved through the basolateral membrane and enter the

bloodstream without further hydrolysis. Transporters located on the basolateral membrane move proteins out of the enterocyte and into circulation and transport protein into the enterocyte for cell maintenance.

Nutrition and intestinal epithelial growth

Intestinal epithelial growth can be regulated by the presence of absence of lumenal nutrient. During TPN or fasting, where the intestinal tract is deprived of nutrient, result in mucosal atrophy associated with decreased mass of the small intestinal mucosa and epithelial lining, decreased proliferation and increased apoptosis in the crypts and reduced villus height (170-175). The effects of TPN or fasting can be quickly reversed with refeeding, indicating that the intestinal epithelium is highly responsive and quick to adapt to changes in lumenal content. The changes in mucosal architecture due to fasting or TPN are associated with changes in plasma levels and local expression of IGF1 and GLP-2, positive regulators of intestinal growth (170-175). In *Drosophila*, fasting results in reduced n ISC numbers and proliferation and refeeding reverses these effects (176,177). Although some studies have examined effects of obesity on mucosal mass and crypt/villus homeostasis, direct effects of obesity on ISCs were not defined and are addressed in this work. A second area of study was to examine ADF, a diet similar to CR, that may have opposite effects of obesity, on ISCs and overall changes in crypt/villus homeostasis, as this diet is becoming increasingly popular and emerging evidence suggest it ADF or other intermittent feeding diets can be a clinically relevant alternative to CR.

Hypotheses and questions addressed

This work examined the effect of obesity or ADF on ISCs using both *in vivo* and *in vitro* approaches. Based on previous work, we set forth the following central hypothesis: The intestine will adapt to obesity or ADF and associated changes in insulin levels by regulating ISC number, ISC proliferation, intrinsic ability to survive in culture or to differentiate (Figure 1.14).

Specific questions to address this hypothesis include:

1. Does HFD induce obesity and hyperinsulinemia in Sox9-EGFP animals?
2. Does DIO increase ISC number, proliferation and change number of Paneth, goblet and EECs?
3. Is ISC intrinsic function, assessed by survival and enteroid forming efficiency, altered during DIO?
4. Are effects of DIO linked to the insulin/IGF pathway?
5. Does ADF decrease body weight and insulin levels similar to animal studies in CR?
6. Does ADF maintain or decrease ISC number or proliferation?

7. Does ADF affect intestinal crypt/villus morphology?

8. Are changes observed in ADF animals associated with changes in the insulin/IGF pathway?

Figures and Tables

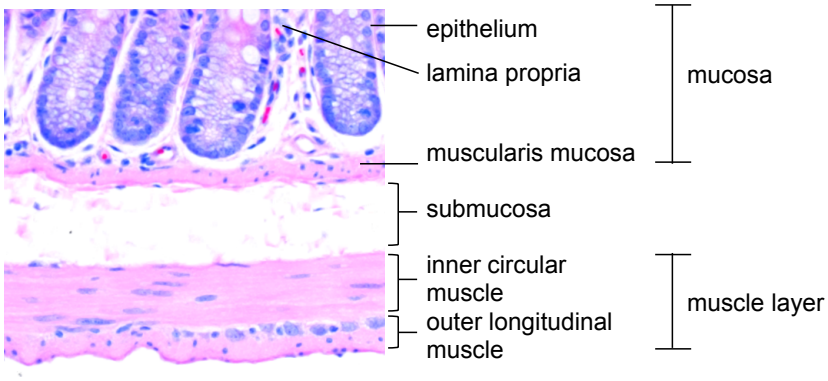

Figure 1.1:Histological representation of the layers of the mammalian intestine.
The intestine contains an inner mucosa layer composed of the epithelium (facing the lumen), underlying lamina propria and muscularis mucosa, a submucosal layer and muscle layer composed of an inner circular and outer longitudinal muscle layer.

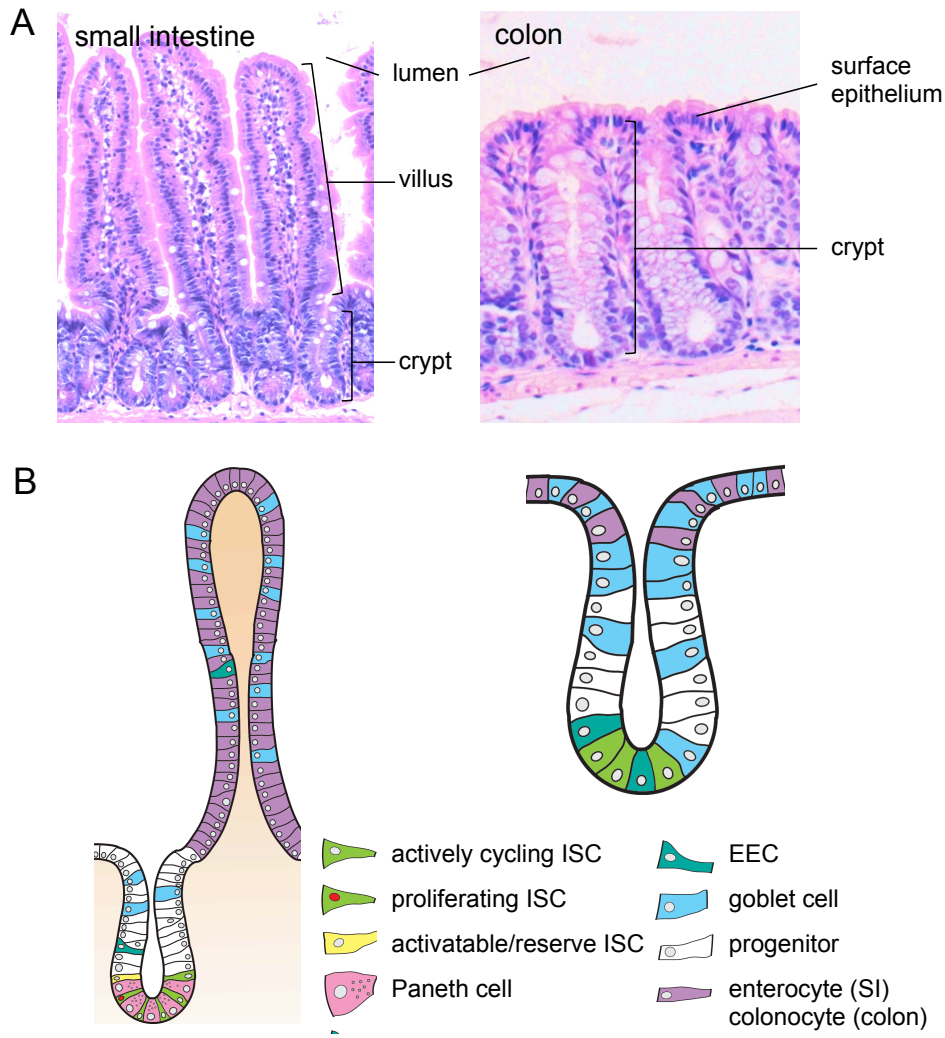

Figure 1.2: Structure and cell types of the small intestinal and colonic epithelium.
(A) Histological sections of the small intestinal and colonic epithelium illustrating morphological differences between regions. The small intestinal (SI) epithelium is organized into crypts and villi, while the colonic epithelium contains crypts and surface epithelium. (B) Schematic of cell types of the small intestinal and colonic epithelium. The small intestinal epithelium is organized into crypts and villi. Crypts contain intestinal stem cells (ISCs) and progenitors, differentiated Paneth cells and cells with enteroendocrine cell (EEC) phenotype located at the position thought to be occupied by activatable/reserve ISC. Villi contain differentiated enterocytes, EEC and goblet cells. The colonic epithelium contains only crypts and surface epithelium, containing colon stem cells, progenitors and differentiated goblet cells, EEC and colonocytes.

Table 1.1: mRNAs or proteins enriched in different small intestinal and colonic epithelial cell types that serve as biomarkers

Intestinal epithelial cell type	Enriched mRNAs or proteins
Actively cycling intestinal stem cell	*Lgr5, Ascl2, Olfm4*
Activatable/Reserve intestinal stem cell	*Bmi1, Lrig1, Hopx*
Progenitors	*Atoh1, Hes1, Ngn3*
Paneth cells	*Lyz, Mmp7, defensins/cryptidins*
Enteroendocrine cells	*Chga, Tac1, Gcg, Cck*
Goblet cells	*Muc2, Tff3*
Enterocytes (Small intestine) Colonocytes (Colon)	Small intestine: *Sim, Alpi, Lct* Colon: *Car1, Car2*

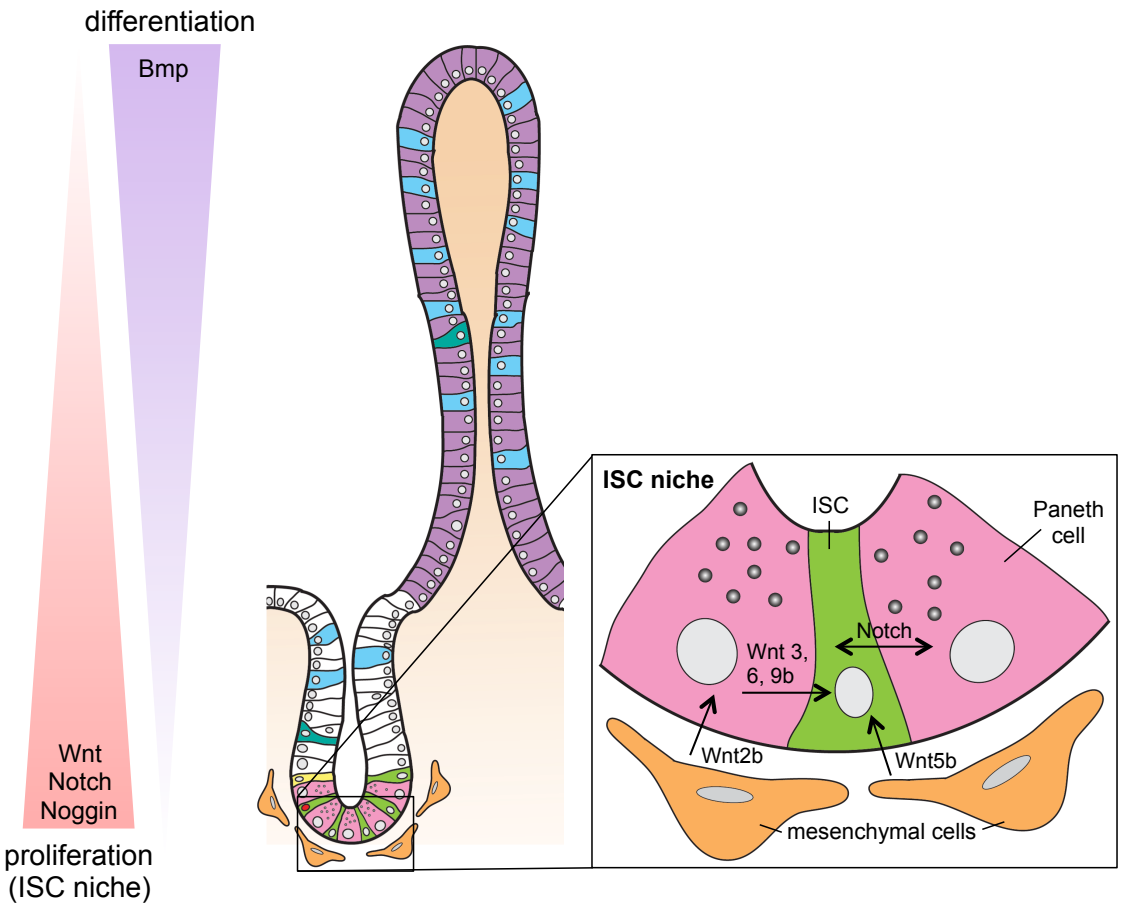

Figure 1.3: Signaling pathways present along crypt/villus axis control ISC maintenance, proliferation and differentiation.
Wnt and Notch activation and Bmp inhibition through Bmp inhibitors such as Noggin are greatest at the crypt base and decreases up the crypt/villus axis. Activation of Wnt, Notch and inhibition of Bmp pathways contribute to the ISC niche required for ISC maintenance, proliferation and differentiation. ISC niche factors including Wnt and Notch ligands are derived from underlying mesenchymal cells and neighboring Paneth cells. Bmp signaling is involved in differentiation and is observed at highest levels at the villus and decreases traveling down to the crypt.

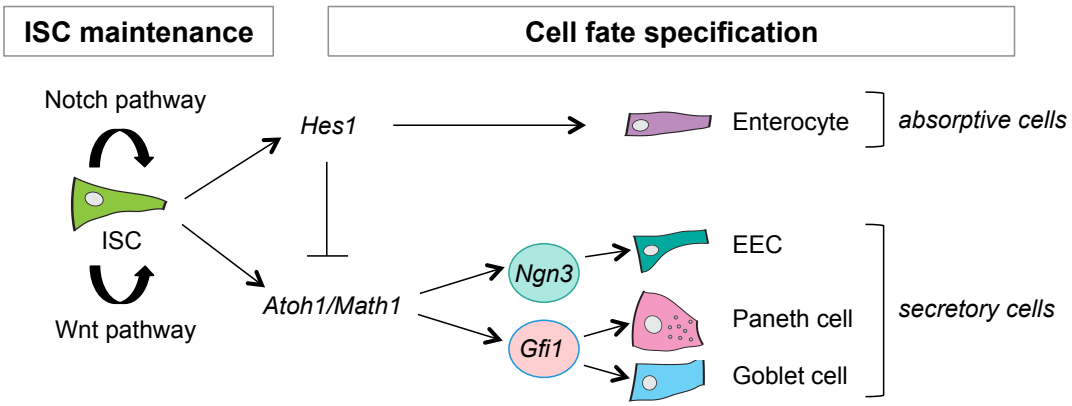

Figure 1.4: Wnt and Notch pathways control ISC maintenance and cell fate specification.
In ISC, Wnt and Notch pathways are required for ISC maintenance and proliferation and cell fate specification. Notch target gene *Hes1* promotes differentiation to enterocyte lineage while suppressing the secretory linage through suppression of *Atoh1/Math1*. Wnt signaling promotes secretory cell fate by increasing transcription of Wnt target gene *Atoh1/Math1*. Lineage specific transcription factors downstream *Atoh1/Math1* further control secretory cell type. *Gfi1* promotes differentiation to Paneth or goblet cell fate while *Ngn3* dictates differentiation to enteroendocrine cells (EEC).

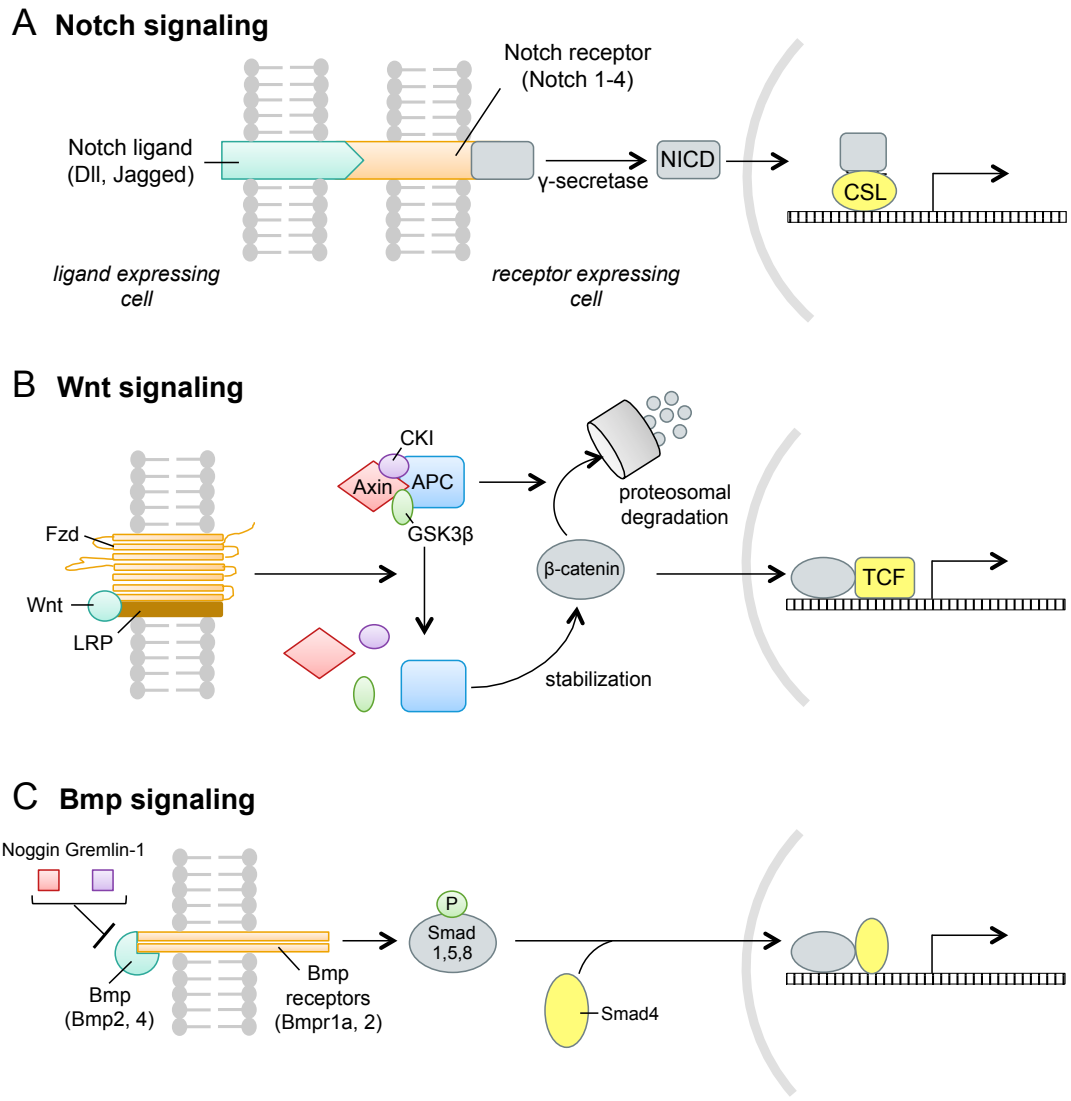

Figure 1.5: Signaling pathways involved in ISC maintenance and cell fate specification.
Notch, Wnt and Bmp signaling act in concert to control ISC maintenance and specification of differentiated lineages. (A) Notch signaling occurs when a Notch ligand binds to a Notch receptor expressed on an adjacent cell. Binding results in cleavage of the Notch intracellular cytoplasmic domain (NICD) by γ-secretase. NICD translocates to the nucleus and binds to the CSL transcription factor to turn on Notch regulated genes. (B) Wnt signaling involves Wnt ligand binding to its receptor consisting of Frizzled (Fzd) and lipoprotein receptor-related protein (LRP) receptors resulting in inhibition of β-catenin degradation. Stabilized cytoplasmic β-catenin travels to the nucleus and binds with the TCF family of transcription factors to increase transcription of Wnt target genes. (C) Bmp ligands bind to membrane bound Bmp receptors leading to phosphorylation of Smad proteins. Phosphorylated Smad proteins bind to Smad4 and travel to the nucleus to regulate gene transcription. Noggin and Gremlin-1 inhibit Bmp signaling by blocking binding of Bmp ligands to receptors. Adapted from (178)

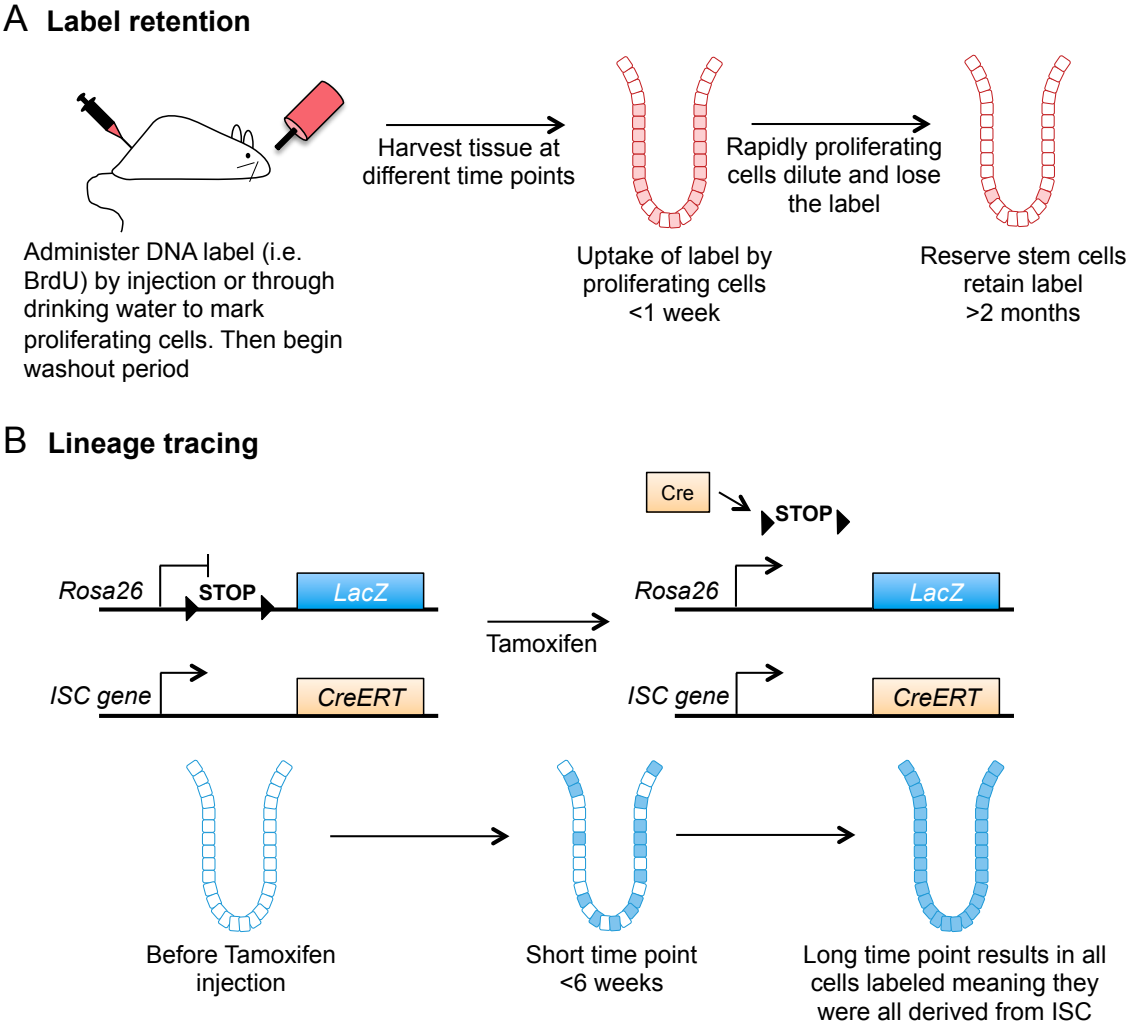

Figure 1.6: Methods for identifying stem cells.
(A) Label retention methods are used to identify slowly cycling reserve stem cells by administration of a DNA label to mark all proliferating cells followed by a washout period. Highly proliferative cells will divide and dilute out the label while slowly cycling stem cells will retain the label and can be visualized by histological methods. (B) Lineage tracing methods to identify stem cells require a inducible CreERT element downstream the promoter of the gene of interest crossed with a reporter mouse. Tamoxifen administration will result in removal of the transcriptional stop sites flanked by loxP sites (filled triangles) by Cre recombinase permanently turning on reporter expression in cells expressing the gene of interest. All progeny will inherit the reporter mark resulting in ribbons of labeled cells, indicating they were originally derived from a stem cell. Adapted from (179)

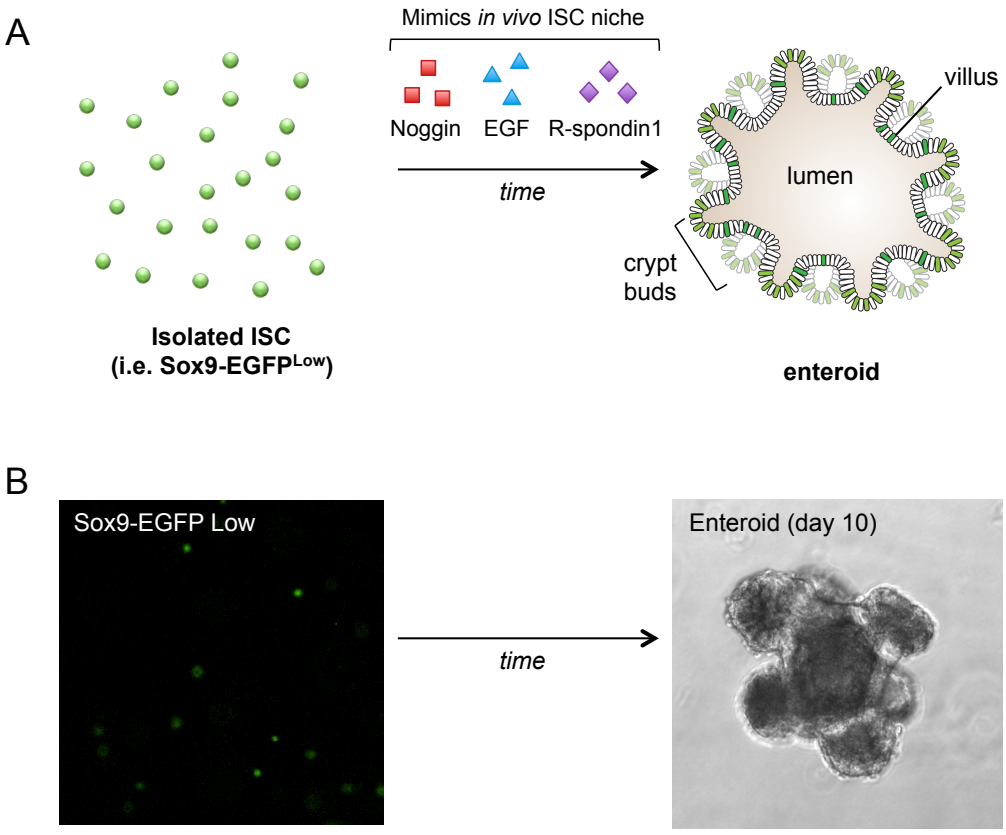

Figure 1.7: Isolated ISCs form enteroids with time *in vitro*.
(A) Schematic showing isolated ISC from reporter models such as the Sox9-EGFP mouse model can be grown *in vitro* using a Matrigel-based culture system supplemented with factors that mimic the ISC niche developed by (53). In time, isolated ISC will form enteroids complete with crypt buds and a lumen, and all differentiated cell types. (B) Isolated Sox9-EGFP Low ISCs are able to be grown in this culture system (adapted by (57)) to yields enteroids with crypt buds, lumen and differentiated cell types, indicating intrinsic function and stemness ability.

Table 1.2: Summary of select ISC reporter mouse models

Marker	ISC population	Mouse model	Type of genomic integration	Linage tracing
Sox9	Low: CBC ISC High: +4/reserve ISC	Sox9-EGFP	BAC transgenic (random integration)	No
Lgr5	CBC ISC	Lgr5-EGFP-IRES-CreERT2 Lgr5-lacZ	Knock-in (targeted integration)	Yes
Olfm4	CBC ISC	Olfm4-IRES-EGFPCreERT2	Knock-in (targeted integration)	Yes
Bmi1	+4/reserve ISC	Bmi1-IRES-CreERT2 Bmi1-EGFP	Knock-in (targeted integration)	Yes
Hopx	+4/reserve ISC	Hopx-IRES-CreERT2 Hopx-EGFP	Knock-in (targeted integration)	Yes
Lrig1	+4/reserve ISC	Lrig1-IRES-CreERT2	Knock-in (targeted integration)	Yes

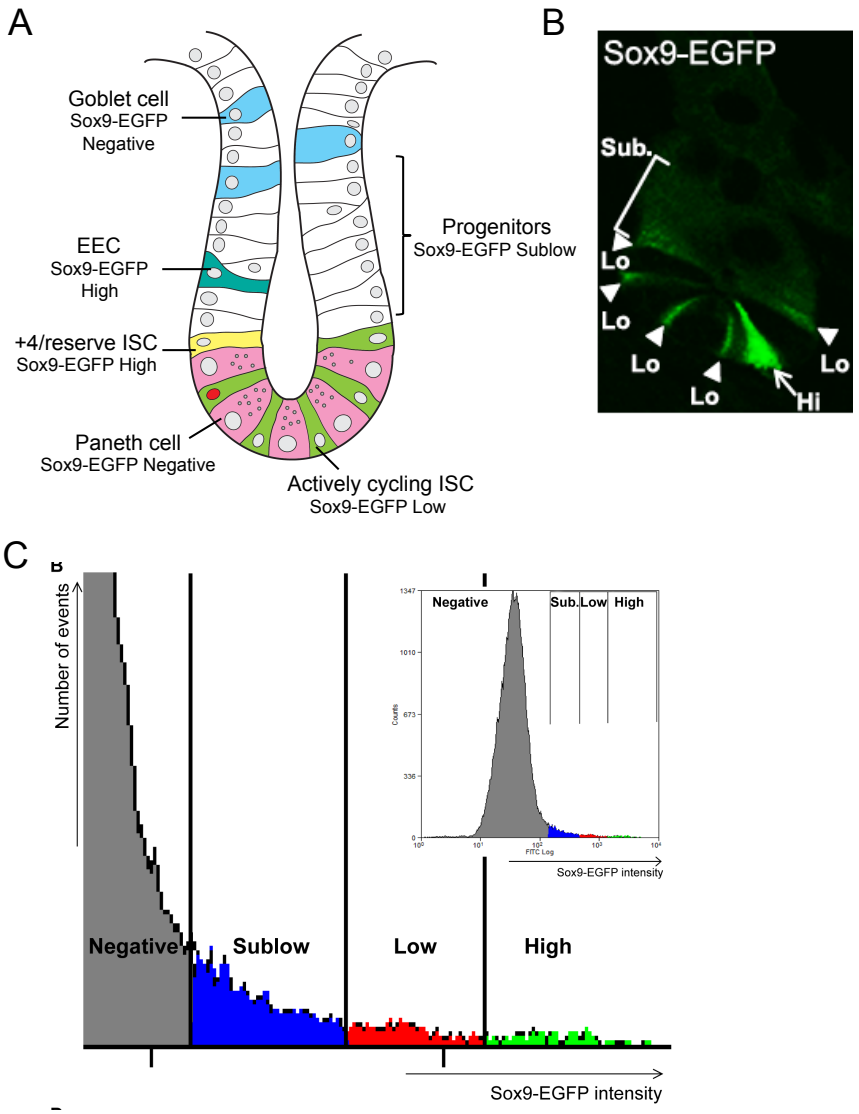

Figure 1.8: Sox9-EGFP reporter gene expression marks different intestinal epithelial cell populations. Sox9-EGFP reporter mouse is a transgenic mouse model expressing a Sox9-EGFP bacterial artificial chromosome (BAC) transgene where large amounts of *Sox9* genomic regulatory sequences regulate EGFP expression. A-B: Different cell types express High, Low, Sublow or no detectable EGFP levels as indicated in the schematic (A) and by immunofluorescence for EGFP (B; Sub: Sublow, Lo: Low, Hi: High). (C) Flow cytometry plot illustrating Sox9-EGFP cell populations can be distinguished by EGFP intensity and used for quantification or isolation by fluorescence activated cell sorting (FACS). Images from (B) and (C) from (13)

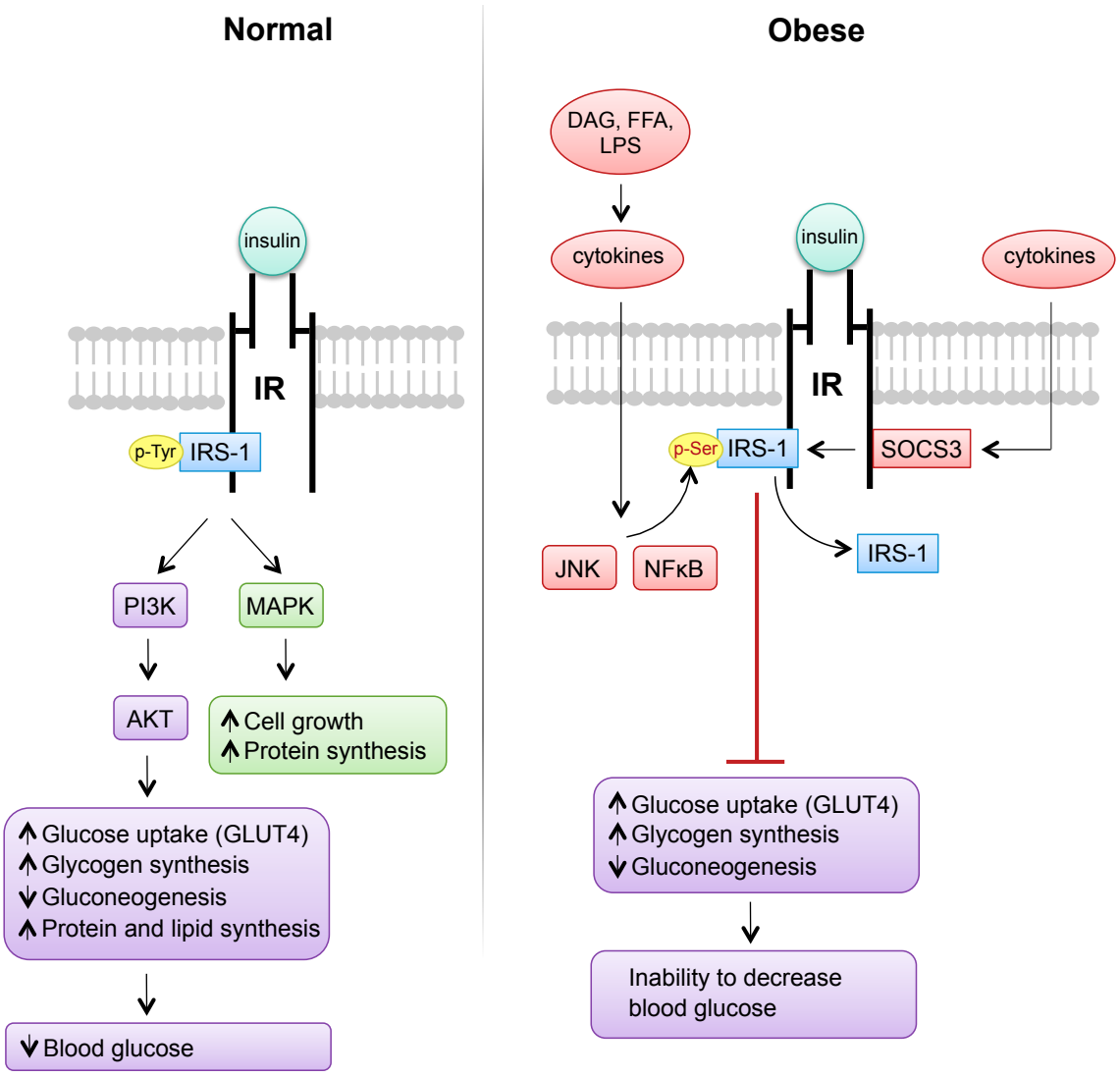

Figure 1.9: Insulin signaling in normal and obese states.
Under normal conditions, insulin signaling begins with insulin binding to and activating insulin receptor (IR) leading to tyrosine phosphorylation of insulin receptor substrate 1 (IRS-1). IRS-1 mediated PI3K/AKT activation results in increased glucose uptake, glycogen, protein and lipid synthesis and decreased gluconeogenesis to lower postprandial blood glucose. IRS-1 can also activate the MAP kinase pathway via MAPK to promote cell growth and protein synthesis. Obesity has been linked to impaired insulin signaling. Increased inflammatory cytokines, and factors promoting increased cytokines such as free fatty acids (FFA) and diacylglycerol (DAG) and lipopolysaccharide (LPS) activate inflammatory JNK and NFκB pathways leading to inactivating serine phosphorylation of IRS-1. Inflammatory cytokines also increase suppressors of cytokine signaling-3 (SOCS3), which binds to IR preventing IRS-1 binding. The lipogenic effects of insulin and preserved during obesity.

Table 1.3: Effects of alternate day fasting (ADF) on fasting glucose, insulin and IGF1 levels in animals

				Fasting levels		
Study	**Animals (Age)**	**Duration**	**Weight change**	**Glucose**	**Insulin**	**IGF1**
Anson et al 2003	C57Bl6 (8 wks)	20 wks	None	Decrease*	Decrease*	Increase*
Wan et al 2003	Sprague-Dawley rats (12 wks)	24 wks	Decrease*	Decrease*	Decrease*	Decrease*
Varady et al 2007	C57Bl6 (7 wks)	4 wks	Decrease*	-	-	Decrease*
Varady et al 2008	C57Bl6 (7 wks)	4 wks (85% ADF)	None	-	-	Decrease*
Varady et al 2009	C57Bl6 (8 wks)	4 wks	None	-	-	Decrease*

*vs. controls at end of study

Table 1.4: Effects of alternate day fasting (ADF) on fasting glucose and insulin in humans

				Fasting levels	
Study	**Subjects**	**Duration**	**Weight change**	**Glucose**	**Insulin**
Heilbronn et al 2005	Both sexes, 20-55yrs, normal weight	3 weeks	Decrease**	No change	Decrease**
Halberg et al 2005	Males, 25rs, normal weight	2 weeks	No change	No change	No change
Varady et al 2009	Both sexes, 45 yrs, obese	8 weeks (75% ADF)	Decrease**	Decrease**	Decrease**
Klempel et al 2013	Females, 40yrs, obese	8 weeks (75% ADF)	Decrease**	No change	No change
Varady et al 2012	Both sexes, 45yrs, normal and overweight	12 weeks (75% ADF)	Decrease*	Decrease*	Decrease*

*vs. controls at end of study; **vs. baseline at end of study

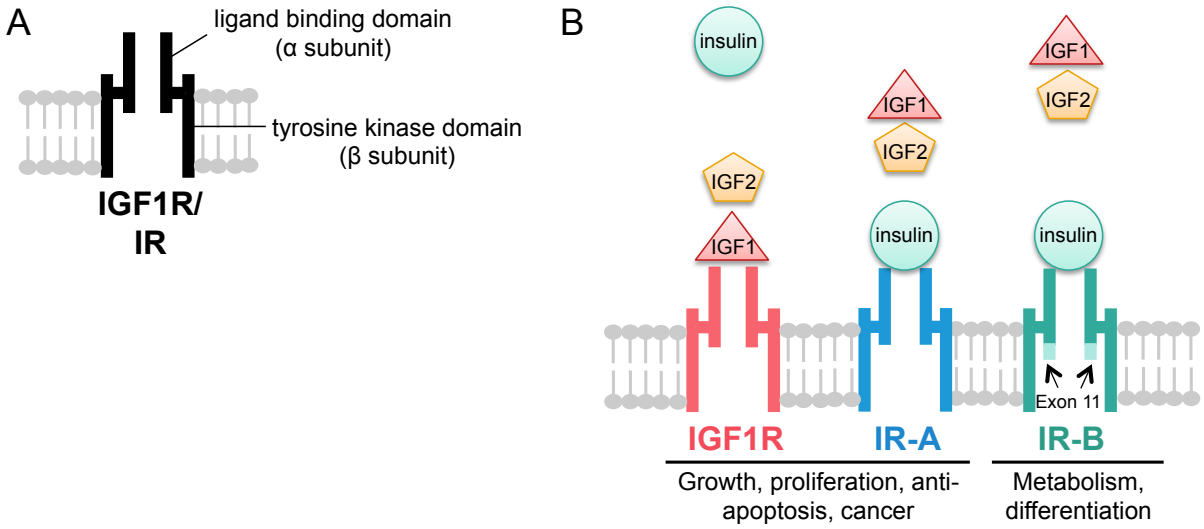

Figure 1.10: IR and IGF1R are tyrosine kinase receptors involved in growth and metabolism
(A) The insulin-like growth factor (IGF1R) and insulin receptor (IR) are highly homologous tyrosine kinase receptors that are composed of an extracellular α subunit where ligand binding occurs and a transmembrane β subunit with tyrosine kinase activity. (B) The insulin/IGF pathway consists of the ligands IGF1, IGF2 and insulin and the receptors IGF1R and two insulin receptor isoforms, IR-A and IR-B. Ligands bind to receptors at differing affinities to mediate growth, proliferation and anti-apoptosis (IGF1R, IR-A) or differentiation and metabolism (IR-B). The proximity of ligands to receptors indicates affinity. Modified from (129)

Table 1.5: Tissue specific effects of insulin by macronutrient

Macronutrient	Tissue	Pathway
Carbohydrate (glucose)	Liver	*Promote glycogen synthesis* *Inhibit gluconeogenesis*
	Adipose tissue	*Promote glucose uptake and glycolysis*
	Skeletal muscle	*Promote glucose uptake and glycolysis*
Fat (fatty acids)	Adipose tissue	*Promotes triglyceride synthesis and storage* *Inhibits lipolysis*
Protein (amino acids)	Liver	*Promotes protein synthesis*
	Skeletal muscle	*Promotes protein synthesis*

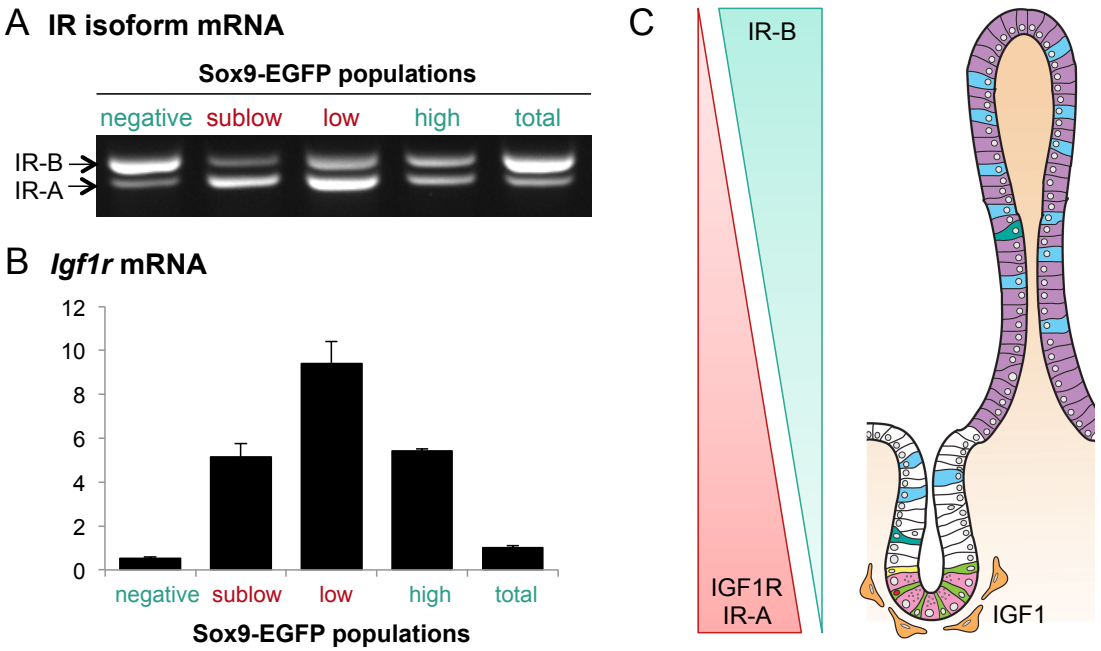

Figure 1.11: Differential expression of the insulin/IGF1 pathway in the intestine.
Evaluation of IR-A, IR-B and *Igf1r* mRNA in Sox9-EGFP sorted cell populations reveals distinct expression differences in specific intestinal epithelial cell types. (A) RT-PCR for IR isoform expression show proliferative progenitors and ISCs (red; Sox9-EGFP Sublow and Sox9-EGFP Low) express predominantly IR-A, while differentiated cells (green; Sox9-EGFP Negative) express greater IR-B levels. Total cells are non-sorted intestinal epithelial cells, which are >90% differentiated enterocytes and therefore express predominantly IR-B. Sox9-EGFP High cells contain both differentiated EEC and slowly cycling reserve ISC and express equal levels of both IR isoforms. (B) qRTPCR on *Igf1r* mRNA in Sox9-EGFP sorted cells reveal enrichment of *Igf1r* in Sox9-EGFP Low ISC and low levels expressed in differentiated Sox9-EGFP Negative cells and total cells. (C) Our data provides a model where IR-A, IR-B and *Igf1r* expression exist in a gradient along the crypt/villus axis. *Igf1r* and IR-A predominate in the proliferative crypts while IR-B is highest in differentiated villi, consistent with known functions of all three receptors. IGF1 produced and secreted by surrounding mesenchymal cells while insulin and IGF1 circulate in the bloodstream (not shown) and can act on the epithelium via its receptors.

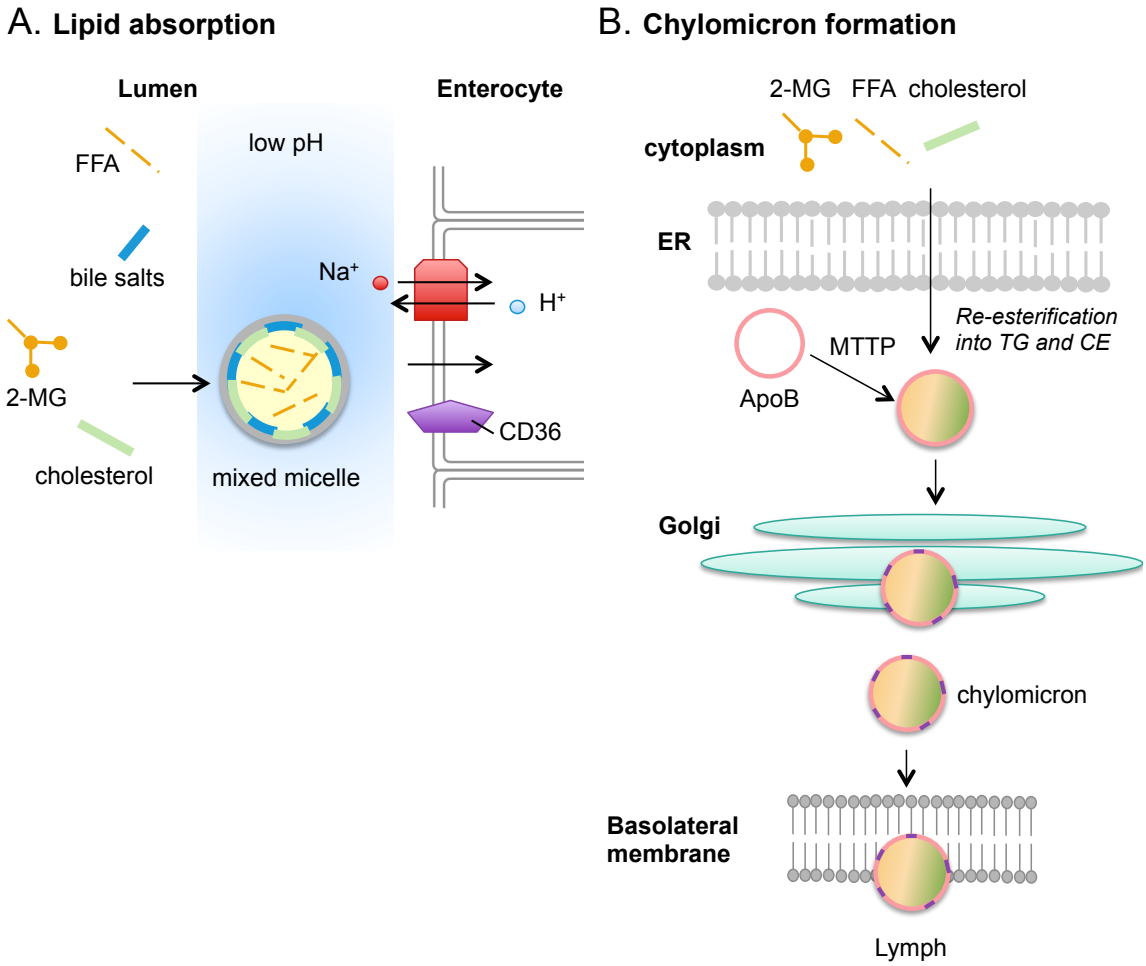

Figure 1.12: Lipids are absorbed by small intestinal enterocytes and repackaged into chylomicrons for distribution to peripheral tissues.
(A) Lipids are digested into 2-monoacylglycerol (2-MG) and free fatty acids (FFA). FFA and 2-MG combine with bile salts and cholesterol to form mixed micelles prior to absorption. Micelles enter enterocytes by diffusion due to an acidic environment or via membrane bound transporter CD36. (B) In enterocytes, FFA and 2-MG are re-esterified to triglycerides (TG) and cholesterol into cholesterol esters (CE) in the endoplasmic reticulum (ER), combine with apolipoproteins in the Golgi apparatus to form chylomicrons. Chylomicrons exit into the lymphatic system to deliver lipids to the venous circulation and peripheral tissues. Adapted from (180).

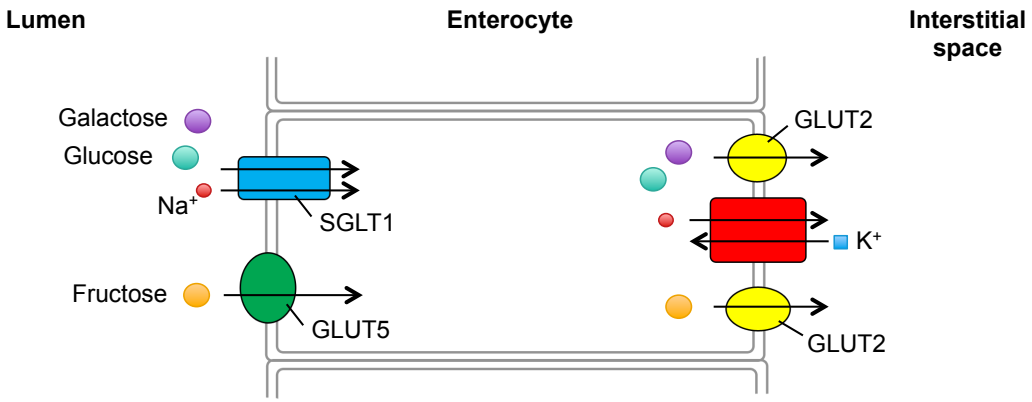

Figure 1.13: Carbohydrate absorption by enterocytes.
Carbohydrates are enzymatically digested into galactose, glucose and fructose prior to absorption through enterocytes. Glucose and galactose absorption is coupled with sodium via the sodium glucose transporter 1 (SGLT1). Fructose absorption occurs through GLUT5. Once inside the cell, all three exist via GLUT2 located on the basolateral membrane while sodium exits by sodium-potassium pump into the interstitial space and then bloodstream. Adapted from (180).

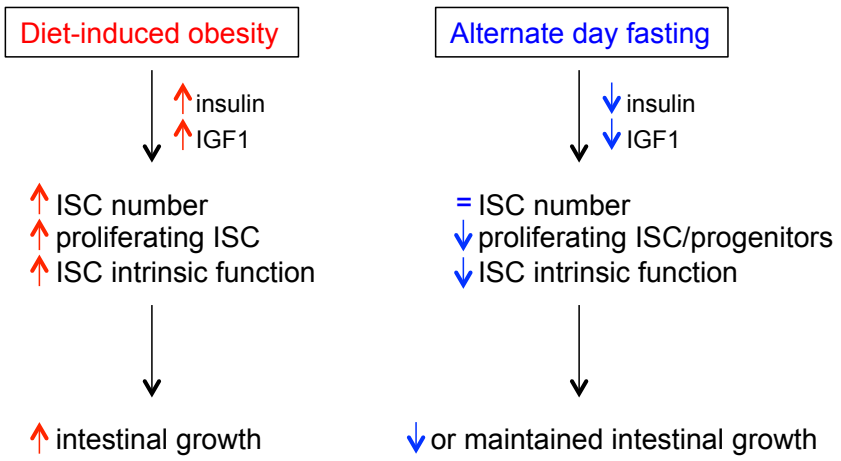

Figure 1.14: Intestinal adaptation to obesity and alternate day fasting involves changes in ISC number, proliferation and function.
The central hypothesis of the following dissertation is that diet-induced obesity, associated hyperinsulinemia and elevated IGF1 levels will increase intestinal stem cell (ISC) number, proliferation and intrinsic function to increase intestinal epithelial growth during hypercaloric conditions, while alternate day fasting, a diet producing similar benefits as calorie restriction, will lead to decreased insulin and IGF1 levels. We hypothesize alternate day fasting will preserve ISC number but decrease ISC or progenitor proliferation and ISC intrinsic function in order to decrease or maintain intestinal epithelial growth.

CHAPTER 2: IMPACT OF DIET-INDUCED OBESITY ON INTESTINAL STEM CELLS: HYPERPROLIFERATION BUT IMPAIRED INTRINSIC FUNCTION THAT REQUIRES INSULIN/IGF1[1]

Introduction

The functional consequences of obesity have been extensively studied in liver, skeletal muscle and adipose tissue, but much less is known about the effect of obesity on the intestinal epithelium, the initial site of nutrient absorption. The highly proliferative small intestinal epithelium is composed of crypts, containing proliferating cells, terminally differentiated Paneth cells and some goblet and enteroendocrine cells (EEC), and villi composed of primarily post-mitotic differentiated enterocytes, but also goblet cells and EEC. The small intestinal epithelium is renewed every 3-7 days depending on the species and region. Constant renewal involves proliferation of intestinal stem cells (ISC), which reside at the crypt base. ISC give rise to more actively dividing progenitors, also termed transit-amplifying cells, which differentiate into post-mitotic lineages as they exit the crypts, or migrate to the crypt base (1,181,182). Intestinal epithelial homeostasis is dependent on a tightly regulated balance between ISC and progenitor proliferation, differentiation and the constant loss of differentiated cells at the villus tip.

The small intestinal epithelium is highly responsive to changes in nutrient intake or exposure to luminal nutrient. In rodents, fasting or total parenteral nutrition (TPN) leads to rapid reductions in small intestinal epithelial mass, associated with reduced proliferation in the crypts and increased apoptosis in crypts and villi (170-175). This is a logical physiological adaptation to a reduced need for nutrient absorption. In duodenum and jejunum and to a lesser extent ileum, refeeding can rapidly reverse the fasting-induced atrophy of the epithelium. Until recently, it was not possible to directly assess impact of nutrient status on ISC. Since landmark studies in 2007, Lgr5 and multiple other proteins have been identified as biomarkers of actively cycling ISC (also termed crypt based columnar cells, CBC) (3,58). Development of transgenic reporter mice expressing fluorescent proteins downstream of the promoters driving ISC biomarker expression has permitted direct evaluation of ISC *in vivo* (3,56) and isolation and assessment of ISC intrinsic function *in vitro*. In 3D culture systems, ISC develop into spherical

[1] This chapter previously appeared in *Endocrinology*. The original citation is as follows: Mah AT, Van Landeghem L, Gavin HE, Magness ST, Lund PK. (2014) Impact of diet-induced obesity on intestinal stem cells: hyperproliferation but impaired intrinsic function that requires insulin/IGF1 *Endocrinology*.Sep;155(9):3302-14.

structures termed enterospheres that are composed of multiple cells, reflecting ISC survival and proliferation. With increased time in culture, enterospheres grow and form more complex structures termed enteroids that show a lumen, crypt buds and contain ISC and all differentiated lineages (54). Enterosphere and enteroid yield from isolated ISC is a useful measure of ISC survival and growth capacity. A recent study using Lgr5 reporter mice demonstrated that long-term calorie restriction (CR) reduced villus height and proliferation of progenitors but increased both numbers and proliferation of ISC (121). CR also enhanced the ability of isolated ISC to survive, grow and yield enteroids (121). The ability of CR to enhance ISC number and function was linked to diminished mTORC signaling in Paneth cells, neighboring niche cells that provide trophic support to ISC (54). Other studies performed in *Drosophila* demonstrated that fasting decreased ISC number, which was restored upon refeeding (176,177), strengthening the concept that ISC respond and adapt to altered nutrient availability. Compared with fasting, the impact of over-nutrition as seen in diet-induced obesity (DIO) has not been as extensively studied. Depending on the model and duration of obesogenic diet, DIO has been linked to altered crypt-villus homeostasis, particularly increased villus height but variable effects on crypt cell proliferation (70,96,183). Importantly, the impact of DIO specifically on ISC is not defined.

In this study, we sought to define the effects of DIO, specifically on ISC using the Sox9-EGFP reporter mouse model. In the intestine of this model, different expression levels of the Sox9-EGFP transgene mark different intestinal epithelial cell types (56,57). The highest expression levels of Sox9-EGFP (Sox9-EGFP High) are found in cells co-expressing or enriched for EEC markers and *Bmi1*, *Hopx* and *Dcamkl1*, markers linked to a 'reserve' population of cells that can function as ISC in some situations (5,6,13,184). Lower Sox9-EGFP expression marks cells that have been termed Sox9-EGFP Low ISC because they are highly enriched for *Lgr5* and other biomarkers of actively cycling ISC and are capable of self-renewal and multipotency *in vivo* and *in vitro* (13,56,57,185). In healthy, *ad libitum* fed Sox9-EGFP mice, only Sox9-EGFP Low cells can survive and form enteroids in 3D culture. Sublow EGFP expression (Sox9-EGFP Sublow) mark progenitors, and cells negative for EGFP (Sox9-EGFP Negative) correspond to enterocytes, Paneth and goblet cells based on enrichment of markers of these differentiated cells (13,56,57). This model therefore permits us to test the impact of dietary interventions on Sox9-EGFP Low ISC and also on the other cell populations expressing different levels of Sox9-EGFP. Our study tested the hypothesis that DIO promotes ISC proliferation and expansion to increase small intestinal epithelial mass.

It is well established that changes in crypt cell proliferation and intestinal mass induced by fasting and refeeding correlate with changes in circulating insulin-like growth factor 1 (IGF1) and local intestinal expression of *Igf1* that derives from the pericryptal mesenchyme (175). Enterotrophic effects of IGF1 have been demonstrated and IGF1 is able to prevent atrophy of the small intestinal epithelium induced by TPN (141). Since DIO due to long-term high fat diet (HFD) promotes insulin resistance associated with elevated circulating insulin (76) and increased free IGF1 in the circulation (166,186), we examined whether DIO-induced changes in ISC correlated with plasma insulin or IGF1 and whether ISC from DIO mice showed altered responsiveness to insulin or IGF1 *in vitro*.

Results

Diet-induced obesity in Sox9-EGFP mice

Sox9-EGFP mice were fed a low fat standard chow or HFD for 20 weeks to induce DIO. Male and female mice responded similarly to HFD feeding and were combined in all analyses. Sox9-EGFP mice fed HFD showed significantly higher body weight by 7 weeks on diet (+24 ± 5%). This effect was maintained and more dramatic (+38 ± 5%) by 20 weeks on diet (Figure 2.1a) and accompanied by an increase in percent fat mass and a decrease in percent lean mass (Figure 2.1b). Following 20 weeks on diet, DIO mice exhibited elevated plasma glucose, insulin and IGF1 (Figures 2.1c-e). DIO mice also exhibited significantly higher jejunal *Igf1* mRNA levels (Figure 2.1f).

Impact of DIO on small intestine weight, length and jejunal crypt and villus morphometry

As shown in Table 2.1, DIO resulted in a small but significant decrease in intestinal length and a non-significant trend for decreased overall intestinal weight so that weight per unit length did not change significantly. Crypt-villus morphometry was measured in jejunum, a major region of nutrient absorption. Villus height was increased in DIO mice (+18 ± 7%; Figure 2.2a-b). Crypt depth did not differ between DIO and controls, but crypt density was significantly increased in DIO mice (+12 ± 4%; Figure 2.2a, c), indicating an increase in the number of crypts feeding onto the heightened villi. Percentage of fissioning crypts was similar in DIO and controls.

DIO selectively increases number of ISC and ISC in S-phase

Total number of cells per crypt section and total number of cells labeled with the S-phase marker EdU per crypt section did not differ in DIO mice *versus* controls (Figure 2.2d-e). We used the Sox9-EGFP reporter mouse to assess if DIO affected numbers of Sox9-EGFP Low ISC or crypt-based Sox9-EGFP High cells that express the EEC marker Chromogranin A (ChgA), but also contain a population of 'reserve' ISC-like cells activated to proliferate after injury (13). Sox9-EGFP High cells were distinguished from Sox9-EGFP Low cells by both high intensity of

EGFP and ChgA expression (Figure 2.2f). As shown in Figures 2F and 2G, there was a small but significant increase in the number of Sox9-EGFP Low ISC but not Sox9-EGFP High cells per crypt section. Co-labeling with EdU was used to quantify the numbers of Sox9-EGFP Low and Sox9-EGFP High cells in S-phase. DIO resulted in a significant increase in the percentage of Sox9-EGFP Low ISC co-labeled with EdU, but no significant change in the proportion of Sox9-EGFP High EdU positive cells per crypt section (Figure 2.2h-i). While the total numbers of Sox9-EGFP Low cells per crypt section were increased by 25 ± 6.0%, there was a greater increase in the number of EdU positive Sox9-EGFP Low cells per crypt section (+48.1 ± 19.3%) indicative of ISC hyperproliferation and/or altered cell cycle time. Flow cytometry, performed as an independent measure of the proportion of Sox9-EGFP Low ISC in entire jejunum of control and DIO mice, revealed a significant increase in the percentage of Sox9-EGFP Low ISC in DIO mice compared to controls (Figure 2.2j). Collectively, the morphometry, histology and flow cytometry data demonstrate that DIO results in increased total numbers of Sox9-EGFP Low ISC and percentage of ISC in S-phase, which may be required to support the increased crypt density and villus height even though total numbers of cells per crypt are unchanged.

DIO mice have decreased numbers of Paneth and goblet cells

To evaluate if increased villus height and increased ISC proliferation in DIO mice were associated with changes in differentiated lineages, we compared numbers of Paneth, goblet and EEC in DIO mice *versus* controls. Quantification of lysozyme positive cells revealed a 25.7 ± 3.1% decrease in the number of Paneth cells per crypt section in DIO mice compared to controls (Figure 2.3a-b). Mucin2 staining revealed that numbers of goblet cells were significantly decreased in DIO mice in both crypts (-33.6 ± 4.6%) and villi (-24.4 ± 4.6%) compared to controls (Figure 2.3c-d). EEC number evaluated by the number of ChgA positive cells revealed no differences between control and DIO mice in either crypt or villus (Figure 2.3e-f). Taken together, these data suggest DIO mice exhibit significantly reduced numbers of Paneth and goblet cells and no change in EEC, providing indirect evidence that the increased villus height likely involves increased number or size of enterocytes, the other major differentiated villus lineage.

Sox9-EGFP Low ISC isolated from DIO mice have reduced ability to form enterospheres and enteroids in culture

ISC were isolated by FACS using dispersed epithelial preparations from control and DIO Sox9-EGFP reporter mice. High throughput qRTPCR on isolated Sox9-EGFP cell populations demonstrated an appropriate and similar gradient

of EGFP and *Sox9* mRNA across the sorted cell populations from control and DIO mice (Figure 2.4a-b). Sox9-EGFP High cells were enriched for mRNAs encoding EEC marker *Chga* and 'reserve' ISC marker *Hopx* (Figure 2.4c-d) and Sox9-EGFP Negative cells were enriched in *Lct* mRNA, a brush border enzyme expressed by absorptive enterocytes (Figure 2.4e). Importantly, Sox9-EGFP Low cells isolated from both control and DIO mice were both similarly enriched for the mRNA encoding the ISC marker *Lgr5* (Figure 2.4f). Consistent with selective hyperproliferation of ISC in DIO mice observed by histology and EdU, Cyclin D1 (*Ccnd1*) mRNA was increased only in Sox9-EGFP Low cells from DIO mice versus control and not in any other cell population (Figure 2.4g).

To assess whether the *in vivo* increase in Sox9-EGFP Low ISC proliferation in DIO mice translated to increased intrinsic ISC function, we compared the ability of Sox9-EGFP Low cells isolated from DIO and control mice to survive, expand and form enterospheres/enteroids in 3D culture. In this *in vitro* assay, low density ISC are plated at day 0 and the number of structures formed are counted every other day for 12 days. Because of low-density plating, enterosphere/enteroids derive primarily from single ISC. This assay is a useful *in vitro* readout for intrinsic function of stem cells in terms of survival and growth. In addition to Sox9-EGFP Low cells, we also tested Sox9-EGFP High, Sox9-EGFP Sublow and Sox9-EGFP Negative cells to establish if DIO altered 'stemness' in populations other than actively cycling Sox9-EGFP Low ISC. Consistent with previous findings in chow fed mice, Sox9-EGFP Negative, Sox9-EGFP Sublow and Sox9-EGFP High cells from control mice did not survive or expand to form enterospheres/enteroids, and this was also the case in DIO mice (data not shown). Sox9-EGFP Low ISC isolated from both control and DIO mice were able to survive and form enterospheres/enteroids in 3D culture (Figure 2.5a). Enterospheres were quantified starting at day 4 when these structures are large enough to count reliably. No significant difference was seen in the percentage of enterospheres formed from Sox9-EGFP Low ISC isolated from DIO or control mice at day 4-post plating, although there was a trend for lower numbers in DIO mice (Figure 2.5b). By day 6 post plating, Sox9-EGFP Low ISC isolated from DIO mice yielded fewer enteroids than controls and numbers of enteroids formed from DIO ISC remained significantly lower until the end of the culture at day 12 post plating (Figure 2.5b). While sizes of 3D enteroids are difficult to quantify, qualitative evaluation indicated a reduced size of enterospheres/enteroids formed from ISC isolated from DIO mice versus controls as shown in the examples in Figure 2.5a. These data indicate that despite increased numbers and proliferation of ISC in DIO mice *in vivo*, the intrinsic *in vitro* survival and growth capabilities of ISC isolated from DIO mice are impaired relative to ISC isolated from controls. This provides novel evidence that DIO alters ISC intrinsic function.

Insulin and/or IGF1 treatment rescues functional defect of ISC isolated from DIO mice

DIO mice are hyperinsulinemic, display elevated plasma IGF1 levels (Figures 1D and 1E), and have significantly higher local intestinal *Igf1* mRNA expression (Figure 2.1f). Additionally, plasma insulin levels were found to be positively and significantly correlated with abundance of Sox9-EGFP Low ISC evaluated by flow cytometry in the same animals (Figure 2.6a). We therefore hypothesized that the reduced *in vitro* survival and growth of ISC from DIO mice might reflect an acquired dependence on elevated insulin or IGF1. To test whether the decrease in enterosphere/enteroid formation seen in ISC from DIO mice could be rescued by supplementation of cultures with insulin and/or IGF1, isolated ISC from control and DIO mice were treated with standard growth factor conditions (EGF, Noggin and R-Spondin 1) alone or plus insulin, IGF1 or insulin and IGF1 combined. Consistent with prior results (Figure 2.5), in this independent series of experiments, Sox9-EGFP Low ISC from DIO mice formed fewer enteroids than controls when plated in standard growth factor conditions alone (Figure 2.6b). Neither insulin, IGF1 nor both affected enteroid yield from ISC isolated from control mice. In contrast, insulin, IGF1 or insulin and IGF1 combined resulted in a significant >3-fold increase in the number of enteroids formed from Sox9-EGFP Low ISC isolated from DIO mice (Figure 2.6b) compared to ISC from DIO mice cultured in standard growth factor conditions. In fact, the mean number of enteroids formed from IGF1 treated ISC from DIO mice significantly exceeded the number formed from ISC of control mice cultured under standard GF conditions ($p<0.05$) and a similar trend was observed in DIO ISC treated with insulin ($p=0.07$) or insulin and IGF1 ($p=0.17$) (Figure 2.6b). Insulin, IGF1 or both therefore 'rescued' the defect in survival and growth of DIO ISC. qRTPCR on FACS isolated Sox9-EGFP Low ISC and other populations revealed that IGF1 receptor (*Igf1r*) mRNA was significantly enriched in Sox9-EGFP Low ISC, suggesting that ISC may be particularly responsive to IGF1 (Figure 2.6c). In contrast, *Ir* mRNA was significantly enriched in Sox9-EGFP High cells (Figure 2.6d). However neither levels of *Igf1r* mRNA nor *Ir* mRNA differed in Sox9-EGFP Low ISC isolated from DIO versus control mice suggesting that receptor down-regulation, at least at the mRNA level, did not accompany differences in enteroid forming ability or dependence on exogenous insulin/IGF1 in isolated ISC from DIO mice. Our prior studies demonstrated that IR isoform A (IR-A), a receptor that can mediate proliferative actions of insulin or IGFs, is the predominant IR isoform in Sox9-EGFP Low ISC compared to the metabolic IR-B isoform (139). We performed RT-PCR to evaluate if DIO resulted in changes in relative proportions of the two IR isoforms. We found no significant changes in relative expression of the two isoforms, with IR-A being expressed at >2 fold the levels of IR-B in ISC from control and

DIO mice. (Figure 2.6e-f). Thus, ISC from DIO mice require the presence of elevated insulin and/or IGF1 to maintain their intrinsic function *in vitro* but this does not reflect reduced levels of either *Igf1r* or *Ir* at least at the level of mRNA expression. Wnt signaling is a key pathway involved in ISC function. We therefore assessed levels of two known Wnt targets, *Myc* and *Axin2* in Sox9-EGFP Low ISC isolated from DIO and control mice. Both *Myc* and *Axin2* mRNAs were significantly lower in ISC isolated from DIO mice compared to controls (-20.5 ± 8.5% and -24.4 ± 9.3%, respectively). Decreased Wnt activation in ISC isolated from DIO mice could therefore contribute to their reduced enteroid forming ability.

Discussion

In this study, we used the Sox9-EGFP reporter model to directly examine the impact of DIO due to chronic HFD exposure on Sox9-EGFP Low ISC, which share a similar gene signature to actively cycling $Lgr5^{+}$ ISC (13) and are able to survive and form enteroids in culture (57). We provide new evidence that DIO leads to increased numbers of jejunal Sox9-EGFP Low ISC, increased ISC proliferation as measured by EdU and increased expression of *Ccnd1* mRNA specifically in Sox9-EGFP Low ISC, but does not affect total crypt cell number, crypt depth or total EdU positive cells per crypt. DIO was associated with increased crypt density and villus height, supporting a model whereby the increased numbers of ISC and ISC in S-phase support the increased number of crypts which in turn feed cells onto longer villi as an adaptation to hypercaloric load (Figure 2.7).

Our results are consistent with recent findings that report increases in villus height and numbers of Ki67 or BrdU positive cells per crypt with long-term HFD feeding (70,96). However our study provides, to our knowledge, the first evidence that DIO preferentially expands and promotes proliferation of Sox9-EGFP Low ISC. Our prior studies on Sox9-EGFP High cells, which are enriched for EEC markers (13), and evidence from the literature indicate that a subpopulation of secretory cells, EEC or Paneth cells or their immediate progenitors can be activated to proliferate and adopt a stem cell phenotype upon injury (12,13). Our findings indicate that DIO does not increase EdU positive Sox9-EGFP High cells and that Sox9-EGFP High cells from DIO mice do not acquire the ability to generate enterospheres/enteroids in culture suggesting that in contrast to injury models, DIO does not activate Sox9-EGFP High cells to expand, proliferate or adopt functional characteristics of stem cells. Thus DIO selectively promotes hyperproliferation of the more actively cycling Sox9-EGFP Low ISC.

Our findings show that concomitant with increased villus height and ISC hyperproliferation, DIO mice have reduced numbers of Paneth cells in crypts, reduced goblet cells on crypts and villi and no change in EEC

suggesting that increased villus height likely reflects increased numbers or size of absorptive enterocytes. Other studies have reported reduced goblet cells in obese mice (66,92), while some reports have suggested changes in numbers of specific EEC (66,187,188). To our knowledge, this is the first report of reduced Paneth cell number in DIO mice. This is potentially interesting since Paneth cells are reported to secrete factors such as Wnts, which provide trophic support to ISC. However *in vivo*, despite reduced Paneth cell numbers, DIO ISC still hyperproliferate and expand and the ISC expansion correlates with plasma insulin levels.

We used a 3D Matrigel based culture system to directly test if the *in vivo* hyperproliferation of Sox9-EGFP Low ISC was associated with enhanced ability of these cells to generate enterospheres/enteroids *in vitro*. Surprisingly, the number of enterospheres/enteroids derived from isolated Sox9-EGFP Low ISC was reduced in DIO mice versus controls indicating impaired rather than enhanced intrinsic function of DIO ISC when isolated from their *in vivo* environment. This suggested that some extrinsic signal in the *in vivo* setting that promotes survival or proliferation of ISC from DIO mice may be deficient in the *in vitro* system. In support of this possibility, supplementation of culture medium with insulin and/or IGF1, which are increased in plasma of DIO mice, was able to rescue the impaired enteroid forming ability of Sox9-EGFP Low ISC from DIO mice to levels equal to or greater than that observed in Sox9-EGFP Low ISC from controls. Interestingly, addition of insulin, IGF1 or both factors combined did not affect the yield of enteroids from control Sox9-EGFP Low ISC. Since DIO mice exhibited elevated circulating levels of insulin and IGF1 and elevated locally expressed *Igf1* mRNA *in vivo*, we interpret these findings as novel evidence that ISC from DIO mice develop a 'dependence' or responsiveness to exogenous insulin or IGF1 for their survival or increased proliferation normally not seen in control ISC. At the mRNA level, we found no evidence for reduced levels of *Igf1r, Ir* or IR-A in Sox9-EGFP Low ISC from DIO mice versus controls suggesting that the dependence on exogenous insulin/IGF1 may result from a mechanism other than down-regulation of receptor expression. We cannot exclude altered expression of Igf1r or Ir at the protein level, but this is difficult to quantify considering the small numbers of ISC that can be collected. The significant decrease in Wnt targets *Myc* and *Axin2* mRNAs in Sox9-EGFP Low ISC isolated from DIO mice suggest that reduced Wnt activation may contribute to impaired enteroid forming ability of Sox9-EGFP Low ISC. This could reflect reduced Wnt ligand exposure *in vivo* due to reduced Paneth cell numbers. Impaired Wnt signaling is also seen in other tissues during obesity such as the hypothalamus and bone (189,190). In other systems, insulin and IGFs are known to activate β-catenin/TCF, known downstream mediators of Wnt activation (191-193). Thus the ability of insulin and IGF1 to

promote enteroid forming ability of DIO ISC may reflect their ability to compensate for Wnt down-regulation. Additional studies of the Wnt pathway or insulin/IGF/Wnt interactions in ISC of DIO mice represent an interesting future direction.

It is noteworthy that CR reduced progenitor proliferation and led to a reduction in villus height of similar magnitude to the increase in villus height observed here with DIO, but similar to DIO, CR resulted in selective ISC expansion and hyperproliferation based on numbers of cells labeled with the ISC biomarker *Olfm4* and BrdU (121). However the mechanisms leading to selective increases in ISC numbers and proliferation appear to differ in CR and DIO. In CR, increased ISC number and proliferation *in vivo* were associated with enhanced enteroid formation *in vitro*, which depended on paracrine interactions with Paneth cells and increased responsiveness of Paneth cells to insulin appeared to enhance intrinsic ISC enteroid forming abilities (121). In contrast, our study suggests that despite increased ISC numbers and hyperproliferation in DIO *in vivo*, isolated ISC exhibit impaired intrinsic function that can be rescued with insulin or IGF1.

In summary, our study provides novel evidence in rodents that *in vivo* DIO increases ISC number and this correlates with elevated plasma insulin and is associated with ISC hyperproliferation and decreased Paneth and goblet cell number. However *in vitro* analyses of isolated ISC from DIO mice demonstrate impaired intrinsic function that can be reversed by insulin and/or IGF1, indicating that DIO leads to an acquired dependence of ISC on insulin or IGF1.

Materials and Methods

Animals/Diet

Sox9-EGFP mice contain a BAC transgene with ~226.5kb of *Sox9* genomic regulatory region that drive EGFP expression (56,57) and are maintained as heterozygotes on an outbred CD-1 background. Genotyping was performed as described in (56). Adult male and female Sox9-EGFP mice (7-10 weeks old) were randomly divided to receive either low fat chow (14% kcal from fat; Prolab RMH3000) or HFD (45% kcal from fat; Research Diets D12451) *ad libitum*. Published literature on inbred C57Bl/6J mice demonstrated frank obesity and insulin resistance after 16 weeks on the 45% kcal from fat HFD (76). To ensure obesity and hyperinsulinemia, Sox9-EGFP mice were maintained on the diet for 20 weeks. Body weight was measured weekly. Body composition was assessed by magnetic resonance imaging (EchoMRI, Houston, TX) after 20 weeks on diet. All mice were euthanized between 09:30-11:00 with a lethal dose of Nembutal (150µg/g/body weight). The Institutional Animal Care and Use

Committee (IACUC) of the University of North Carolina at Chapel Hill (Chapel Hill, NC) approved all animal studies.

Plasma hormone measurements

Animals were not fasted prior to euthanasia; therefore any measured hormone or glucose levels were in mice allowed to feed *ad libitum*. Blood was collected by cardiac puncture. Plasma was obtained by centrifugation at 2500 rpm for 6 minutes. Plasma for IGF1 assays was processed by acid-ethanol extraction to remove IGF binding proteins as described in (194). ELISA kits were used to measure plasma glucose (Cayman Chemical, Ann Arbor, MI), insulin (Mercodia, Uppsala, Sweden) and IGF1 (R&D, Minneapolis, MN) levels, according to manufacturer's instructions.

Tissue Harvest for Histology

Entire small intestine was collected, flushed to remove contents and weight and length measured. To mark cells in S-phase, 5-ethynyl-2'deoxyuridine (EdU, Sigma, St. Louis, MO) was administered by intraperitoneal injection (100μg/25g body weight) to animals 90 minutes prior to euthanasia. For histological analysis, small intestine was divided into three segments: the most proximal and distal 10cm were considered duodenum and ileum, respectively. The remaining middle segment was considered jejunum and used in all subsequent studies.

Histological analyses

All quantitative histological analyses were performed by an investigator blinded to diet groups. Morphometric analyses were performed on zinc formalin fixed, paraffin embedded, hematoxylin and eosin stained cross sections as described in (195,196). Crypt density was calculated by dividing the number of well-oriented crypts per millimeter of submucosal circumference. Immunofluorescence analyses were performed as described in (13). Briefly, jejunum was opened longitudinally and fixed in fresh 4% paraformaldehyde followed by 24-hour incubations in 10% and 30% sucrose. Frozen 5-7μm sections were cut and mounted for staining. To visualize cells in S-phase, sections were stained with EdU using the Click-iT EdU AlexaFluor 594 Kit following manufacturer's instructions (Invitrogen, Carlsbad, CA). For other immunofluorescence stains, sections were incubated overnight in the following primary antibodies: chicken α-GFP (1:500; Aves Labs, Tigard, OR), rabbit α-chromogranin-A (1:400; Abcam, Cambridge, MA), rabbit α-lysozyme (1:500; Leica Biosystems, Buffalo Grove, IL) and rabbit α-mucin2 (1:200; Santa Cruz Biotechnology, Santa Cruz, CA). The following secondary antibodies were used at 1:500: goat α-chicken-AlexaFluor 488 (Invitrogen, Carlsbad, CA) and goat α-rabbit Cy3 (Jackson ImmunoResearch Laboratories, West Grove, PA). DAPI containing mounting medium was used to visualize nuclei (Electron Microscopy Sciences,

Hatfield, PA). Images were captured using an inverted fluorescence microscope (Olympus IX83, Tokyo, Japan) fitted with a digital camera (ORCA-Flash4.0 C11440, Hamamatsu, Japan). The number of positively stained cells per crypt or villus section was counted in at least 20 crypts or villi/animal. Individual positive cells were confirmed by DAPI nuclear staining. Confocal images were photographed using the Leica SP2 Laser Scanning Confocal Microscope (Leica Microsystems, Wetzlar, Germany).

Intestinal epithelial cell dissociation for flow cytometry and fluorescence activated cell sorting (FACS)

Preparation of jejunal epithelial cells for flow cytometry and FACS was carried out as described in (13). For flow cytometry studies, dead cells were excluded based on uptake of propidium iodide (Sigma, St. Louis, MO) and quantification of Sox9-EGFP Low ISC was performed using a Cyan flow cytometer and Summit v4.3 software (Beckman Coulter, Fullerton, CA). Sox9-EGFP cell populations were sorted using the MoFlo XDP cell sorter (Beckman Coulter, Fullerton, CA) using gating parameters as described in (13,57). $CD45^+$ (BioLegend, San Diego, CA), $CD31^+$ (BioLegend, San Diego, CA), and Annexin-V^+ (Life Technologies, Carlsbad, CA) cells were excluded prior to sorting. Sort efficiency was assessed by post-sort cell analysis to establish the percentage of populations that fall within the previously established gates.

RNA isolation and high throughput quantitative real-time PCR by Fluidigm

Total RNA was isolated from whole thickness jejunum or FACS isolated epithelial cells using the RNeasy Mini Kit (Qiagen, Venlo, The Netherlands) per manufacturer's instructions. For high throughput qRTPCR of FACS isolated cells, RNA quality was assessed by the 2100 Bioanalyzer (Agilent Technologies, Santa Clara, CA) and high quality RNA was included for gene expression studies using the Fluidigm BioMark HD system per manufacturer's instructions (Fluidigm, South San Francisco, CA). *Igf1* is expressed in intestinal mesenchyme (128,197) and so *Igf1* mRNA was quantified on total RNA extracted from whole thickness segments of jejunum. Total RNA was reverse transcribed using the High Capacity cDNA Reverse Transcription Kit with RNase inhibitor (Applied Biosystems, Carlsbad, CA), qRTPCR reactions were performed in duplicate using the Rotor-Gene 3000 and analyzed using Rotor-Gene software version 6.0.23 (Qiagen, Venlo, The Netherlands). All qRTPCR data were normalized to the invariant control gene *ActB*. For FACS isolated samples, data were also normalized to non-sorted intestinal epithelial samples or Sox9-EGFP Low ISC from control animals sorted on the same day in the same run to control for any technical variability across cell preparations and/or sorting procedures. The following TaqMan primer/probesets were used *ActB*: Mm00607939_s1, *Igf1*: Mm00439560_m1, *Sox9*: Mm00448840_m1, *Chga*:

Mm00514341_m1, *Hopx*: Mm00558630_m1, *Lct*: Mm01285112_m1, *Lgr5*: Mm00438890_m1, *Ccnd1*: Mm00432359_m1, *Igf1r*: Mm00802831_m1, *Insr*: Mm01211875_m1, *Myc* Mm00487804_m1 and *Axin2* Mm00443610_m1 (Applied Biosystems). EGFP mRNA was assessed as described in (13).

RT-PCR for insulin receptor (IR) isoform expression

2µg cDNA was used for RT-PCR using primers that amplify the A and B isoforms of the IR as described in (139). Densitometry was performed using ImageJ (http://rsbweb.nih.gov/ij/).

***In vitro* culture of FACS-isolated Sox9-EGFP cell populations**

Culture experiments were carried out using methods originally described by Sato et al. for $Lgr5^+$ cells and adapted for Sox9-EGFP Low ISC by Gracz et al (53,57). In all studies, ISC were plated at low density and cultured in growth factor reduced Matrigel (BD Biosciences, San Jose, CA) with a standard growth factor cocktail (EGF: R&D, Minneapolis, MN, Noggin: PeproTech, Rocky Hill, NJ and R-Spondin 1: R&D, Minneapolis, MN). To assess responsiveness to insulin or IGF1, ISC from control or DIO mice were cultured plus or minus insulin (Sigma, St. Louis, MO), IGF1 (Genentech, San Francisco, CA) or insulin and IGF1, added at a concentration of 50ng/ml every other day. Enterospheres are predominantly seen at day 2 –4 post plating and starting at day 6-8, they typically grow and develop into enteroids. Number of enterospheres/enteroids formed was counted every other day by an investigator blinded to treatment groups until day 12 post plating (end of study). Quantification and photographs were taken at 10x objective.

Statistical Analysis

Data are expressed as mean ± SEM. For control and DIO groups, n≥20 for entire study. Subsets of animals were used for different experiments. All experimental results include ≥3 independent pairs of animals. Body weights were compared between diet groups by repeated measures ANOVA. For high throughput qRTPCR experiments, differences between Sox9-EGFP populations were compared using one-way ANOVA followed by pairwise comparisons using Holm-Sidak post-hoc test. Impact of diet on individual Sox9-EGFP populations was assessed using paired t-test on cells isolated from DIO and chow fed control littermate pairs sorted in the same run. ISC culture studies were performed on ISC isolated from Sox9-EGFP littermate pairs fed either HFD or chow. ISC were isolated from these littermate pairs by FACS and plated on the same day in any given experiment. Paired t test was therefore used to assess impact of diet on cultured ISC or their response to insulin, IGF1 or both. All remaining data

were compared using Student's t-test as appropriate. In all analyses, $p<0.05$ was considered statistically significant. All statistical analyses were performed using SigmaPlot 12.0

Figures and Tables

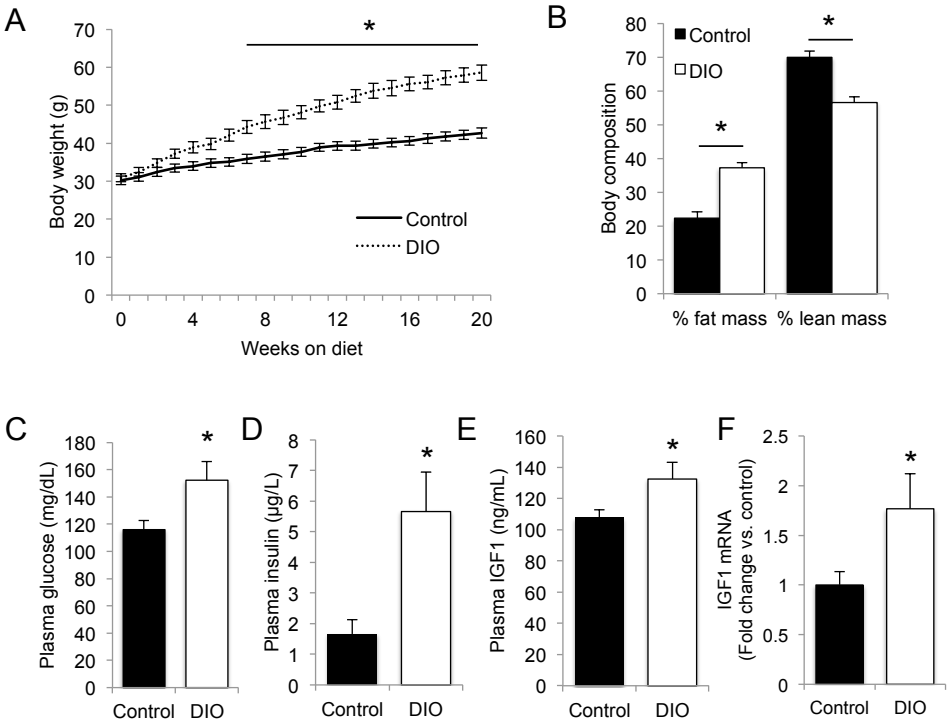

Figure 2.1: High fat diet feeding for 20 weeks increases body weight and fat mass leading to diet-induced obesity (DIO), elevated plasma glucose, insulin and IGF1 levels.
(A) Body weight over 20 weeks in mice fed low fat chow (control) or high fat diet to induce DIO. (B) Body composition of control versus DIO mice measured by magnetic resonance imaging after 20 weeks on diet. C-E: Circulating plasma concentrations of (C) glucose, (D) insulin and (E) insulin-like growth factor 1 (IGF1). F: qRTPCR measured *Igf1* mRNA from jejunum. Data expressed as mean ± SEM. *$p<0.05$ DIO versus control, repeated measures ANOVA (A) or unpaired t-test (B-F), $n\geq5$

Table 2.1: Measures of intestinal morphology and morphometry in diet-induced obesity (DIO)

Measure	Control	DIO	p-value
	mean ± sem	mean ± sem	
Small intestine length (cm)	46.7 ± 1.0	43.6 ± 1.3	**0.02***
Small intestine weight (g)	1.9 ± 0.1	1.8 ± 0.1	0.35
Small intestine weight/length (g/cm)	0.04 ± 0.002	0.04 ± 0.002	0.73
Jejunal crypt depth (μm)	70.1 ± 2.5	66.1 ± 0.8	0.14
Jejunal villus height (μm)	282.1 ± 8.0	333.8 ± 18.8	**0.02***
Jejunal crypt density (#/mm submucosal circumference)	18.4 ± 0.6	20.6 ± 0.7	**0.04***
Jejunal crypt fission (% of total cross section)	0.92 ± 0.1	1.15 ± 0.2	0.31

*$p<0.05$; unpaired t-test; $n\geq5$ per group

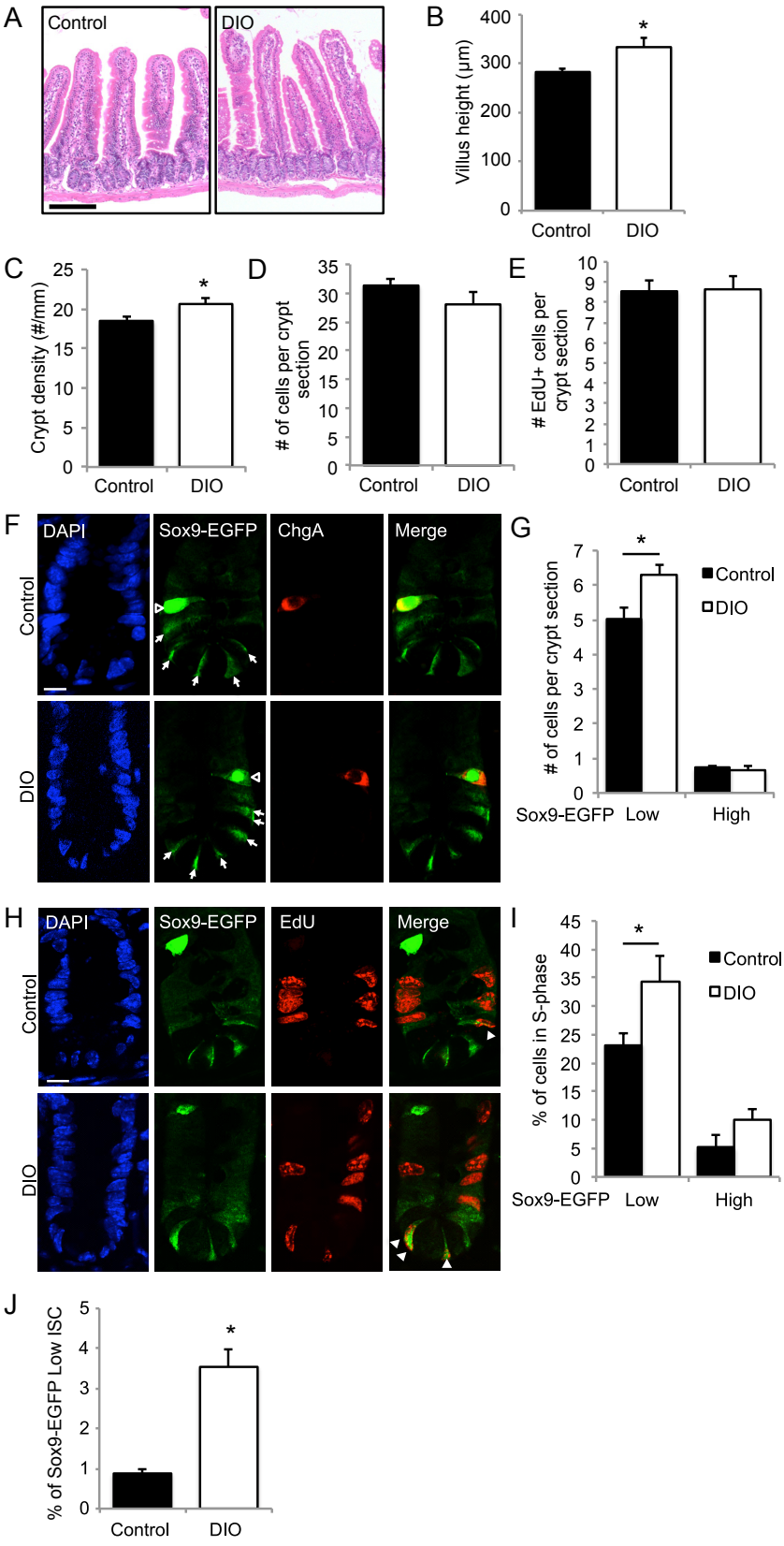
A
Control
DIO
B
Villus height (μm)
400
300
200
100
0
*
Control
DIO
C
Crypt density (#/mm)
25
20
15
10
5
0
*
Control
DIO
D
# of cells per crypt section
35
30
25
20
15
10
5
0
Control
DIO
E
EdU+ cells per crypt section
10
9
8
7
6
5
4
3
2
1
0
Control
DIO
F
DAPI
Sox9-EGFP
ChgA
Merge
Control
DIO
G
# of cells per crypt section
7
6
5
4
3
2
1
0
*
Control
DIO
Sox9-EGFP Low
High
H
DAPI
Sox9-EGFP
EdU
Merge
Control
DIO
I
% of cells in S-phase
45
40
35
30
25
20
15
10
5
0
*
Control
DIO
Sox9-EGFP Low
High
J
% of Sox9-EGFP Low ISC
5
4
3
2
1
0
*
Control
DIO

Figure 2.2: Increases in villus height, crypt density, ISC number and proportion of ISC in S-phase in DIO versus control mice.
(A) Representative hematoxylin & eosin stained photographs depicting crypt-villus architecture of intestinal epithelium from control and DIO mice. Images were taken at 10x magnification. Scale bar = 100μm. (B) Villus height in control and DIO mice. (C) Crypt density quantified by number of crypts per mm submucosal circumference in control and DIO mice. (D) Number of cells per crypt in control and DIO mice. (E) Number of cells in S-phase measured by EdU positive staining per crypt. (F) Representative images of crypt sections stained with DAPI (blue), GFP (Sox9-EGFP; green) and Chromogranin-A (ChgA; red). Sox9-EGFP Low ISC (white arrows) and Sox9-EGFP High cells (open triangles) were defined by intensity of EGFP staining. (G) Quantification of Sox9-EGFP Low and Sox9-EGFP High cells. (H) Representative images of crypt sections stained with DAPI, GFP and EdU (red). Dual positive Sox9-EGFP Low and EdU cells are denoted by the filled triangles. EdU: 5-ethynyl-2'-deoxyuridine. Images were taken at 63x magnification. Scale bar = 20μm. (I) Percentage of Sox9-EGFP Low or Sox9-EGFP High cells positive for EdU. (J) Relative abundance of Sox9-EGFP Low cells assayed by flow cytometry and expressed as the percentage of total cells that fall in Sox9-EGFP Low gates. Data expressed as mean ± SEM. *$p<0.05$ DIO versus control, unpaired t-test, $n\geq5$

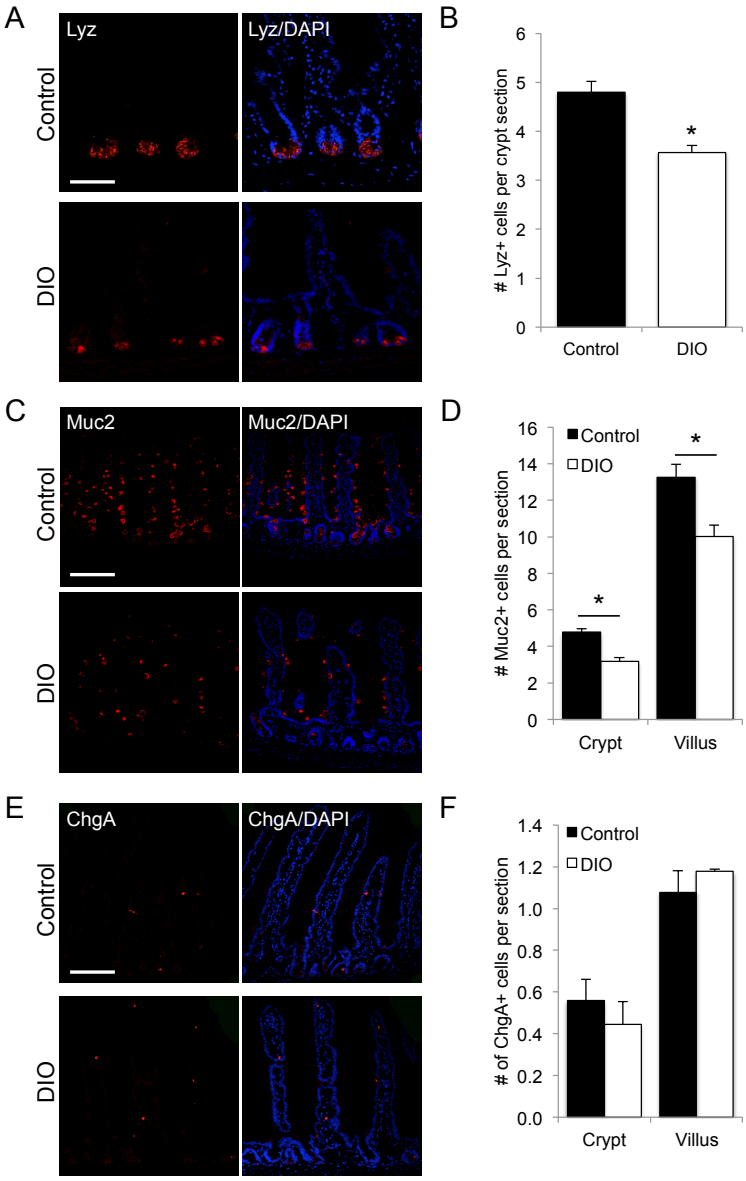

Figure 2.3: Decreased Paneth and goblet cells but no change in EECs in DIO mice versus controls.
A, C and E: Representative immunofluorescent images of jejunal sections stained with (A) lysozyme (Lyz), (C) mucin2 (Muc2) or (E) Chromogranin-A (ChgA). B, D and F: Quantification of (B) Lyz positive Paneth cells, (D) Muc2 positive goblet cells and (F) ChgA positive EECs in DIO versus control mice. All images were taken at 20x magnification. Scale bar = 50µm. Data expressed as mean ± SEM. * $p<0.05$ DIO versus control, unpaired t-test, $n\geq4$

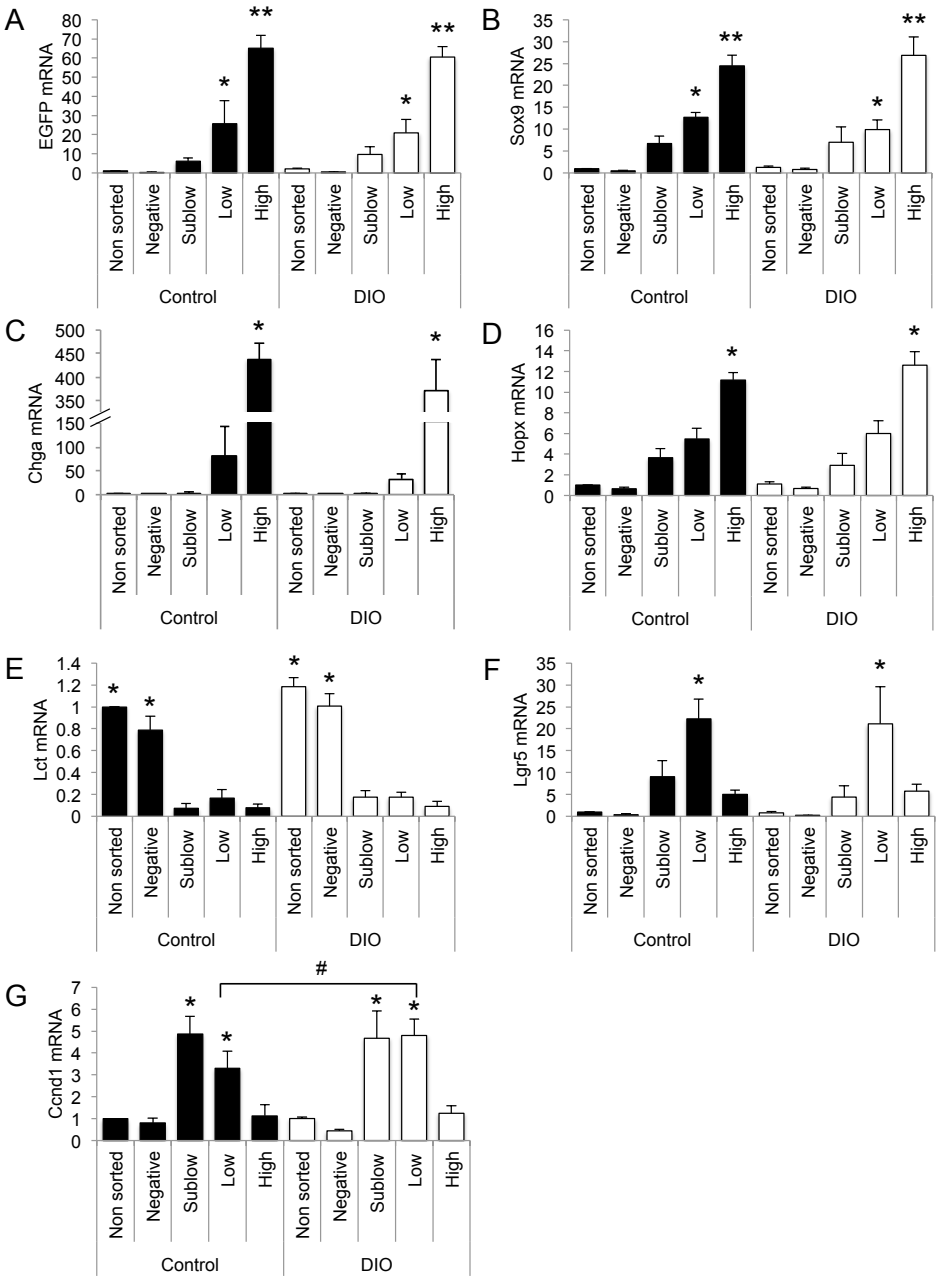

Figure 2.4: Sox9-EGFP Low ISCs from DIO mice are enriched for appropriate biomarkers and show elevated cyclin D1 mRNA.

High throughput qRTPCR on FACS isolated Sox9-EGFP cells from control and DIO mice assessed levels of mRNAs encoding (A) EGFP, (B) *Sox9*, (C) *Chga*, (D) *Hopx*, (E) *Lct*, (F) *Lgr5* and (G) *Ccnd1*. Data expressed as mean ± SEM. * or ** $p<0.05$ versus all other Sox9-EGFP populations; $^{\#}$ $p<0.05$ in DIO versus control Sox9-EGFP Low ISCs. Differences between Sox9-EGFP populations compared by one-way ANOVA, Holm-Sidak and between diets by paired t-test, $n\geq3$

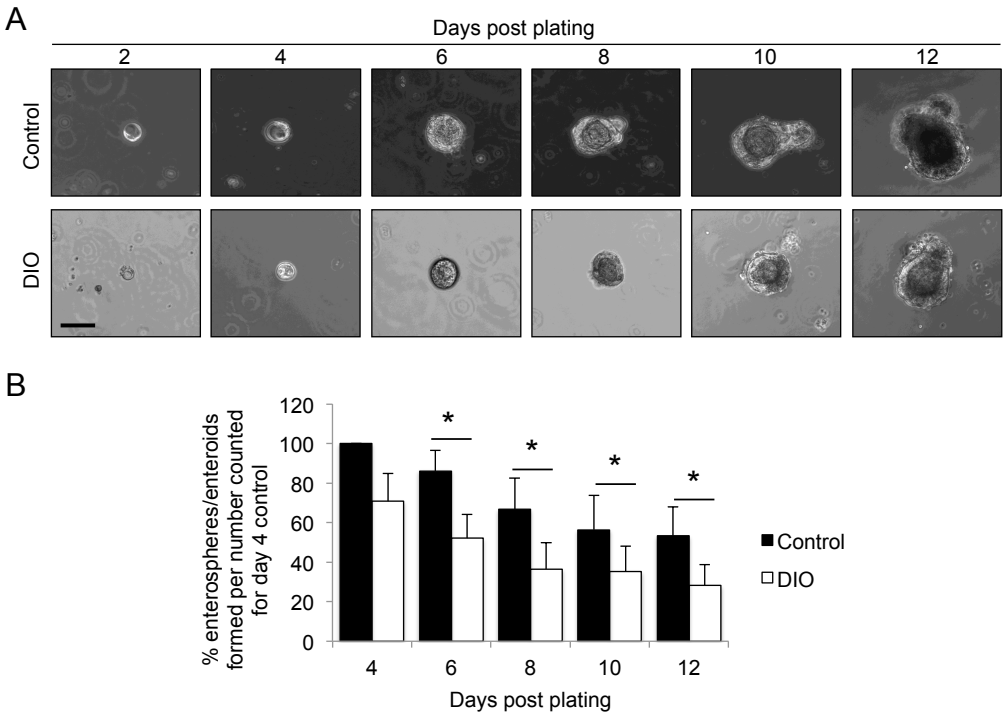

Figure 2.5: Sox9-EGFP Low ISCs from DIO mice exhibit reduced enteroid-forming ability.
(A) Time course of enterosphere/enteroid formation by ISCs isolated from control and DIO mice. Images were taken at 10x magnification. Scale bar = 100μm. (B) Quantification of enterosphere/enteroids formed starting at day 4 until day 12. Data expressed as mean percentage versus enteroids formed in control at day 4 ± SEM. *$p<0.05$ DIO versus control, paired t-test, $n\geq6$ independent pairs performed in duplicate or triplicate.

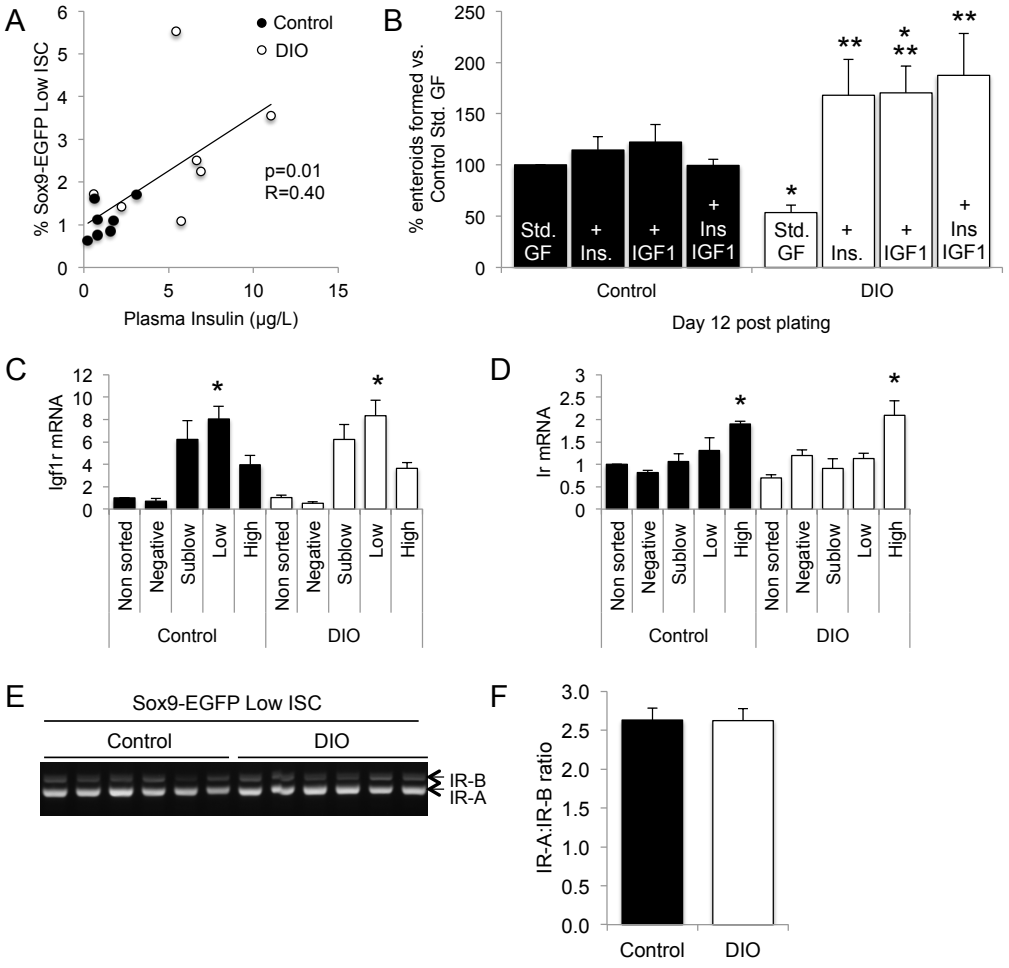

Figure 2.6: Plasma insulin positively correlates with percentage of Sox9-EGFP Low ISCs and treatment of ISC from DIO mice with insulin, IGF1 or both rescues decreased intrinsic *in vitro* function.
(A) Linear regression analysis of plasma insulin levels and percentage of Sox9-EGFP Low ISC in individual mice. (B) Enteroid formation at day 12 from Sox9-EGFP Low ISC isolated from control or DIO mice cultured with standard growth factors (Std. GF) as described in *Materials and Methods* or Std. GF plus insulin (Ins.), IGF1 or Ins. and IGF1. Data expressed as mean ± SEM. * $p<0.05$ versus control cultured with Std. GF alone; ** $p<0.05$ versus DIO Std. GF alone, paired t-test, n=3 for ISC isolated from 3 independent littermate pairs each cultured in duplicate. C-D: High throughput qRTPCR measured (C) *Igf1r* and (D) total *Ir* mRNA. (E) RT-PCR on Sox9-EGFP Low ISCs measured IR isoform expression. (F) Ratio of IR-A to IR-B expression quantified in control *versus* DIO Sox9-EGFP Low ISC. Data expressed as mean ± SEM. * $p<0.05$ versus all Sox9-EGFP cell populations, one-way ANOVA, Holm-Sidak, $n\geq3$.

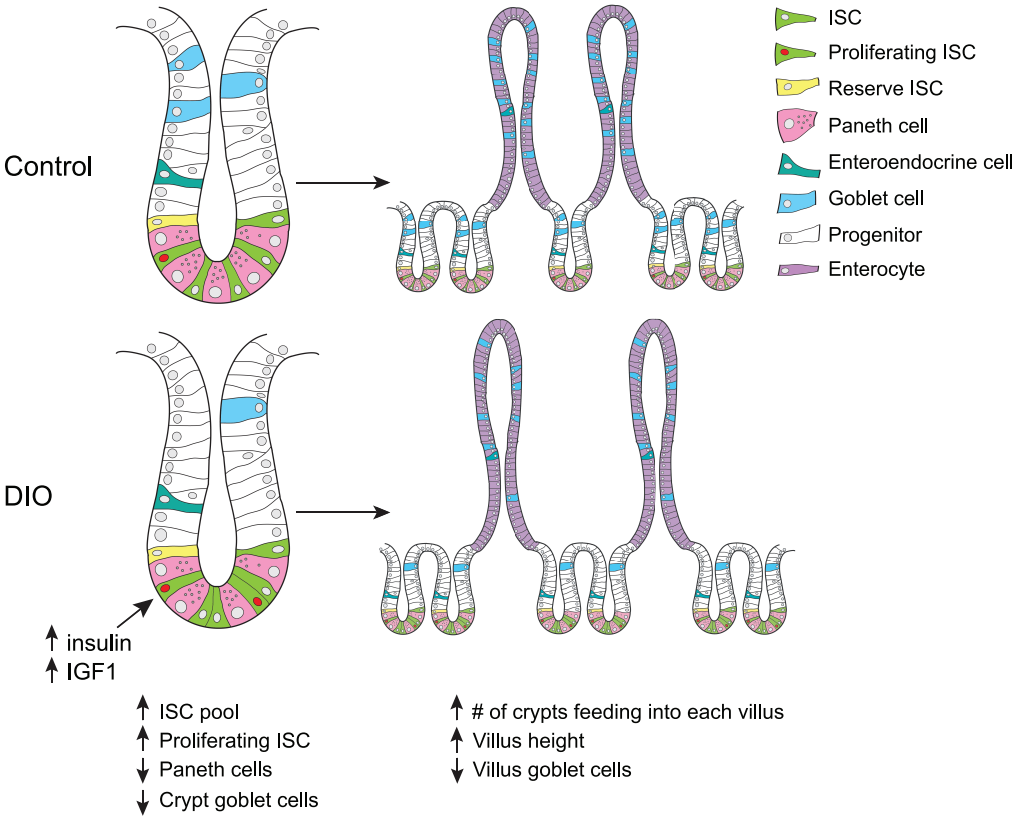

Figure 2.7: Proposed model of impact of DIO on ISC number, function and crypt-villus homeostasis. We provide a model where intestinal adaptation to DIO increases the number of total and proliferating ISC associated with elevated plasma insulin and IGF1 and local *Igf1* mRNA. The expansion in the ISC pool is associated with increases in the number of crypts feeding onto each villus resulting in heightened villi. DIO also decreases crypt-based Paneth cells and crypt and villus goblet cells, which may favor a greater mass of villus enterocytes that may enhance absorptive capacity during hypercaloric conditions.

CHAPTER 3: ALTERNATE DAY FASTING SELECTIVELY ALTERS INTESTINAL PROGENITOR POOL ASSOCIATED WITH DECREASED INTESTINAL PROLIFERATION WITHOUT REDUCTION IN FOOD INTAKE

Introduction

Daily calorie restriction (CR), defined as 20-40% reduction in calories without malnutrition, is still one of the most common strategies for weight loss (100,101). Until recently, it has been widely accepted that CR results in numerous health benefits including increasing lifespan and delaying the onset of chronic diseases (198,199). However, those health benefits require strict adherence to long-term CR, which in humans, is difficult to maintain (98,99). Recently a new diet regimen has emerged as a potentially more feasible alternative to CR, called intermittent feeding. Variations of intermittent feeding include alternate day fasting (ADF) or modified ADF. Complete ADF consists of cyclic patterns of unrestricted access to food for 24 hours followed by a 24-hour fasting period. Modified ADF regimens allow for CR on "fast" days so that there is no day where 100% fasting occurs. Reviews comparing intermittent feeding diets show that ADF is as effective as CR in promoting weight loss and reducing markers of chronic disease risk (103,110,200,201). ADF and CR can improve metabolic parameters such as lowering plasma insulin and glucose and increasing the ratio of subcutaneous versus visceral adipose tissue (103,110). Dietary restriction studies on the intestine are limited, but focused on short-term fasting or longer-term CR. However the effect of ADF on the intestinal epithelium, the tissue responsible for nutrient digestion and absorption, has not been fully studied.

The intestine is anatomically divided into two main regions, the small intestine and the colon. Both regions are lined with a monolayer of cells called intestinal epithelial cells. The small intestinal epithelium is composed of crypts and villi, while the colonic epithelium contains crypts and surface epithelium. The highly adaptive intestinal epithelium is renewed every 3-7 days depending on region and species (1). Renewal is accomplished by intestinal stem cells (ISCs) at the crypt base. ISCs divide to renew themselves and generate early progenitors, which continue to divide before they differentiate into multiple functional lineages. In the small intestine, villus-based terminally differentiated enterocytes, responsible for nutrient digestion and absorption, comprise >90% of total the epithelial cell population. Other differentiated lineages include goblet cells, enteroendocrine cells (EECs) primarily located on

villi but a few cells are located in the crypt, and Paneth cells. In the colon, stem cells are less well-defined but are thought to divide slowly to yield more rapidly dividing progenitors, which differentiate into goblet cells, EECs and colonocytes with both absorptive and secretory functions.

The intestinal epithelium can rapidly adapt its growth rate to changes in luminal nutrient. Available data indicate that fasting more profoundly affects the mass of duodenal or jejunal epithelium than ileum or colon and that upper small intestine restores its normal mass with 24-hours of refeeding after a prolonged fast (175). Decreased intestinal mass observed during fasting is associated with decreased mucosal proliferation while increased proliferation occurs to restore mucosal mass during refeeding (171,173,175). Recent evidence showed CR decreased proliferation in the small intestinal epithelium but enhanced the capacity of ISCs to yield enteroids *in vitro* indicating intestinal adaptation to CR involved changes in ISCs and proliferating progenitors (121). In the colon, CR reduced the number of colon tumors in preclinical models of colon tumorigenesis (202-207). These effects were associated with decreased colonic epithelial cell proliferation (208). Whether the effect of ADF on the small intestinal or colonic epithelium is similar to that observed in CR models is unknown. Based on the recent data observed in intestines from CR animals, the present study aimed to assess whether ADF affected growth of the small intestinal epithelium, and particularly number or proliferation of ISCs and progenitors. To accomplish this, we used the a unique mouse model established to study ISCs and their progenitors based on intensity levels of enhanced green fluorescent protein (EGFP).

The Sox9-EGFP transgenic mouse model allows us to directly assess the effects of ADF on proliferation and numbers of ISC and progenitors in the small intestine. In the Sox9-EGFP mouse, different levels of Sox9-EGFP transgene expression mark different cell types in the small intestine. Cells expressing high levels of Sox9-EGFP (Sox9-EGFP High) mark EECs and a subset of reserve ISC. Low levels of Sox9-EGFP (Sox9-EGFP Low) mark actively cycling ISCs, sublow levels of Sox9-EGFP mark progenitors (Sox9-EGFP Sublow) and cells negative for Sox9-EGFP (Sox9-EGFP Negative) correspond primarily to enterocytes, but also contain Paneth and goblet cells (13,56,57).

The insulin/insulin-like growth factor (IGF) system is a well-established pathway regulated by nutrition and involved in intestinal proliferation. Enterotrophic effects are mediated by the insulin receptor (IR) and IGF1R. IR exists in two functionally distinct isoforms; IR isoform-A (IR-A) mediates the growth promoting actions of insulin while IR isoform-B (IR-B) mediates the metabolic actions of insulin. Our lab has demonstrated differential

expression of *Igf1r*, total *Insr*, IR-A and IR-B in ISCs and progenitors versus differentiated lineages (139,209) and that IR-B expression can slow the growth of colorectal cancer cell lines (139).

We hypothesized that ADF would preserve the ISC pool but would reduce either ISC or progenitor proliferation. We also examined the effect of ADF on growth parameters, proliferation and the role of IR and IGF1R in colon due to the effect of CR on colon proliferation and tumorigenesis (202-207). Our findings indicate profound effects of ADF on metabolism despite identical food intake to *ad libitum* fed mice. These effects were associated with preferential and more dramatic effects on progenitors and not ISC proliferation in the small intestine and significant reductions in proliferation in the colon.

Results

Decreased body weight, fat mass and fasting circulating triglycerides in ADF mice despite no change in food intake

Mice (7-8 week old) were exposed to constant chow *ad libitum* (control) or *ad libitum* feeding or fasting for alternating 24-hour periods (ADF) over 20 weeks. During this time, controls steadily gained weight as expected while ADF mice maintained body weight At 20 weeks after start of diet, ADF mice gained no weight from baseline and weighed 25% less than controls ($p<0.05$; Figure 3.1a). This difference in weight gain was in the absence of decreased food intake in ADF-fed animals. ADF animals ate twice as much as controls on feed days resulting in no difference in net food intake compared to controls (Figure 3.1b). Fasting plasma triglycerides were significantly lower in ADF animals by 26% ($p<0.05$; Figure 3.1c). ADF mice had significantly lower fat mass than controls at the end of a feed or fast cycle. This was evident by both MRI for percentage of fat mass and by weight of gonadal fat (Figure 3.1d-f). Fasting levels of plasma insulin did not differ between control and ADF groups, however ADF animals displayed higher levels, although still physiologically low, of glucose and IGF1 compared to controls (Table 3.1).

Increased CO_2 production, O_2 consumption and respiratory exchange ratio (RER) in ADF mice

To assess whether changes in body composition were due to changes in metabolic activity, mice were placed in metabolic chambers and measurements were taken for 24-hours with and without food after acclimating for 2 days. RER was significantly higher in ADF mice during a 24-hour feed period compared to all other groups, consistently near 1.0, indicating use of solely carbohydrates for ATP production. RER of control fed mice was around 0.85 indicating that controls use both carbohydrates and fat for energy. RER did not differ between fasted groups (Figure

3.2a). The increased RER in ADF mice in the fed state was associated with significant increases in VO_2 and VCO_2 compared to controls (Figure 3.2b-c). During feed periods, ADF mice displayed a significant increase in heat production compared to controls, potentially due to increased food intake during feed days (Figure 3.2d). Activity was measured by beam breaks in multiple dimensions during fed and fast periods. There were no significant differences in activity in either fed or fast states between control and ADF mice (Figure 3.2e).

Impact of ADF on jejunal morphology, ISC and progenitors and proliferation

Since ADF altered many metabolic parameters, we examined the effect of ADF on the intestine, the tissue responsible for nutrient absorption. Small intestinal mass and length were not different between control or ADF mice in a fed state or after fasting (Table 3.2). After a fast cycle, long-term ADF did not affect villus height, however crypt depth was modestly but significantly reduced by 11% associated with a significant 11% decrease in crypt cell number versus controls ($p<0.05$; Figure 3.3a-d).

To directly assess impact of ADF on ISCs or progenitors and proliferation, we performed flow cytometry to quantify changes in proportion of Sox9-EGFP Sublow progenitors and Sox9-EGFP Low ISCs. Numbers of Sox9-EGFP Low ISCs, total cells in S-phase (EdU labeled) or co-labeled Sox9-EGFP Low ISC and EdU cell per crypt were evaluated by histology. Note that because we were interested in the effect of ADF on fasting levels of circulating hormones, much of our current intestinal data is gathered from *ad libitum* fed control animals or long-term ADF animals both after a fast cycle. We observed no change in the number of Sox9-EGFP Low ISCs quantified by histology (Figure 3.3e). Flow cytometry confirmed histology results showing no change in the percentage of Sox9-EGFP Low ISC between *ad libitum* fed controls or ADF animals following a fast cycle (Figure 3.3f) indicating ISC numbers are not affected by ADF after fasting. Flow cytometry, used to quantify Sox9-EGFP Sublow progenitors, which are unable to be visualized by histology, revealed that ADF animals following a fast cycle had a significantly greater percentage of Sox9-EGFP Sublow progenitors than *ad libitum* fed controls following a fast cycle (Figure 3.3f). To assess proliferation, we quantified the number of EdU positive cells and found a significant decrease of number of EdU positive cells per crypt section in fasted ADF animals compared to controls (Figure 3.3g-h). The percentage of Sox9-EGFP Low ISCs that were EdU positive was similar between groups indicating decreased proliferation was not due to decreased ISC proliferation (Figure 3.3i). Flow cytometry data from *ad libitum* fed controls and ADF animals following a fed cycle demonstrated that the increase in

progenitors observed in ADF fasted animals (Figure 3.3e) was reversed in ADF animals following feeding (Figure 3.3j).

Effects of ADF on colon morphology and proliferation

Like in the small intestine, colon mass and length did not differ between control and ADF following a fed or fast cycle (Table 1). Growth parameters were assessed in distal colon since it is the site of tumor formation. Unlike the jejunum, colon crypt depth was significantly increased by 9% in ADF mice versus controls and this was associated with a significant 16% increase in the number of cells per colonic crypt ($p<0.05$; Figure 3.4a-b). To assess whether changes in colon crypt depth were due to changes in proliferation, we quantified EdU positive cells in colon crypts of ADF and control mice following a fast cycle. We found that despite increased colonic crypt depth, ADF mice displayed a significant decrease in EdU positive cells, as observed in the jejunum, compared to controls (Figure 3.4c-d). To evaluate whether decreased proliferation is associated with changes in gene expression, we assessed mRNA levels of Cyclin D1 (*Ccnd1*), a gene involved in cell-cycle progression from G1 to S-phase in isolated colonic epithelium from fasted ADF and *ad libitum* fed control animals following a fast cycle. Consistent with decreased proliferation, ADF animals displayed significantly decreased *Ccnd1* mRNA (Figure 3.4e) confirming observed decreased number of EdU^+ cells by histology.

Insulin receptor isoform expression in colon of ADF and controls

Due to its role in proliferation, we assessed changes in the insulin/IGF1 pathway. There was no significant differences in *Igf1r* and total *Insr* mRNA in ADF colonic epithelium compared to controls (Figure 3.5a-b). To evaluate whether the decreased proliferation observed in ADF animals following a fast cycle compared to *ad libitum* fed controls following a fast cycle was due to changes in IR isoform expression, we measured IR isoform mRNA by RT-PCR. Analysis of whole thickness distal colon revealed ADF animals following a fast cycle express a greater ratio of IR-B versus IR-A compared to controls fasted during the same period (Figure 3.5c).

Discussion

Reported effects of ADF on weight loss have been variable. However, beneficial metabolic effects of ADF occur even in the absence of any weight loss or decreased overall food intake (103,110,200). We chose to study 20-week ADF to evaluate the long-term impact of ADF on the intestine. After 20 weeks of ADF, despite no change in food intake or activity compared to controls, animals weighed significantly less than *ad libitum* fed controls due to a lack of weight gain, rather than weight loss associated with lower fat mass as measured by MRI and decreased gonadal

fat weight. Thus ADF, despite equivalent food intake, leads to reduced body fat versus mice allowed to feed *ad libitum* for the same period or those allowed to feed *ad libitum* and then experience the same fasting period. We did not observe decreased insulin in our ADF animals as reported in other rodent models (102,107). Surprisingly, we found ADF animals displayed increased relative fasting glucose and IGF1, despite studies reporting glucose and IGF1-lowering effects of ADF (104-107). However, it is important to note that levels of glucose and IGF1 in ADF animals were still physiologically low. The observed increase in circulating glucose in ADF animals may indicate increased hepatic glucose output during fasting periods or may reflect the increased food intake during both light and dark cycles in ADF animals. Indirect calorimetry revealed that during feeding, ADF mice have adapted to rapidly use primarily carbohydrates from food as an energy source, leaving little to be stored as fat whereas control mice use a mixture of fat and carbohydrates for energy, leaving unutilized glucose to be converted to fatty acids and stored in adipose tissue. Our data are consistent with a recent study, which demonstrated that restricted feeding improved hepatic glucose and lipid metabolism (119). ADF mice however displayed an increase in heat production on feed days, presumably due to diet-induced thermogenesis, which is expected due to the significant increase in food intake. Importantly, we found no significant differences in activity between control and ADF groups, indicating any effects we observe in ADF animals were not due to differences in activity. Taken together, these data confirm previous evidence that ADF can improve body composition without changing overall food intake or activity and is associated with changes in nutrient metabolism.

Our primary goal was to evaluate the effect of ADF on the intestinal epithelium, and directly assess changes in jejunal ISCs and progenitors because of its role in nutrient absorption. We report new evidence that ADF resulted in decreased jejunal crypt depth associated with proportionate decreases in crypt cell number and decreased in proliferation or cells in S-phase. We recently reported that diet-induced obesity selectively expands jejunal ISC number and increases ISC proliferation (209) and therefore predicted that we would observe maintained ISC numbers but decreased ISC and progenitor proliferation in ADF. However ADF did not affect ISC number or ISC proliferation after a fast cycle suggesting that ISC are preserved during ADF and indicating that similar food intake over a prolonged period of ADF maintains ISC number and proliferation. This is different than what is reported in CR, where CR increased ISC number and proliferation (121), indicating that although ADF and CR may produce similar results in other factors, the effects of both diets on ISC number and proliferation are distinctly different from each other.

Despite no changes in ISC number or proliferation, we did find novel evidence that ADF selectively expands the percentage of Sox9-EGFP Sublow progenitors after a fast cycle, and this was associated with decreased progenitor proliferation, or increased cell-cycle time. This expansion of progenitors is reversed after a fed cycle in ADF animals. Taken together, these data are intriguing and suggests that during a fast cycle after prolonged ADF, there is an accumulation of progenitors potentially poised to exit the crypts for when food becomes available. After feeding, the increase in progenitors in ADF animals is lost suggesting rapid differentiation to adapt to presence of lumenal nutrient (Figure 3.6). While we observed changes in proliferation, we have not ruled out changes in apoptosis levels between ADF and controls. However, evidence from fasting and refeeding studies suggest limited to no effect on apoptosis (210,211).

While the goal of this study was to investigate the direct effects of ADF on the small intestinal epithelium, we observed decreased proliferation in the colonic epithelium associated with increased colon crypt depth and colon cell number. This suggests that ADF may be decreasing progenitor proliferation or increasing cell cycle time in the colon or increasing differentiated lineages but not at the expense of crypt depth or crypt cell number and is a future area for study. There is evidence that fasting increases cell cycle time in the colon, by increasing G1 (212). Our observations are consistent with complementary studies that have shown ADF decreases cell proliferation in other cell types such as prostate and T-cells (105,117).

Beneficial effects of dietary restriction on colon carcinogenesis have been documented (202-206). Cell proliferation is thought to be one early event that precedes carcinogenesis; therefore we investigated the potential role of the insulin/IGF system in mediating the observed decrease in colonic epithelial cell proliferation. Decreased proliferation was associated with a trend for decreased *Igf1r* and total *Insr* expression in colon epithelium. Insulin or IGF signaling via IR-A can mediate changes in proliferation and IR-A expression is up-regulated in numerous types of cancer (129,130). Our lab has shown that the balance of IR isoform expression dictates the role of IR in proliferation, where forced IR-B expression reduces proliferation in CRC cell lines (139). We show that ADF promotes IR-B expression, indicating up-regulation of IR-B may mediate decreased colon proliferation. A limitation in these data is that analysis of IR isoform expression was performed on whole thickness colon, rather than isolated epithelium. Studies to confirm epithelial specific IR-B up-regulation in ADF animals are currently in progress. Our data showing ADF mice displaying decreased colonic cell proliferation in the distal colon, the site of colon

tumorigenesis, indicates that ADF may be protective against tumorigenesis by slowing colonic epithelial proliferation.

We reported major effects of ADF on the intestine after a fast cycle. Because of the highly adaptive nature of the intestinal epithelium, evaluating the intestinal epithelium following a feed cycle is of great interest. Ongoing studies are currently underway to assess jejunal ISC number and proliferation, colon proliferation and differentiated lineages after a feed cycle. We predict ADF animals will display longer villi and increased proliferation following a feed cycle compared to after a fast cycle as well as controls.

In our study, we used 100% restriction on fast days, however emerging research is indicating that 100% restriction is not necessary to see the beneficial effects of ADF. Modified and complete ADF trials in humans demonstrate high adherence rates, indicating feasibility (103,110-114). Additionally, studies using high fat diet on alternating days also produce beneficial results similar to ADF using standard chow (104,118-120). This is highly translatable to humans as it is probable that humans who restrict their diet might not necessarily have to change their diet quality. Longer-term ADF studies need to be performed to gain insight on chronic ADF adherence. However it is becoming clear that ADF confers some protective effects as seen in CR studies and may be a more feasible and successful alternative to improving metabolic health in humans. ADF may also contribute to decreased chronic disease risk, particularly tumorigenesis by decreasing cell proliferation.

Materials and Methods

Animals/Diet

Sox9-EGFP mice express a BAC transgene containing genomic regulatory regions of *Sox9* that drive EGFP expression (56,57). Mice are maintained on an outbred CD-1 background and bred as heterozygotes. Genotyping was performed as described in (56). Adult Sox9-EGFP mice (8 weeks old) were randomly divided into one of two groups: control and ADF. Both groups were fed standard rodent chow with control mice receiving food *ad libitum* every day throughout the study and ADF mice receiving alternating 24-hour cycles of *ad libitum* access to food followed by removal of food for 24 hours over a total of 20 weeks. Food was removed or added every day at 17:00. Body weight was measured weekly after a 24-hour feed period for ADF mice. Prior to euthanasia, body composition was measured by magnetic resonance imaging (MRI; EchoMRI, Houston, TX). Animals were euthanized at 10:00 following either a fed or fast period. All animal studies were approved by the Institutional Animal Care and Use Committee (IACUC) of the University of North Carolina at Chapel Hill (Chapel Hill, NC).

Tissue Harvest

Ninety minutes prior to euthanasia, animals were given an intraperitoneal (IP) injection of 5-ethynyl-2'deoxyuridine (EdU, 100µg/25g body weight, Invitrogen, Carlsbad, CA) to mark cells in S-phase. Animals were euthanized with a lethal dose of Nembutal (150µg/g body weight) following either a fast or feed period, allowing for comparisons between ADF fed and *ad libitum* fed controls or ADF fasted and *ad libitum* fed controls following the same fast cycle. Gonadal fat was dissected and weighed. Small intestine and colon were removed, cleaned and flushed prior to measuring weight and length. Small intestine was divided into three segments, the proximal 10 cm was considered duodenum, the distal 10 cm was considered ileum and the remaining segment was considered the jejunum and was the focus of studies on small intestine. Colon was divided into proximal and distal regions.

Blood/plasma hormone measurements

At time of euthanasia, blood was collected by cardiac puncture. Plasma was separated by centrifugation for 6 minutes at 2500 rpm. ELISA kits measuring plasma triglycerides (Pointe Scientific, Canton, MI), insulin (Mercodia, Uppsala, Sweden), and IGF1 (R&D Systems, Minneapolis, MN) were used following manufacturer's instructions. Following an overnight fast, blood glucose measurements were performed on blood from the tail vain and measured using the OneTouch Ultra glucometer (LifeSpan, Milpitas, CA). Values are expressed as an average of duplicate readings.

Metabolic phenotyping

Food intake, CO_2 production, O_2 consumption, activity and heat production were measured using an indirect calorimetry system (TSE Systems, Chesterfield, MO), Prior to placement in the system, mice were weighed for pre-chamber body weight. Mice were then individually housed at room temperature under a 12:12-h light-dark cycle and allowed to adapt for 48 hours. The following metabolic parameters were measured for the next 48 hours where control and ADF groups were *ad libitum* fed for 24 hours followed by 24 hours without food. Food intake was measured in both groups during *ad libitum* access to food. CO_2 production, O_2 consumption and heat production values were normalized to body weight. Respiratory exchange ratio (RER) was calculated using CO_2 production and O_2 consumption. Activity was measured by infrared beam breaks in multiple dimensions.

Histological analyses

All analyses were performed by investigators blinded to diet groups. Jejunal and distal colon cross sections were fixed in 10% Zinc formalin and paraffin embedded for morphometric analyses. Hematoxylin and eosin (H&E)

stained sections were used to measure crypt depth and villus height by measuring the length from the crypt base to the crypt/villus junction (crypt depth) and from the crypt/villus junction to the villus tip (villus height) in well-oriented crypts and villi. Images and measurements were performed using the Axio Imager.A2 (Zeiss, Thornwood, NY), ProgRes CF Scan camera and the ProgRes Capture Pro 2.7 software (Jenoptik, Jena, Thuringia, Germany). For immunofluorescence, jejunum and distal colon were opened longitudinally and fixed in 4% paraformaldehyde overnight followed by sequential overnight incubations in 10 and 30% sucrose prior to embedding and freezing in OCT. Frozen sections (5-7μm) were cut and mounted onto positively-charged slides. Sections were stained for GFP using a chicken α-GFP (1:500; Aves Labs, Tigard OR) primary antibody at 4ºC overnight followed by a 2-hour incubation in a goat α-chicken-Alexa Fluor 488 (1:500; Invitrogen, Carlsbad, CA) secondary antibody at room temperature. To visualize cells in S-phase, slides were stained using the Click-iT EdU Alexa Fluor 594 kit following manufacturer's instructions (Life Technologies, Carlsbad, CA). Nuclei were visualized and using DAPI-containing mountain medium (Fluoro-Gel II with DAPI; Electron Microscopy Sciences, Hatfield, PA). Quantification was performed by counting the number of positive cells and total cell number in 30 well-oriented crypts/animal. Images were captured using the Olympus IX83 inverted fluorescence microscope (Olympus, Tokyo, Japan) fitted with the ORCA-Flask4.0 digital camera (Hamamatsu, Hamamatsu City, Japan).

Jejunal epithelium isolation for flow cytometry studies

Preparation of jejunal epithelial cells for flow cytometry was carried out as described in (13). Cell debris was excluded by forward-scatter/side-scatter gating. Dead cells were assessed by uptake of propidium iodine and excluded. Quantification of Sox9-EGFP Sublow and Sox9-EGFP Low cells was performed using the Cyan flow cytometer and Summit 4.3 software (Beckman Coulter, Pasadena, CA). Analysis was performed following published gating strategies (57) based on gates set for *ad libitum* fed control animals.

Jejunal and colonic epithelium isolation for gene expression studies

Jejunum was flushed with 1X PBS, opened longitudinally and incubated in 30mM EDTA/1.5mM DTT/PBS on ice for 15 minutes. Tissue was moved to 30mM EDTA/PBS and incubated at 37ºC for 8 minutes. Tissue was shaken vigorously and remnant tissue discarded. Cells were pelleted at 1500rpm for 5 minutes at 4ºC and washed two times with 1X PBS. Distal colon was treated as described for jejunum, but was incubated in 30mM EDTA/1.5mM DTT/PBS for 20 minutes and 30mM EDTA/PBS for 10 minutes since these longer incubations have proved necessary for efficient yield of crypts.

RNA isolation, reverse transcription and quantitative real-time PCR (qRTPCR)

Total RNA was isolated using the RNeasy Mini Kit following manufacturer's instructions (Qiagen, Valencia, CA). 0.5µg RNA was reverse transcribed to cDNA by the High Capacity cDNA Reverse Transcription Kit (Applied Biosystems, Carlsbad, CA). Quantitative real-time PCR (qRTPCR) was performed using Platinum Quantitative PCR SuperMix-UDG (Invitrogen, Carlsbad, CA) and the following TaqMan primer/probe sets (Applied Biosystems, Carlsbad, CA): *ActB*: Mm00607939_s1, *Ccnd1*: Mm00432359_m1, *Igf1r*: Mm00802831_m1 and *Insr*: Mm01211881_m1. Samples were run in duplicate and gene expression was calculated using the standard curve method and normalized to the invariant control *ActB*.

RT-PCR for IR isoform

RT-PCR on 0.5µg cDNA was performed using primers designed to amplify the IR-A and IR-B isoforms as described in (139). Densitometry was performed using ImageJ software.

Statistical Analysis

Data are expressed as mean ± SEM. Overall an $n \geq 15$ in control and ADF group was used. Subsets of animals were used for particular analyses and specific *n* is stated in the legend. Body weights over the 20 weeks of control *ad libitum* feeding or ADF were compared by repeated measures ANOVA followed by Tukey's post-hoc comparison test. We wanted to test differences between control and ADF groups after a fed or fast period, therefore comparisons between control and ADF group after a fed or fast state was assessed by Student's t-test. All analyses were performed using GraphPad Prism 6 software (La Jolla, CA). In all analyses, $p<0.05$ was considered statistically significant.

Figures and Tables

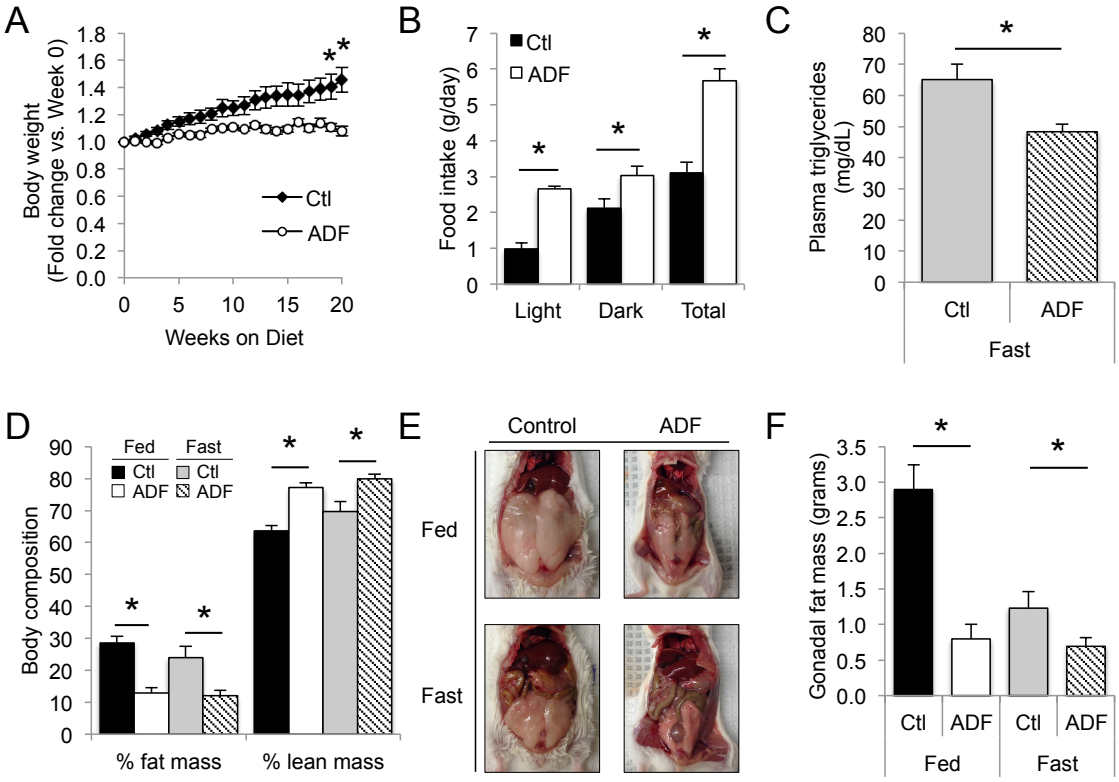

Figure 3.1: ADF prevents weight gain while decreasing fat and plasma triglycerides despite no change in food intake.
(A) Body weight over 20 weeks in mice fed chow *ad libitum* (Ctl) or every other day (ADF). Weight was measured after a 24-hour feed period in ADF group. (B) 24-hour food intake by light/dark cycle between diets measured by indirect calorimetry in control and ADF mice during 24-hour feeding cycle and after 16 weeks on ADF. (C) Fasting circulating triglycerides between diets. (D) Body composition analysis measured by MRI between diets after 24-hour fed or fast period in ADF mice or in *ad libitum* controls after fast cycle. (E) Representative images of gonadal fat pads between diets. (F) Gonadal fat mass between diets after a 24-hour fed or fast period. Data expressed as mean ± sem. *$p<0.05$, one-way ANOVA, Tukey post-hoc test (A) or unpaired t-test; $n\geq5$ per group

Table 3.1: Plasma metabolic parameters in ADF vs. control mice

	Control	ADF
	mean ± sem	mean ± sem
Glucose (mg/dL)	45.6 ± 1.2	75.2 ± 6.7*
Insulin (µg/L)	0.2 ± 0.01	0.4 ± 0.1
IGF1 (ng/mL)	32.0 ± 3.7	80.0 ± 7.9*

*$p<0.05$; unpaired t-test; $n \geq 4$ per group

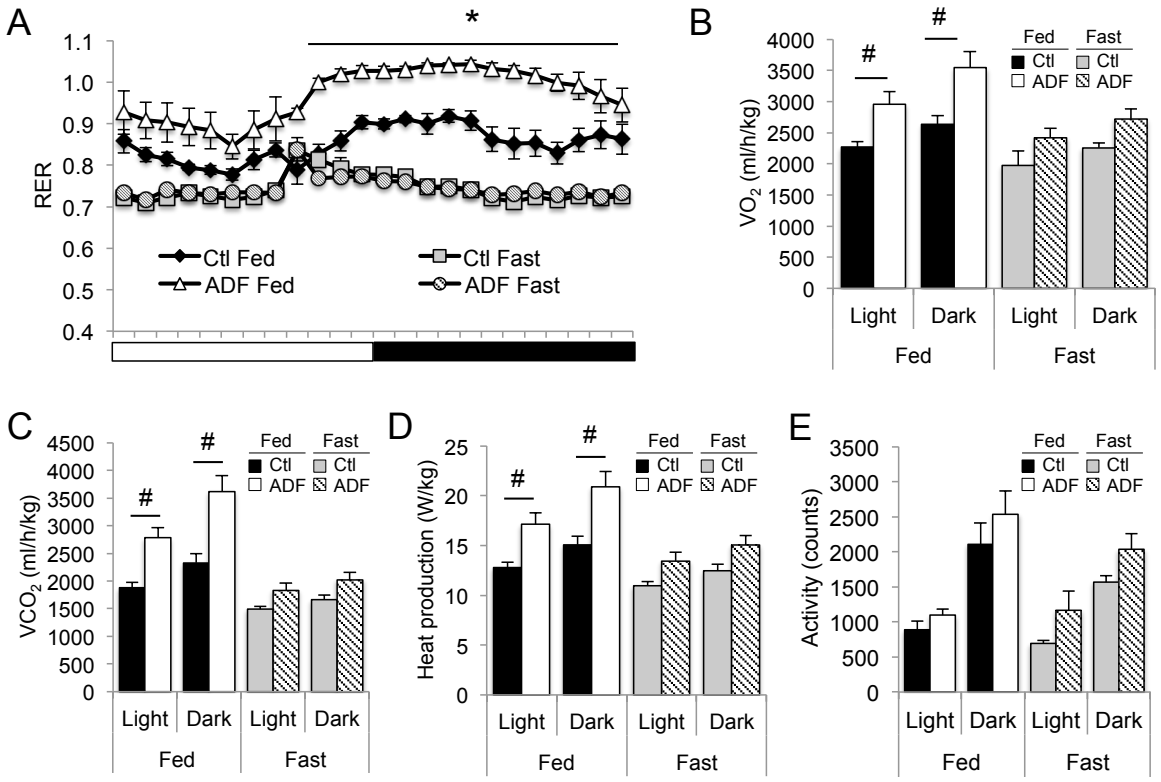

Figure 3.2: ADF animals burn more carbohydrates and produce more heat compared to controls despite no difference in activity.

Indirect calorimetry during a 24-hour period with food (fed) or without food (fast) between control and ADF animals measured (A) respiratory exchange ratio (RER; white bar: light cycle, black bar: dark cycle), (B) oxygen consumption (VO_2), (C) carbon dioxide production (VCO_2), (D) heat production and (E) activity during light and dark cycles. Data expressed as mean ± sem. *$p<0.05$ vs. control fed, #$p<0.05$; one-way ANOVA, Tukey post-hoc test (A) or unpaired t-test (B-E); $n\geq4$ per group

Table 3.2: Intestinal weight and length measurements in ADF vs. control mice

Measure	Fed		Fast	
	Control	ADF	Control	ADF
	mean ± sem	mean ± sem	mean ± sem	mean ± sem
Small intestine length (cm)	49.8 ± 1.4	50.7 ± 2.4	51.5 ± 2.2	52.2 ± 1.3
Small intestine weight (g)	1.96 ± 0.11	2.04 ± 0.30	1.81 ± 0.16	2.04 ± 0.10
Colon length (cm)	12.6 ± 0.2	13.1 ± 0.5	13.1 ± 0.4	13.0 ± 0.3
Colon weight (g)	0.42 ± 0.03	0.45 ± 0.08	0.44 ± 0.03	0.45 ± 0.02

n≥5 per group

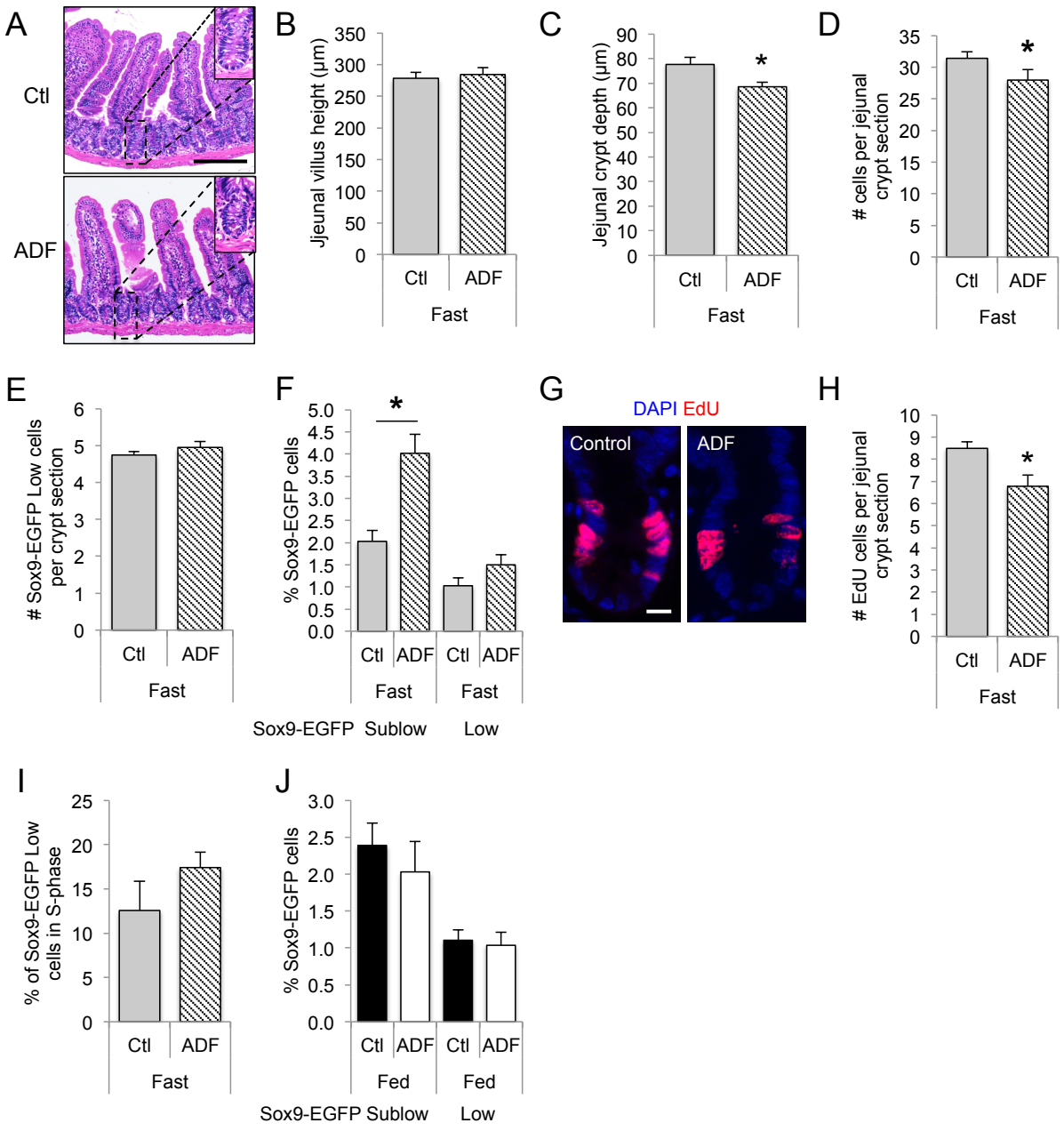

Figure 3.3: ADF decreases jejunal crypt depth and increases non-proliferating progenitor pool following a fast cycle.

(A) Representative images of jejunal crypt/villus units between *ad libitum* fed controls following a fast cycle and ADF animals after a fast cycle. B-D. Measurements of jejunal (B) villus height, (C) crypt depth and (D) crypt cell number between control and ADF animals (both after fast cycle). (E) Number of Sox9-EGFP Low ISCs per crypt section quantified by EGFP intensity in control and ADF (both after fast cycle). (F) Flow cytometry analysis of Sox9-EGFP Sublow and Sox9-EGFP Low populations in control and ADF (both after fast cycle). G. Representative images of EdU (red) and DAPI (blue; nuclei) staining. (H) Quantification of EdU positive cells per crypt section. (I) Number of Sox9-EGFP Low and EdU dual-labeled cells expressed as a percentage of total Sox9-EGFP Low cells. (J) Flow cytometry analysis of Sox9-EGFP Sublow and Low populations following fed cycle. Images were taken at (A) 10x or (A inset and G) 40x magnification. Scale bar: (A) 100µm or (G) 20µm. Data expressed as mean ± sem. *p<0.05, unpaired t-test; n≥3 per group.

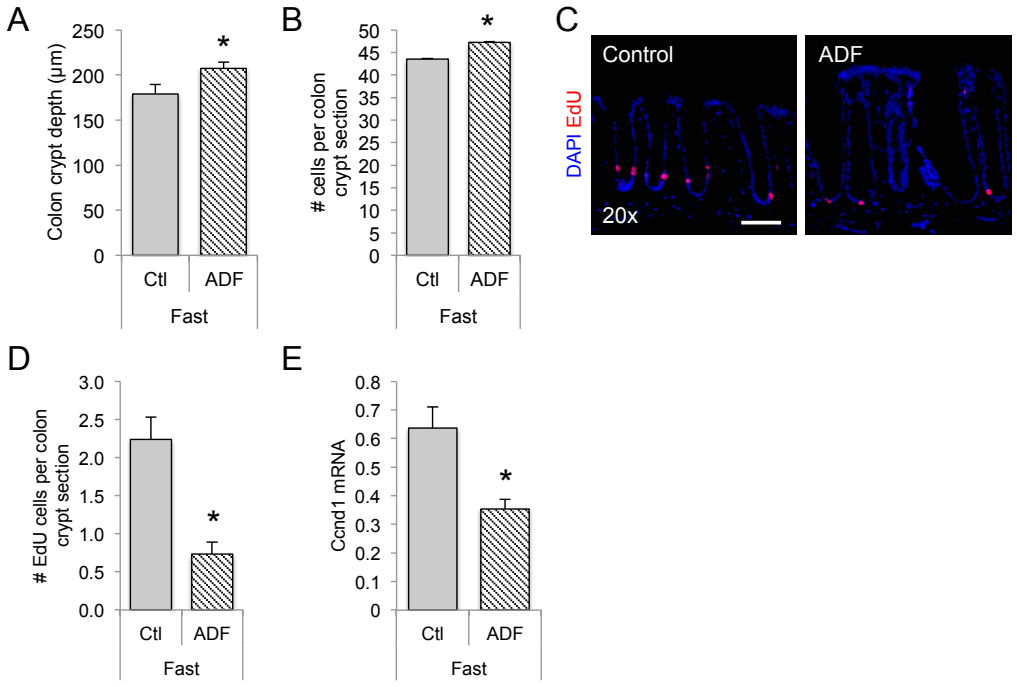

Figure 3.4: ADF increases colon crypt depth and cell number but decreases proliferation.
A-B. Morphological measurements of (A) colon crypt depth and (B) colon crypt cell number between *ad libitum* control and ADF groups (both after fast cycle). (C) Representative images of EdU (red) and DAPI (blue; nuclei) stained colon crypt sections. (D) Quantification of EdU positive cells per colon crypt section between diets. (E) qRTPCR measuring *Ccnd1* mRNA. Images were taken at 20x magnification. Scale bar: 100µm. Data expressed as mean ± sem. *$p<0.05$, unpaired t-test; $n\geq4$ per group.

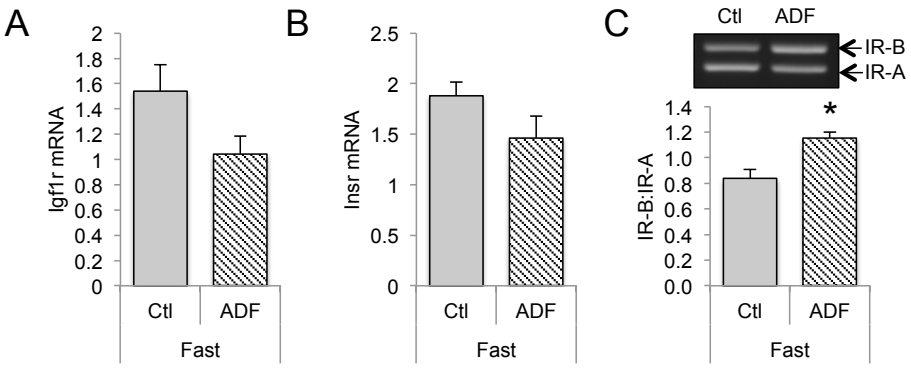

Figure 3.5: Decreased proliferation associated with increased IR-B in colon.
qRTPCR measured (A) *Igf1r* and (B) *Insr* mRNA in colon epithelium of *ad libitum* control and ADF animals both following a fast cycle. (C) RT-PCR assessed IR isoform ratio in colon (IR-B: top band, IR-A: bottom band). Data expressed as mean ± sem and normalized to invariant control *ActB*. *$p<0.05$, unpaired t-test; $n\geq3$ per group.

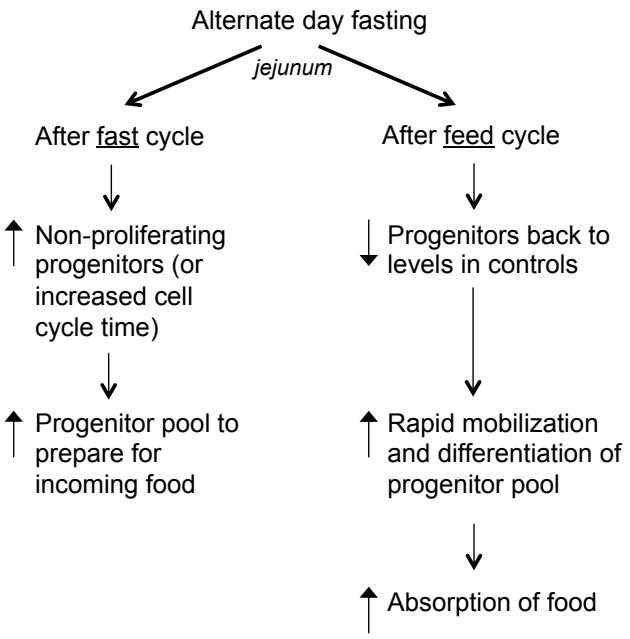

Figure 3.6: Progenitors are highly adaptive to feed and fast cycles in ADF animals to maximize food absorption.
Proposed model of the effect of ADF on progenitors where after a fast cycle, there is an increase in non-proliferating progenitors due to decreased proliferation or prolonged cell cycle time leading to an expansion in the pool of progenitors to prepare for incoming food. When food is available after a feed cycle, the progenitor pool returns to basal levels indicating a rapid mobilization and differentiation of the progenitor pool in order to facilitate absorption of food.

CHAPTER 4: EFFECTS OF OBESITY AND INTERMITTENT FEEDING ON ISCS AND PROGENITORS: SIGNIFICANCE, POTENTIAL MECHANISMS AND FUTURE DIRECTIONS

Obesity and associated hyperinsulinemia are at epidemic proportions and are associated with adverse consequences including increased risk of gastrointestinal cancers and chronic inflammation. The latter has been linked to impaired barrier function of the intestinal epithelium. Prior to this work, it had been reported that one adaptation of the intestinal epithelium in obesity was an increase in villus height, an adaptation that provides more mass of digestive and absorptive enterocytes (70,96). It was unknown whether this adaptation, and obesity or hyperinsulinemia was associated with altered number or function of ISCs or progenitors, cells that proliferate and constantly renew the intestinal epithelium maintaining digestive and absorptive mass and barrier function. Only in 2007 did the biomarkers and tools to directly study ISCs emerge. This dissertation focused on exploring the effect of obesity and hyperinsulinemia on ISC. We show, for the first time that DIO selectively increased ISC number and ISC proliferation. This comes at a cost of impaired intrinsic ISC function defined as the ability to yield enteroids *in vitro*, and a dependence on excess insulin or IGF1 for intrinsic function.

As well as obesity, we were interested in whether a dietary regimen that led to improved metabolism, reduced fat and particularly reduced plasma insulin affected the intestinal epithelium and preferentially or specifically ISCs or their progenitors. We explored an intermittent feeding model because this was emerging as a diet that could limit weight gain or reverse adverse effects of obesity. Using an ADF model, we demonstrated remarkable reductions in fat mass despite equivalent food intake and activity. We demonstrated that ADF decreased proliferation in the small intestine and colon, but that in the small intestine, it is not due to reductions in ISC proliferation, rather proliferation in the progenitor region. This discussion will explore significance of findings, additional potential mechanisms to explain them, remaining questions and possible future directions.

Intestinal epithelium adaptation to obesity and hyperinsulinemia

Selective expansion and proliferation of ISCs and decreased Paneth and goblet cells in obesity

We reported, for the first time, that DIO selectively increased ISC number and proliferation. DIO also increased crypt density and villus height. Together, these findings support a model where the intestine adapts to

obesity by increasing the ISC pool via selectively increasing ISC proliferation associated with an increased number of crypts feeding onto each villus resulting in increased villus height (Figure 4.1). DIO also decreased number of secretory Paneth and goblet cells, indicating obesity increases the absorptive enterocyte linage to digest and absorb the increased caloric load. Changes in differentiated cell types indicate DIO leads to altered cell fate specification and promote the absorptive lineage at the expense of the secretory lineage. The effect of obesity on cell fate determination directly in ISCs and progenitors is not known. Sakar et al. reported decreased *Atoh1* and increased *Hes1* expression in mucosal scrapings of obese versus control animals (66). We would propose a model that ISCs or progenitors from DIO animals would display increased Notch signaling and *Hes1* expression and decreased Wnt and *Atoh1* expression, resulting in increasing absorptive enterocytes (Figure 4.2). We are able to use the Sox9-EGFP mouse model to isolate ISCs and progenitors and assess changes in transcription factors and gene expression signatures dictating secretory versus absorptive fate specification. It is noteworthy that emerging literature in other organ systems links increased Notch signaling to obesity (213,214). Notch is also linked to cancer growth (20), therefore elevated Notch in obesity and especially in ISCs would be relevant to mechanisms driving cancer risk in obesity.

One main limitation of this study was we evaluated the effect of DIO at one time point. The time chosen was aimed at evaluating the impact of existing obesity and particularly hyperinsulinemia on ISCs. We recognize that performing a time course experiment over the course of development of DIO would reveal at what time intrinsic ISC function declines and starts to depend on exogenous insulin or IGF1. Another limitation is that our studies do not directly assess the effect of a particular dietary component on ISCs. The ISC enteroid culture system provides a useful model system to more directly evaluate the effect of specific dietary components on ISC function or fate specification. High throughput systems developed in the Magness lab will be particularly useful for such applications (215).

Paneth cells and ISC function

Paneth cells contribute to the ISC niche and changes in Paneth cell function or factors secreted can alter ISC number or function. In 2012, Yilmaz et al reported that CR enhanced ISC number and function and promoted intestinal regeneration by inhibiting mTORC1 activity specifically in Paneth cells. This led to increased *Bst1* mRNA and generation of cyclic ADF ribose, which acted on neighboring ISCs to promote proliferation. They concluded that CR promoted ISC number by favoring self-renewal, decreasing the number of progenitors and preserving the

stem cell pool for when calorie intake increases. (121) This study was the first to couple changes in nutrient intake to Paneth cell mediated ISC function.

Potential impact of reduced Paneth and goblet cells in DIO

Reduced Paneth and goblet cells during DIO may have important implications for adverse consequences of obesity since these cells contribute to host defense against potential pro-inflammatory stimuli in the lumen such as microbes. In our recent follow-up study, we found similar reductions in Paneth cells in obese C56Bl6 mice (216). Intriguingly, mRNAs encoding Paneth cell anti-microbial peptides were increased indicating functional changes in Paneth cells. Such increases in antimicrobial mRNAs were noted in obese humans despite decreased lysozyme protein levels (217). Further analyses of Paneth cells in DIO such as RNA or proteomic analyses would be of considerable interest. The Sox9-EGFP model permits Paneth cell isolation based on high CD24 expression and negative expression of the Sox9-EGFP reporter (215).

Paneth cells are known to secrete trophic factors and more recently enhance enteroid formation in a contact dependent manner. Reduced Paneth cells therefore seem unlikely to account for the ISC hyperproliferation *in vivo* or the defective intrinsic function in isolated cultured ISCs. We cultured isolated crypts, containing both ISCs and Paneth cells, from DIO and control animals. Crypt culture experiments revealed similar results as single ISC culture experiments; reduced crypt budding (proxy for ISC expansion) in enteroids formed from crypts isolated from DIO animals versus controls. These data provide indirect evidence that the decreased intrinsic ISC function cannot be rescued by the presence of Paneth cells or their secreted mediators. Since crypt culture is an indirect way to assess Paneth cell and ISC interaction, future studies should more directly evaluate the relationship between Paneth cells and ISCs during obesity. These would involve culturing control Paneth cells with DIO ISCs or DIO Paneth cells with control ISCs and assess enteroid formation.

Mechanisms underlying obesity associated ISC hyperproliferation

We were interested in the potential role of the insulin/IGF system in the observed ISC hyperproliferation in DIO animals. We evaluated mRNA levels of *Igf1r* and *Insr* (total and IR-A and IR-B) and these were not different in ISCs from DIO mice. However, mRNA levels of *Igf1r* and IR-A remained high in Sox9-EGFP Low ISCs versus all other cell populations isolated from DIO animals indicating that DIO-ISCs are still expressing the two receptors at high levels compared to other Sox9-EGFP cell populations. Insulin/IGF1 signaling is typically assessed by phosphorylation of receptors and downstream signaling molecules such as IRS-1. Numbers of Sox9-EGFP Low

cells were not high enough to yield sufficient protein to look at regulation of receptor or IRS phosphorylation. Evidence for effect of insulin on ISC stem from significant positive correlations between plasma insulin and ISC number. The fact that excess insulin or IGF1 rescued the intrinsic enteroid-forming defect in ISCs from DIO mice provides important evidence for altered response to insulin/IGF. We propose that long-term exposure to high insulin or IGF1 levels promotes ISC 'dependence' on these levels. Future studies to directly examine molecular mediators linked to differential response would be of interest. Recent studies from our lab have shown that IGF1 treatment by osmotic mini-pump increases the number of Sox9-EGFP Low ISCs, indicating that IGF1 preferentially expands this cell population, similar to what we see in DIO (Van Landeghem et al, under review). This same study defines genes selectively increased in ISCs by IGF1, which could be explored in ISCs from DIO mice. However, other mediators of proliferation that are increased during obesity exist. Figure 4.3 illustrates potential mediators such as pro-inflammatory cytokines and adipokines and ER stress that can contribute to ISC hyperproliferation and are topics that should be explored further.

Cytokines and adipokines

The link between intestinal inflammation and cell proliferation is highlighted by the relationship between inflammation and carcinogenesis. Pro-inflammatory signaling pathways are common mediators of CRC and patients with IBD are at increased risk for developing CRC (218). Our lab has shown HFD increases intestinal inflammation and expression of pro-inflammatory cytokines such as TNFα in the intestine, prior to onset of obesity and hyperinsulinemia (76). Inflammation was apparent in multiple cell types including intestinal epithelial cells and underlying immune and endothelial cells as assessed by NFkB-GFP reporter mice indicating multiple sources of inflammation during obesity (76). Our lab has also shown cytokines can promote proliferation of CRC cell lines (219), however we do not know whether inflammatory cytokines can act specifically on ISC to promote proliferation. Gene expression data on Sox9-EGFP sorted cell populations from our lab reveals expression of TNFα receptors *Tnfr1* and *Tnfr2* on Sox9-EGFP Low ISC, indicating ISC are capable of signaling through these receptors (data not shown). Future studies employing the enteroid culture system can be used to more directly test the effect of cytokines on ISC survival or growth by assessing enteroid forming ability, size or proliferation via EdU incorporation.

Leptin, an adipokine that is positively correlated with adipose tissue size, normally functions to suppress food intake, however obese individuals are thought to have developed resistance to its anorexigenic cues. Limited

studies have looked at the effect of leptin on intestinal epithelial cells. Evidence suggested leptin promotes proliferation and inhibits apoptosis of CRC or transformed cell lines but has no mitogenic effect on non-transformed colon epithelial cell lines (220-222). The pro-proliferative effect of leptin is reported to be mediated by production of pro-inflammatory cytokine interleukin-6 (IL-6) (222). While it is unclear if leptin can promote proliferation in a normal setting, future studies can explore the effect of leptin on ISC by treating ISC or enteroids with leptin and assessing its effect on enteroid growth and survival.

ER stress

Obesity is associated with increased ER stress and chronic inflammation in adipose tissue. Obesity induced adipose tissue ER stress is thought to be due to generation of reactive oxygen species due to elevated FFA that lead to protein misfolding or unfolding (223). Evidence for the effect of ER stress on ISCs is conflicting. Heijmans et al. reported decreased *Olfm4*$^{+}$ cells following induction of intestinal epithelial ER stress by conditionally knocking out ER chaperone protein Grp78 (224), while Niederreiter et al reported an increased number of *Olfm4*$^{+}$ cells in intestinal epithelial specific Xbp1$^{-/-}$ animals (225). Despite conflicting evidence, these data indicate ER stress can affect ISC. Intestinal ER stress is linked to increased inflammation (226). Therefore, during obesity, ER stress in the intestine and surrounding mesenteric fat can contribute to increased inflammation and ISC proliferation.

It is noteworthy that Xbp1$^{-/-}$ animals do not develop Paneth cells and authors conclude this is due to inability of Paneth cells to resolve ER stress, leading them to undergo apoptosis (226). Obese subjects displayed elevated levels of ER stress proteins BiP and ATF4 associated with ER stress in Paneth cells (217). These data indicate Paneth cells may be particularly sensitive to ER stress providing a potential mechanism to explain our observed decreased Paneth cell number in DIO animals. The role of ER stress in both ISCs and Paneth cells during obesity and ISC hyperproliferation is something to be explored in the future.

Obesity, proliferation and cancer risk

Many epidemiological studies have linked diet to cancer risk. Obesity increases the risk of developing many cancers especially colon, while CR is protective against carcinogenesis (165,227). Carcinogenesis is a multistep process involving multiple genetic mutations associated with hyperproliferation. Understanding how cellular proliferation is regulated during obesity will help better establish molecular mechanisms underlying tumor formation. While the goals of this dissertation were not to directly study obesity and carcinogenesis, our data point to some potential mechanisms that may link obesity to tumor formation.

Obesity, ISC hyperproliferation and cancer

Hyperproliferation of ISCs as occurs in DIO increases the statistical probability of acquiring genetic mutations that promote tumor formation. Evidence suggests that mutations in ISCs are an initial event that can lead to tumor initiation. *Apc* deletion in *Lgr5*$^{+}$ or *Lrig1*$^{+}$ ISCs resulted in adenoma formation suggesting that mutations acquired in ISC are the cells of origin in intestinal adenomas (228,229). ISC hyperproliferation as seen in DIO may be one mechanism by which obesity is associated with increased risk for tumor formation. Our studies explored the effect of DIO on jejunal ISCs because the jejunum is the main site of nutrient absorption and the ISC are best characterized in the jejunum, however it is currently not known whether ISC hyperproliferation due to DIO occurs in the colon. This would be of great interest as colon tumors are more common than small intestinal tumors. Fortunately, the Sox9-EGFP reporter model also marks CSC and can be used to assess effects of obesity on CSC (230). To understand the role of DIO induced ISC expansion and hyperproliferation in the setting of carcinogenesis, future studies can use the Apc^{Min+} model or azoxymethane/dextran sodium sulfate (AOM/DSS) model of intestinal tumorigenesis in the Sox9-EGFP reporter mouse. The ability to sort Sox9-EGFP Low ISCs from these animals can allow for interrogation of frequency of known mutations linked to tumor initiation in ISCs isolated from obese animals. High-throughput single cell analysis is currently available (215) to assess the number of ISC with mutations in *Apc, B-catenin, Kras* and *p53*. We would hypothesize that obese animals acquire a greater number of mutations in ISCs or acquire mutations at an earlier time point compared to controls (Figure 4.4). These studies would provide novel analysis of obesity induced, ISC specific mutations that can result in tumorigenesis. One limitation of the Sox9-EGFP model is that the differential expression profile of Sox9-EGFP in CSC versus progenitors is not as clear or well defined as in the small intestine. In fact overall CSC are less well characterized than in the ISC of the small intestine. Other models of CSC could be useful (3,8). Our lab also has the Lgr5-EGFP reporter, which is well accepted. Another issue is whether the tumor environment affects reporter expression. High-level Sox9-EGFP expression has been noted in tumors (230) but could reflect tumor environment activating the Sox9-EGFP reporter rather than expanded ISCs.

Role of the intestinal microbiota in proliferation

The intestinal microbiota exists in a symbiotic relationship with the host to aid in host defense, immunity and nutrient absorption. It is becoming more apparent that the changes in microbial composition can alter many biological processes. Studies in germ free animals and microbiota transfer studies highlight the contribution of the

microbiota to host health during obesity and provide the potential use of microbes as therapeutic strategies (85,89,231-235). Therefore, it is important to understand potential roles of the microbiota in obesity associated ISC expansion.

Obesity, microbiota and ISC proliferation

Seminal studies evaluating the effect of diet on the intestinal microbiota have provided evidence that microbiota composition in obesity is significantly altered compared to controls, where obesity decreases the abundance of Bacteroidetes while increasing abundance of Firmicutes (83-85). Whether changes in microbiota composition during obesity can affect ISC expansion and proliferation is unknown. Host recognition of bacterial products occurs through Toll-like receptors (TLRs) and Nod receptors. Although via different pathways, both TLR and Nod signaling converge on activation of NFkB and increased production of pro-inflammatory cytokines and chemokines, which may affect proliferation. Nigro et al showed that ISCs express high levels of *Nod2* mRNA and treatment of ISCs with a Nod2 agonist yielded greater enteroid formation compared to *Nod2*$^{-/-}$ ISCs indicating a role for bacterial signaling in ISC function (236). These data begin to define the relationship between microbes and ISC function and this is an area that warrants increased attention. *In silico* analyses of our microarray dataset of Sox9-EGFP cell populations confirmed prior knowledge that the intestinal epithelium expresses TLRs and Nod receptors (237-239). However, with our dataset, we were able to further assess expression in different intestinal epithelial cell populations and found that *Tlr2*, *4* and *5* were enriched in Sox9-EGFP Low and High cells while *Tlr3* and *9* were enriched in Sox9-EGFP Negative cells. Identifying microbial sub-types that express activators of TLRs enriched in Sox9-EGFP Low and High cells to promote cell proliferation can provide novel insights on the relationship between the microbiota and ISCs such as LPS, which is elevated during obesity and binds/signals through TLR4. Future studies can use the enteroid culture system to treat enteroids with specific bacterial products that activate TLRs or Nod receptors to assess effects on ISC proliferation. Additionally, we have derived Sox9-EGFP animals under germ free conditions to assess the role of the microbiota in DIO associated ISC expansion and proliferation. If the DIO associated effects on ISC are due to the microbiome, colonization of germ-free Sox9-EGFP mice with microbes from control and DIO animals should recapitulate our observed results in conventionally raised animals.

The intestinal microbiome can also be shaped by antimicrobial secretions derived from Paneth cells (240). Therefore changes in Paneth cell number or secretions during obesity may have an effect on microbiome composition. Changes in mRNAs encoding Paneth cell secretions are altered in obese mice (216) and humans (217).

Interestingly, mice deficient for MMP7, an enzyme required for the processing of alpha-defensins – an antimicrobial peptide secreted by Paneth cells, display a change in their microbiota composition favoring *Firmicutes*, similar to what is seen in obese humans (50,85). Evaluating Paneth cell secretions, particularly levels of alpha-defensins, from obese and lean mice may provide novel evidence linking altered Paneth cells to obese microbiome.

Intestinal adaptation to intermittent feeding

Effect of ADF on ISCs, progenitors and intestinal proliferation in jejunum

Figure 4.5 summarizes the effects of ADF on the intestine. We found no effect of ADF on ISC number or ISC proliferation. Evaluating ISC number or proliferation at earlier time points are of interest for future studies as changes might occur at earlier time points after start of ADF. These data are different than what was observed during CR. CR increased number of *Olfm4*$^{+}$ ISCs and CR crypts yielded greater number of enteroids compared to *ad libitum* fed controls (121), indicating that ISC responses to CR and ADF are different. Future studies will test ISC function in ADF animals using ISC and crypt culture methods.

Despite no effect on ISC number or proliferation, ADF significantly increased the pool of non-proliferating progenitors after a fast cycle, which is reversed following a feed cycle. These data support a model where progenitors are highly responsive to feed and fast cycles of ADF by maintaining a large progenitor pool during fasting and rapidly mobilizing the pool to increase differentiated cells during feeding (Figure 4.5). Decreased progenitor proliferation can be explained by increased cell-cycle time. Studies using DNA labels to mark proliferating cells and monitoring time of label washout can provide evidence for differences in cell-cycle time during feed and fast periods. Restoration of progenitor pool following feeding indicates rapid differentiation to handle incoming food. Therefore, intestines of ADF animals could be more efficient at digesting and absorbing nutrients in the proximal small intestine (Figure 4.6). Radiolabeled or fluorescent-conjugated glucose or fatty acids could be administered by oral gavage and radioactivity or fluorescence can be measured in intestinal segments to assess changes in absorption rates and location as well as evaluation of nutrient transporters along the length of the small intestine.

Effect of ADF on colonic epithelium

We reported a significant decrease in colonic epithelial proliferation in ADF animals following a fast cycle compared to *ad libitum* fed controls after same fast cycle. In the colon, fasting doubled while refeeding shortened cell-cycle time (212). Decreased colon proliferation in ADF mice after a fast cycle can be attributed to increased

cell-cycle time and can be assessed as described above for the jejunum. Decreased colon cell proliferation is of great interest, since intestinal cancers are commonly found in the colon and is discussed more below.

Mechanisms underlying decreased proliferation in ADF animals

Factors that are increased during obesity that underlie increased proliferation may mediate decreased proliferation during ADF. Ongoing studies are evaluating potential mechanisms that contribute to changes in proliferation in ADF mice including inflammation, insulin/IGF1 pathway and the intestinal microbiome (discussed in later sections).

Inflammation and ADF

Other diet restriction regimens lowered mRNAs of pro-inflammatory cytokines in white adipose tissue (119). As described above, pro-inflammatory cytokines promoted proliferation in CRC cell lines (219). Investigating gene expression of pro-inflammatory mediators such as TNFα and IL-6 in the intestine, surrounding mesenteric adipose tissue and gonadal adipose tissue will be of interest to test whether ADF animals display decreased inflammation compared to controls (Figure 4.7).

Insulin and IGF1 and ADF

The insulin/IGF1 pathway is a well-documented pathway that exerts trophic effects on the intestine. There is debate as to whether ADF decreases insulin and IGF1 levels as studies have reported conflicting results (103). We reported no change in fasting insulin levels in ADF mice compared to controls, however observed increased IGF1 in ADF animals. Although relatively greater than controls, absolute IGF1 levels were still lower than traditionally reported in mice. Our lab has shown that IR isoform expression can dictate cell proliferation (139). Forced IR-B expression decreased proliferation of CRC cell lines, indicating the role of the metabolic IR in limiting proliferation. We observed a significant increase in IR-B expression in ADF colons compared to controls. This effect was also observed in jejunum (data not shown). One limitation is these data are they were assessed in whole thickness tissue. Ongoing studies on isolated epithelium are directly testing whether increased IR-B expression is present in epithelial cells. We are also able to directly assess if ADF increases IR-B in specific cell types of the small intestinal epithelium, most notably progenitors and ISCs, using the Sox9-EGFP mouse. We would predict Sox9-EGFP Sublow progenitors would express higher levels of IR-B in ADF animals compared to controls, linking IR isoform switching to ADF effects on intestinal epithelial proliferation (Figure 4.7). If ADF does promote IR isoform switching, future studies will look at splicing factors responsible for promoting or inhibiting IR-A versus IR-B

production. This would provide novel evidence that diet is able to affect IR isoform expression by regulating IR splicing.

ADF, decreased proliferation and cancer

ADF animals displayed decreased intestinal proliferation compared to controls consistent with studies in other tissues (104,105,117). There is evidence that ADF is protective against carcinogen/mutagen-induced carcinogenesis (115,116). Decreased colon proliferation is of interest because it is the major site of intestinal cancers. Ongoing studies in the lab are exploring ADF in the setting of intestinal tumorigenesis using the $Apc^{Min/+}$ mouse model. Tumor number and load will be quantified and we predict that ADF animals will display lower numbers of tumors consistent with our decreased proliferation phenotype. This would test primarily the effect of ADF on small intestinal tumors, as $Apc^{Min/+}$ is a model of genetically induced small intestinal tumorigenesis. ADF decreases proliferation in both small intestine and colon. Therefore we can also test the impact of ADF on inflammation associated colon tumorigenesis using the AOM/DSS model and assess tumor formation between ADF and controls. Decreased proliferation due to ADF may be a mechanism by which ADF or other intermittent feeding diets can decrease risk of colon tumor formation, which further promotes this diet as clinically relevant.

Metabolic adaptations to ADF

There was no difference in net food intake or activity between ADF and control animals. Despite this, ADF animals show no increase in body weight over 20 weeks and have reduced body fat relative to *ad libitum* controls (Figure 4.5). During a feed period, ADF mice have a RER near 1.0, indicating animals are using primarily carbohydrates for energy compared to controls, which use both carbohydrates and lipids for energy production during feeding (RER = 0.85). Chausse et al reported similar RER in ADF mice, however found no difference in RER between ADF and controls (241). Differences in results are likely due to the length of intervention. Chausse et al. maintained their animals on ADF for 3 weeks (241), while we examined the chronic effects by subjecting animals to 20 weeks of ADF. This indicates that animals do not adapt by burning more carbohydrates after 3 weeks on ADF and require a longer period. This is a potentially important observation that duration of ADF or other intermittent feeding strategies may be critical to maximize benefit and utilization of carbohydrates. Excess carbohydrates are typically turned into fat by converting glucose to acetyl CoA, a precursor for TG synthesis. The greater efficiency of ADF fed animals to burn carbohydrates provides a mechanism to avoid accumulating excess fat. We do not observe differences in gonadal fat mass between ADF animals after a fed and fast period, indicating

animals are not storing excess carbohydrates consumed on feed days. Instead, ADF animals can be storing excess glucose as glycogen in the liver. Recently published studies show diet restriction alters hepatic glucose metabolism (118,119). Ongoing studies are exploring changes in hepatic liver enzymes related to glycolysis, gluconeogenesis, lipid synthesis and β-oxidation as well as glycogen content to link ADF in our model to improvements in metabolism.

The intestinal microbiota in ADF: effects on metabolism and proliferation

As described earlier, changes in the intestinal microbiota can dictate host health and physiology. The intestinal microbiota aids in nutrient metabolism and regulating epithelial proliferation, making it an intriguing link between the intestinal and metabolic effects of ADF.

Microbiota changes in ADF mice that promote carbohydrate digestion

ADF animals maintain their body weight while decreasing fat mass, despite similar food intake and activity compared to controls. We have shown to our knowledge for the first time that this phenotype is associated with animals utilizing carbohydrates for energy production when fed compared to controls. Because a function of the microbiome is to extract and harvest nutrients from ingested food, ongoing studies are evaluating changes in microbial communities between groups. We predict that the microbiota composition of ADF animals would favor carbohydrate digestion and absorption. A microbiome with increased abundance of Bacteroidetes and Actinobacteria and decreased abundance of Firmicutes are seen during fasting as well as high polysaccharide diet consumption compared to control or Western style diets (242,243) and we predict ADF animals would exhibit similar microbial profiles. Table 4.1 lists a small set of bacteria we hypothesize would be changed in ADF animals due to their roles in carbohydrate metabolism and intestinal proliferation.

Although our understanding of the microbiome has increased in the past decade through the development of high-throughput genomic approaches, understanding the functions of various microbial communities are not advancing at the same pace. Current views are that diet is one major factor that contributes to microbiome differences, however there is limited work on specific bacteria and their designated roles in nutrient metabolism. Carbohydrates are broken down into fermentable monosaccharides by specific microbial derived enzymes called carbohydrate active enzymes (CAZymes) to generate products such as SCFA prior to absorption. Without these enzymes, complex carbohydrates are unable to be fully broken down and would be unavailable to be used by the host. Characterization and regulation of CAZymes have yet to be fully explored. However metagenomic sequencing

of the human microbiota has provided a set of predicted bacteria that potentially contain CAZymes, linking their genomes to carbohydrate metabolism (244). There are >3000 bacteria identified so far to encode for CAZymes and that number is most likely increasing as sequencing data becomes available. We can utilize these data to interrogate our microbiome sequencing obtained from ADF animals. For example, the bacterial genus *Bacteroides* (from the Bacteroidetes phylum) have been shown to be able to degrade polysaccharides and are highly prevalent in the human colon. Levels of *B. thetaiotaomicron*, a member of the *Bacteroides* genus, were positively associated with presence of dietary polysaccharides (245). *Bifidobacterium*, a genus of the Actinobacteria phylum, contains gene sequences linked to carbohydrate metabolism and has been reported to attach and degrade starch particles (246). Recently, the role of Firmicutes in carbohydrate metabolism has begun to be explored. For example, *R. intestinalis*, member of the *Roseburia* genus, has been shown to play roles in carbohydrate degradation and production of the SCFA butyrate, propionate and acetate (244). Butyrate is used by colonocytes for energy and has been shown to be associated with beneficial effects on the colon including anti-inflammatory properties and CRC prevention (247). Propionate has been shown to modulate satiety and glucose homeostasis by promoting EEC hormones peptide YY and GLP-1 but also is a gluconeogenic substrate, which would be counterintuitive if it acts to promote glucose homeostasis. De Vadder et al report that propionate and butyrate increased intestinal gluconeogenesis (before reaching the liver) and activated targets in the brain leading to decreased hepatic gluconeogenesis, improved glucose homeostasis and adiposity (248). Intestinal gluconeogenesis occurs during fasting periods (249). Changes in intestinal gluconeogenesis can also be measured by intestinal gene expression on key gluconeogenic genes such as *Pepck* and *G6pc*. We would hypothesize that the microbiota of ADF animals contain more SCFA-producing bacteria. These data would provide evidence for ADF induced microbial changes that influence nutrient digestion and metabolism.

Microbiota changes in ADF mice associated with decreased intestinal proliferation

In addition to changes in adiposity and carbohydrate metabolism, our data showed significant reductions in both small intestine and colonic epithelial proliferation in ADF animals. Microbial communities can also regulate proliferation and we predict increases in microbes linked to decreased proliferation in ADF animals. For example, *L. murinus*, a member of the *Lactobacillus* genus, is decreased during starvation and reappears following refeeding and has been shown to promote colonic epithelial proliferation via its production of lactate (250). Therefore we

hypothesize that the microbiome of ADF animals will have decreased *L. murinus* and other lactate-producing bacteria, linking altered microbiota to intestinal proliferation.

A recent study by Zarrinpar et al. looked at the effect of time restricted feeding on the intestinal microbiome (120). The goal of their study was to compare restricted feeding and *ad libitum* feeding using HFD as a potential nutritional intervention. They reported microbial differences between animals that were fed HFD *ad libitum* compared to animals that fed chow *ad libitum* or were restricted with HFD, indicating that restricted feeding with HFD produces a microbiome similar to a chow fed animal (120). However they did not compare the microbiome differences between *ad libitum* versus restricted chow fed animals. Our microbiome data from ADF animals will address this gap and based on our data, we predict changes in the microbiome consistent with the phenotype observed in our ADF animals.

Significance and Conclusions

With the identification and validation of ISC biomarkers and generation of mouse models that mark ISCs *in vivo*, we were able to define the functional effects of obesity and intermittent feeding on ISC. DIO selectively expanded the number of ISC associated with increased ISC proliferation, and decreased number of Paneth and goblet cells. Surprisingly, intrinsic ISC function was decreased in ISCs isolated from DIO animals, but was rescued with the addition of excess insulin or IGF1, indicating DIO-ISCs become dependent on the insulin/IGF-rich environment *in vivo* for intrinsic function. This work has provided the foundation for future studies in identifying the clinical implications of ISCs hyperproliferation and decreased Paneth and goblet cells linking obesity to intestinal health. We have also defined the effects of ADF, a clinically relevant diet, on the intestine and showed that ADF slowed intestinal proliferation, decreased body fat and prevented body weight gain associated with changes in carbohydrate utilization and the intestinal microbiota without changes in food intake or activity. Our work adds to emerging evidence that ADF produces beneficial effects on metabolic health and proliferative activity. Because of the poor adherence rates to CR, there is a need for increased attention to ADF or other intermittent feeding diets as an alternative to improving body weight, metabolic health and chronic disease risk in humans. Findings from both our DIO and ADF studies have unveiled the importance of understanding how both can affect ISCs, which can have downstream effects on intestinal and whole body health.

Figures and Tables

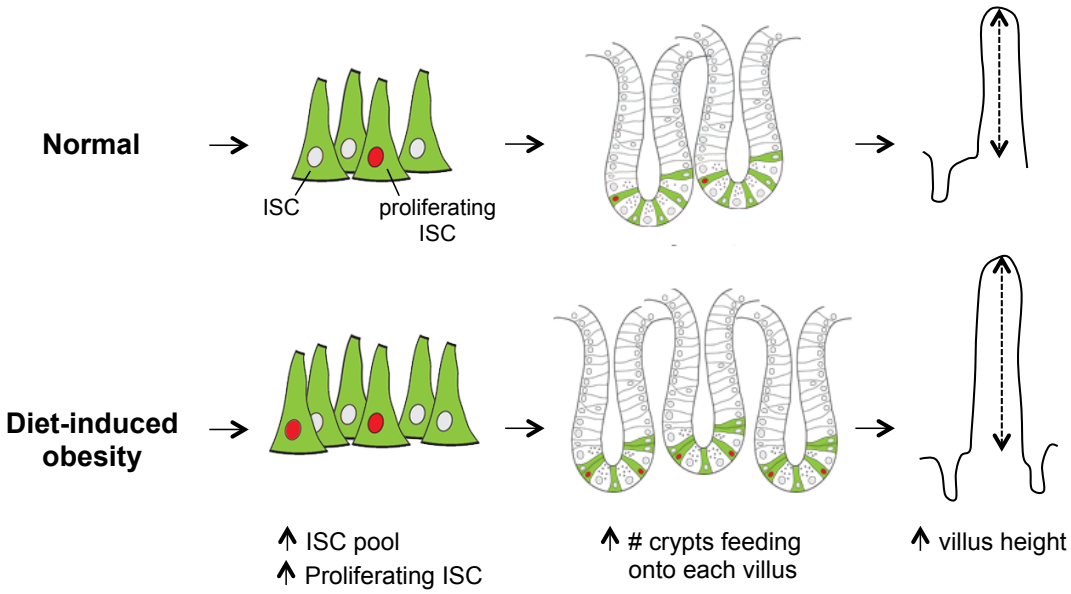

Figure 4.1: Diet-induced obesity (DIO) selectively expands number of total and proliferating ISCs.
Our data provides a model where DIO selectively increases the ISC number and ISC proliferation associated with increased number of crypts feeding onto each villus (crypt density) resulting in increased villus height.

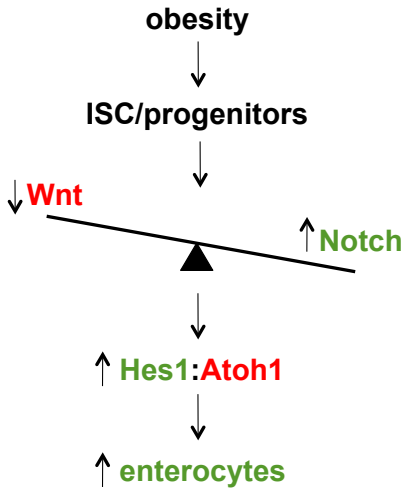

Figure 4.2: Obesity favors enterocyte lineage by increasing Notch signaling in ISCs and progenitors. Proposed model demonstrating that during obesity, Notch signaling is increased and Wnt signaling is decreased in ISCs and progenitors leading to an increase in the *Hes1*:*Atoh1* ratio thereby favoring enterocyte differentiation.

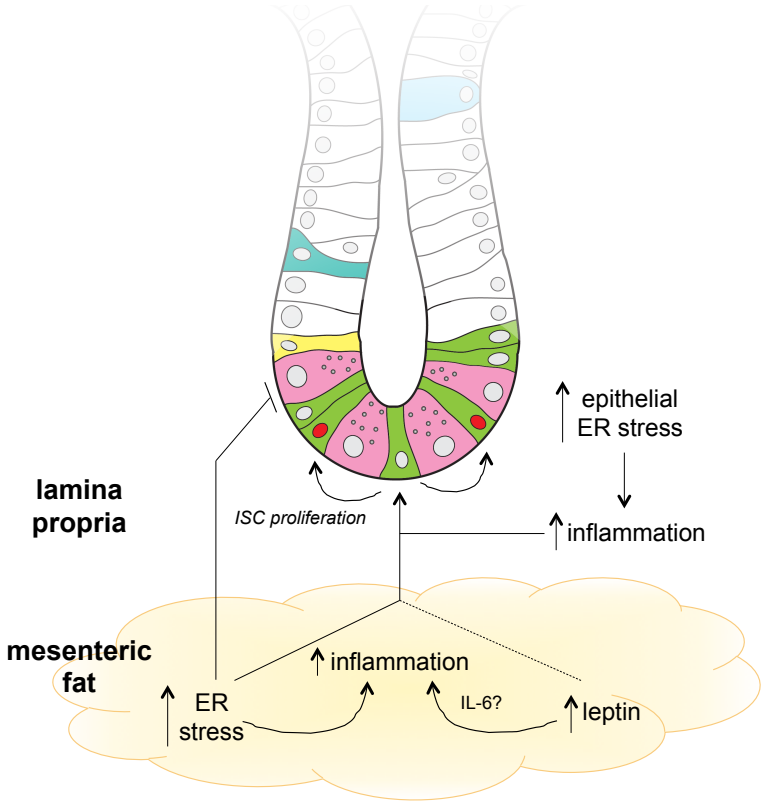

Figure 4.3: Proposed mediators of ISC hyperproliferation in obesity.
Increased levels of inflammation, leptin, and ER stress in the intestine or derived from mesenteric fat surrounding the intestine or underlying lamina propria can contribute to observed ISC hyperproliferation.

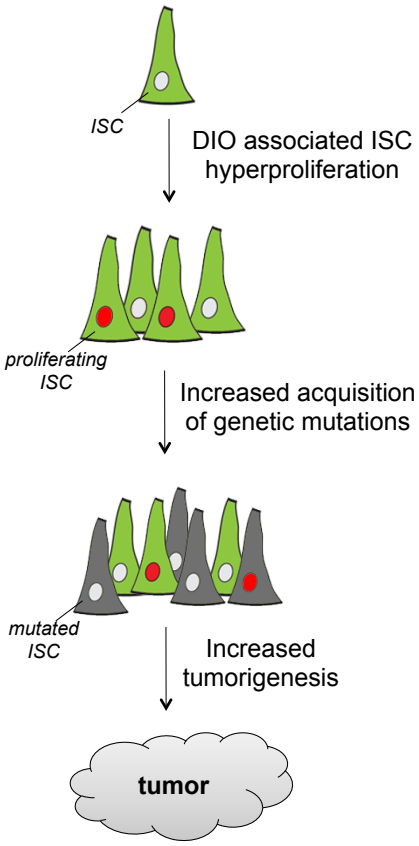

Figure 4.4: ISC hyperproliferation can increase risk of tumor formation.
Increased ISC proliferation can increase the probability of acquiring known genetic mutations linked to intestinal tumorigenesis such as *Apc, Kras* and *p53*. Mutated ISC can increase risk of tumor formation, providing a novel link between obesity and cancer.

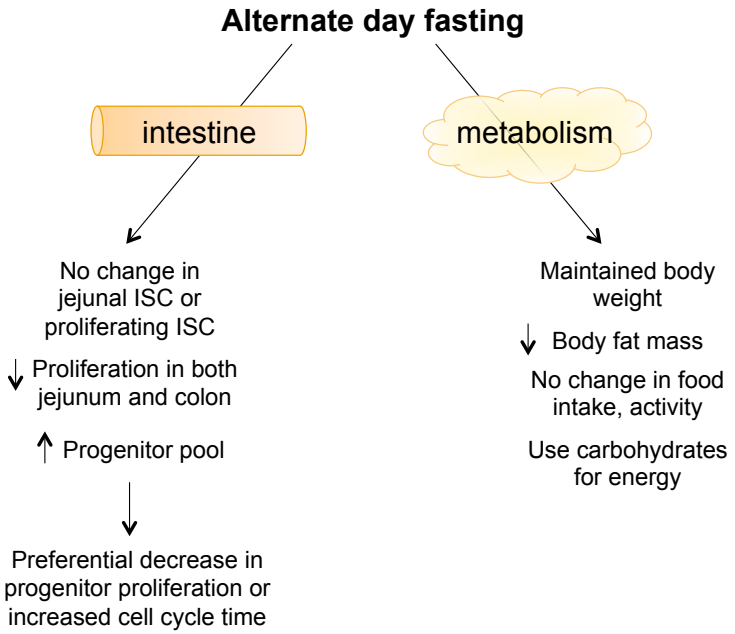

Figure 4.5: ADF improves body mass and maintains body weight while decreasing intestinal proliferation. Our data provides novel evidence that ADF affects the intestinal epithelium by decreasing jejunal and colonic epithelial proliferation and preferentially regulating the pool of progenitors during cycles of feed and fast. ADF also proves to be a diet strategy that potentially has implications for improving metabolic health by decreasing body mass, preventing weight gain and favoring carbohydrate burning, despite no change in food intake or activity.

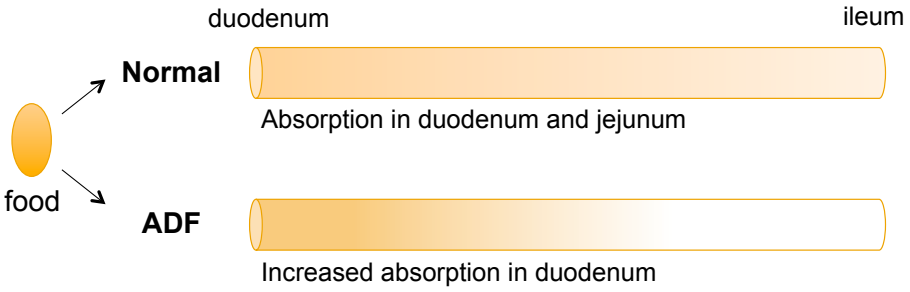

Figure 4.6: Increased absorption efficiency in intestines of ADF animals.
Proposed mechanism that ADF intestines are more efficient at harvesting nutrients from food leading to greater digestion and absorption occurring in the proximal small intestine (duodenum) leaving little food remaining in distal regions (ileum).

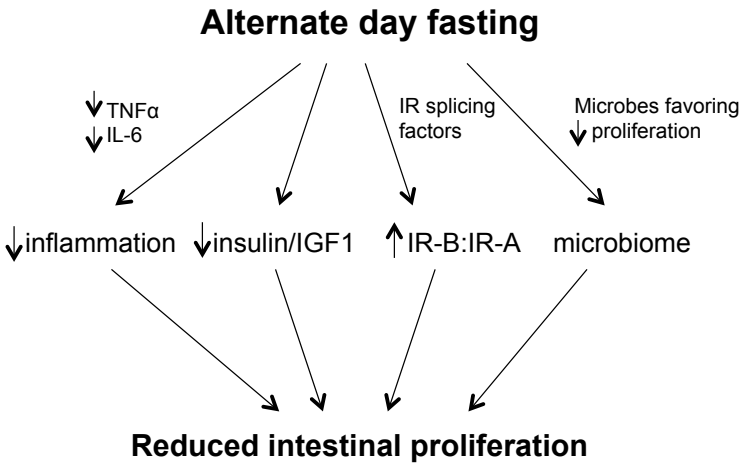

Figure 4.7: Proposed mediators of decreased intestinal proliferation in ADF animals.
Ongoing studies are evaluating the effects of ADF on intestinal inflammation, insulin/IGF1, IR isoform expression and microbiome as potential mechanisms explaining decreased proliferation.

Table 4.1: Predicted bacteria changed in microbiome of ADF animals

Phylum	Genus	Species	Function
Bacteroidetes	Bacteroides	*B. thetaiotaomicron*	Carbohydrate metabolism
Actinobacteria	Bifidobacterium	*B. adolescentis*	Carbohydrate metabolism
Firmicutes	Roseburia	*R. intestinalis*	Carbohydrate metabolism SCFA production
	Lactobacillus	*L. murinus*	Proliferation Lactate production

Green – predicted to increase in ADF animals; Red – predicted to decrease in ADF animals

REFERENCES

1. Cheng H, Leblond CP. Origin, differentiation and renewal of the four main epithelial cell types in the mouse small intestine. V. Unitarian Theory of the origin of the four epithelial cell types. *The American journal of anatomy.* 1974;141(4):537-561.

2. Potten CS, Kovacs L, Hamilton E. Continuous labelling studies on mouse skin and intestine. *Cell and tissue kinetics.* 1974;7(3):271-283.

3. Barker N, van Es JH, Kuipers J, Kujala P, van den Born M, Cozijnsen M, Haegebarth A, Korving J, Begthel H, Peters PJ, Clevers H. Identification of stem cells in small intestine and colon by marker gene Lgr5. *Nature.* 2007;449(7165):1003-1007.

4. Schuijers J, van der Flier LG, van Es J, Clevers H. Robust cre-mediated recombination in small intestinal stem cells utilizing the olfm4 locus. *Stem cell reports.* 2014;3(2):234-241.

5. Sangiorgi E, Capecchi MR. Bmi1 is expressed in vivo in intestinal stem cells. *Nature genetics.* 2008;40(7):915-920.

6. Takeda N, Jain R, LeBoeuf MR, Wang Q, Lu MM, Epstein JA. Interconversion between intestinal stem cell populations in distinct niches. *Science.* 2011;334(6061):1420-1424.

7. Montgomery RK, Carlone DL, Richmond CA, Farilla L, Kranendonk ME, Henderson DE, Baffour-Awuah NY, Ambruzs DM, Fogli LK, Algra S, Breault DT. Mouse telomerase reverse transcriptase (mTert) expression marks slowly cycling intestinal stem cells. *Proceedings of the National Academy of Sciences of the United States of America.* 2011;108(1):179-184.

8. Powell AE, Wang Y, Li Y, Poulin EJ, Means AL, Washington MK, Higginbotham JN, Juchheim A, Prasad N, Levy SE, Guo Y, Shyr Y, Aronow BJ, Haigis KM, Franklin JL, Coffey RJ. The pan-ErbB negative regulator Lrig1 is an intestinal stem cell marker that functions as a tumor suppressor. *Cell.* 2012;149(1):146-158.

9. Munoz J, Stange DE, Schepers AG, van de Wetering M, Koo BK, Itzkovitz S, Volckmann R, Kung KS, Koster J, Radulescu S, Myant K, Versteeg R, Sansom OJ, van Es JH, Barker N, van Oudenaarden A, Mohammed S, Heck AJ, Clevers H. The Lgr5 intestinal stem cell signature: robust expression of proposed quiescent '+4' cell markers. *The EMBO journal.* 2012;31(14):3079-3091.

10. Tian H, Biehs B, Warming S, Leong KG, Rangell L, Klein OD, de Sauvage FJ. A reserve stem cell population in small intestine renders Lgr5-positive cells dispensable. *Nature.* 2011;478(7368):255-259.

11. Yan KS, Chia LA, Li X, Ootani A, Su J, Lee JY, Su N, Luo Y, Heilshorn SC, Amieva MR, Sangiorgi E, Capecchi MR, Kuo CJ. The intestinal stem cell markers Bmi1 and Lgr5 identify two functionally distinct populations. *Proceedings of the National Academy of Sciences of the United States of America.* 2012;109(2):466-471.

12. Buczacki SJ, Zecchini HI, Nicholson AM, Russell R, Vermeulen L, Kemp R, Winton DJ. Intestinal label-retaining cells are secretory precursors expressing Lgr5. *Nature.* 2013;495(7439):65-69.

13. Van Landeghem L, Santoro MA, Krebs AE, Mah AT, Dehmer JJ, Gracz AD, Scull BP, McNaughton K, Magness ST, Lund PK. Activation of two distinct Sox9-EGFP-expressing intestinal stem cell populations during crypt regeneration after irradiation. *American journal of physiology Gastrointestinal and liver physiology.* 2012;302(10):G1111-1132.

14. Schofield R. The relationship between the spleen colony-forming cell and the haemopoietic stem cell. *Blood cells.* 1978;4(1-2):7-25.

15. Fre S, Hannezo E, Sale S, Huyghe M, Lafkas D, Kissel H, Louvi A, Greve J, Louvard D, Artavanis-Tsakonas S. Notch lineages and activity in intestinal stem cells determined by a new set of knock-in mice. *PloS one.* 2011;6(10):e25785.

16. Sato T, van Es JH, Snippert HJ, Stange DE, Vries RG, van den Born M, Barker N, Shroyer NF, van de Wetering M, Clevers H. Paneth cells constitute the niche for Lgr5 stem cells in intestinal crypts. *Nature.* 2011;469(7330):415-418.

17. Schroder N, Gossler A. Expression of Notch pathway components in fetal and adult mouse small intestine. *Gene expression patterns : GEP.* 2002;2(3-4):247-250.

18. Pellegrinet L, Rodilla V, Liu Z, Chen S, Koch U, Espinosa L, Kaestner KH, Kopan R, Lewis J, Radtke F. Dll1- and dll4-mediated notch signaling are required for homeostasis of intestinal stem cells. *Gastroenterology.* 2011;140(4):1230-1240 e1231-1237.

19. van Es JH, van Gijn ME, Riccio O, van den Born M, Vooijs M, Begthel H, Cozijnsen M, Robine S, Winton DJ, Radtke F, Clevers H. Notch/gamma-secretase inhibition turns proliferative cells in intestinal crypts and adenomas into goblet cells. *Nature.* 2005;435(7044):959-963.

20. Noah TK, Shroyer NF. Notch in the intestine: regulation of homeostasis and pathogenesis. *Annual review of physiology.* 2013;75:263-288.

21. Milano J, McKay J, Dagenais C, Foster-Brown L, Pognan F, Gadient R, Jacobs RT, Zacco A, Greenberg B, Ciaccio PJ. Modulation of notch processing by gamma-secretase inhibitors causes intestinal goblet cell metaplasia and induction of genes known to specify gut secretory lineage differentiation. *Toxicological sciences : an official journal of the Society of Toxicology.* 2004;82(1):341-358.

22. Riccio O, van Gijn ME, Bezdek AC, Pellegrinet L, van Es JH, Zimber-Strobl U, Strobl LJ, Honjo T, Clevers H, Radtke F. Loss of intestinal crypt progenitor cells owing to inactivation of both Notch1 and Notch2 is accompanied by derepression of CDK inhibitors p27Kip1 and p57Kip2. *EMBO reports.* 2008;9(4):377-383.

23. Wong GT, Manfra D, Poulet FM, Zhang Q, Josien H, Bara T, Engstrom L, Pinzon-Ortiz M, Fine JS, Lee HJ, Zhang L, Higgins GA, Parker EM. Chronic treatment with the gamma-secretase inhibitor LY-411,575 inhibits beta-amyloid peptide production and alters lymphopoiesis and intestinal cell differentiation. *The Journal of biological chemistry.* 2004;279(13):12876-12882.

24. Jensen J, Pedersen EE, Galante P, Hald J, Heller RS, Ishibashi M, Kageyama R, Guillemot F, Serup P, Madsen OD. Control of endodermal endocrine development by Hes-1. *Nature genetics.* 2000;24(1):36-44.

25. Suzuki K, Fukui H, Kayahara T, Sawada M, Seno H, Hiai H, Kageyama R, Okano H, Chiba T. Hes1-deficient mice show precocious differentiation of Paneth cells in the small intestine. *Biochemical and biophysical research communications.* 2005;328(1):348-352.

26. Ueo T, Imayoshi I, Kobayashi T, Ohtsuka T, Seno H, Nakase H, Chiba T, Kageyama R. The role of Hes genes in intestinal development, homeostasis and tumor formation. *Development.* 2012;139(6):1071-1082.

27. Stanger BZ, Datar R, Murtaugh LC, Melton DA. Direct regulation of intestinal fate by Notch. *Proceedings of the National Academy of Sciences of the United States of America.* 2005;102(35):12443-12448.

28. Gregorieff A, Pinto D, Begthel H, Destree O, Kielman M, Clevers H. Expression pattern of Wnt signaling components in the adult intestine. *Gastroenterology.* 2005;129(2):626-638.

29. van Es JH, Jay P, Gregorieff A, van Gijn ME, Jonkheer S, Hatzis P, Thiele A, van den Born M, Begthel H, Brabletz T, Taketo MM, Clevers H. Wnt signalling induces maturation of Paneth cells in intestinal crypts. *Nature cell biology.* 2005;7(4):381-386.

30. Smith NR, Davies PS, Silk AD, Wong MH. Epithelial and mesenchymal contribution to the niche: a safeguard for intestinal stem cell homeostasis. *Gastroenterology.* 2012;143(6):1426-1430.

31. Korinek V, Barker N, Moerer P, van Donselaar E, Huls G, Peters PJ, Clevers H. Depletion of epithelial stem-cell compartments in the small intestine of mice lacking Tcf-4. *Nature genetics.* 1998;19(4):379-383.

32. Ireland H, Kemp R, Houghton C, Howard L, Clarke AR, Sansom OJ, Winton DJ. Inducible Cre-mediated control of gene expression in the murine gastrointestinal tract: effect of loss of beta-catenin. *Gastroenterology.* 2004;126(5):1236-1246.

33. Kuhnert F, Davis CR, Wang HT, Chu P, Lee M, Yuan J, Nusse R, Kuo CJ. Essential requirement for Wnt signaling in proliferation of adult small intestine and colon revealed by adenoviral expression of Dickkopf-1. *Proceedings of the National Academy of Sciences of the United States of America.* 2004;101(1):266-271.

34. Pinto D, Gregorieff A, Begthel H, Clevers H. Canonical Wnt signals are essential for homeostasis of the intestinal epithelium. *Genes & development.* 2003;17(14):1709-1713.

35. Kim KA, Kakitani M, Zhao J, Oshima T, Tang T, Binnerts M, Liu Y, Boyle B, Park E, Emtage P, Funk WD, Tomizuka K. Mitogenic influence of human R-spondin1 on the intestinal epithelium. *Science.* 2005;309(5738):1256-1259.

36. Giles RH, van Es JH, Clevers H. Caught up in a Wnt storm: Wnt signaling in cancer. *Biochimica et biophysica acta.* 2003;1653(1):1-24.

37. Markowitz SD, Bertagnolli MM. Molecular origins of cancer: Molecular basis of colorectal cancer. *The New England journal of medicine.* 2009;361(25):2449-2460.

38. Shroyer NF, Helmrath MA, Wang VY, Antalffy B, Henning SJ, Zoghbi HY. Intestine-specific ablation of mouse atonal homolog 1 (Math1) reveals a role in cellular homeostasis. *Gastroenterology.* 2007;132(7):2478-2488.

39. Yang Q, Bermingham NA, Finegold MJ, Zoghbi HY. Requirement of Math1 for secretory cell lineage commitment in the mouse intestine. *Science.* 2001;294(5549):2155-2158.

40. VanDussen KL, Samuelson LC. Mouse atonal homolog 1 directs intestinal progenitors to secretory cell rather than absorptive cell fate. *Developmental biology.* 2010;346(2):215-223.

41. Shroyer NF, Wallis D, Venken KJ, Bellen HJ, Zoghbi HY. Gfi1 functions downstream of Math1 to control intestinal secretory cell subtype allocation and differentiation. *Genes & development.* 2005;19(20):2412-2417.

42. Jenny M, Uhl C, Roche C, Duluc I, Guillermin V, Guillemot F, Jensen J, Kedinger M, Gradwohl G. Neurogenin3 is differentially required for endocrine cell fate specification in the intestinal and gastric epithelium. *The EMBO journal.* 2002;21(23):6338-6347.

43. He XC, Zhang J, Tong WG, Tawfik O, Ross J, Scoville DH, Tian Q, Zeng X, He X, Wiedemann LM, Mishina Y, Li L. BMP signaling inhibits intestinal stem cell self-renewal through suppression of Wnt-beta-catenin signaling. *Nature genetics.* 2004;36(10):1117-1121.

44. Haramis AP, Begthel H, van den Born M, van Es J, Jonkheer S, Offerhaus GJ, Clevers H. De novo crypt formation and juvenile polyposis on BMP inhibition in mouse intestine. *Science.* 2004;303(5664):1684-1686.

45. Johansson ME, Phillipson M, Petersson J, Velcich A, Holm L, Hansson GC. The inner of the two Muc2 mucin-dependent mucus layers in colon is devoid of bacteria. *Proceedings of the National Academy of Sciences of the United States of America.* 2008;105(39):15064-15069.

46. Van der Sluis M, De Koning BA, De Bruijn AC, Velcich A, Meijerink JP, Van Goudoever JB, Buller HA, Dekker J, Van Seuningen I, Renes IB, Einerhand AW. Muc2-deficient mice spontaneously develop colitis, indicating that MUC2 is critical for colonic protection. *Gastroenterology.* 2006;131(1):117-129.

47. Clevers HC, Bevins CL. Paneth cells: maestros of the small intestinal crypts. *Annual review of physiology.* 2013;75:289-311.

48. Hodin CM, Lenaerts K, Grootjans J, de Haan JJ, Hadfoune M, Verheyen FK, Kiyama H, Heineman E, Buurman WA. Starvation compromises Paneth cells. *The American journal of pathology.* 2011;179(6):2885-2893.

49. Teltschik Z, Wiest R, Beisner J, Nuding S, Hofmann C, Schoelmerich J, Bevins CL, Stange EF, Wehkamp J. Intestinal bacterial translocation in rats with cirrhosis is related to compromised Paneth cell antimicrobial host defense. *Hepatology.* 2012;55(4):1154-1163.

50. Salzman NH, Hung K, Haribhai D, Chu H, Karlsson-Sjoberg J, Amir E, Teggatz P, Barman M, Hayward M, Eastwood D, Stoel M, Zhou Y, Sodergren E, Weinstock GM, Bevins CL, Williams CB, Bos NA. Enteric defensins are essential regulators of intestinal microbial ecology. *Nature immunology.* 2010;11(1):76-83.

51. van der Flier LG, Clevers H. Stem cells, self-renewal, and differentiation in the intestinal epithelium. *Annual review of physiology.* 2009;71:241-260.

52. Furness JB, Rivera LR, Cho HJ, Bravo DM, Callaghan B. The gut as a sensory organ. *Nature reviews Gastroenterology & hepatology.* 2013;10(12):729-740.

53. Sato T, Vries RG, Snippert HJ, van de Wetering M, Barker N, Stange DE, van Es JH, Abo A, Kujala P, Peters PJ, Clevers H. Single Lgr5 stem cells build crypt-villus structures in vitro without a mesenchymal niche. *Nature.* 2009;459(7244):262-265.

54. Stelzner M, Helmrath M, Dunn JC, Henning SJ, Houchen CW, Kuo C, Lynch J, Li L, Magness ST, Martin MG, Wong MH, Yu J. A nomenclature for intestinal in vitro cultures. *American journal of physiology Gastrointestinal and liver physiology.* 2012;302(12):G1359-1363.

55. Li N, Yousefi M, Nakauka-Ddamba A, Jain R, Tobias J, Epstein JA, Jensen ST, Lengner CJ. Single-cell analysis of proxy reporter allele-marked epithelial cells establishes intestinal stem cell hierarchy. *Stem cell reports.* 2014;3(5):876-891.

56. Formeister EJ, Sionas AL, Lorance DK, Barkley CL, Lee GH, Magness ST. Distinct SOX9 levels differentially mark stem/progenitor populations and enteroendocrine cells of the small intestine epithelium. *American journal of physiology Gastrointestinal and liver physiology.* 2009;296(5):G1108-1118.

57. Gracz AD, Ramalingam S, Magness ST. Sox9 expression marks a subset of CD24-expressing small intestine epithelial stem cells that form organoids in vitro. *American journal of physiology Gastrointestinal and liver physiology.* 2010;298(5):G590-600.

58. van der Flier LG, van Gijn ME, Hatzis P, Kujala P, Haegebarth A, Stange DE, Begthel H, van den Born M, Guryev V, Oving I, van Es JH, Barker N, Peters PJ, van de Wetering M, Clevers H. Transcription factor achaete scute-like 2 controls intestinal stem cell fate. *Cell.* 2009;136(5):903-912.

59. Ogden CL, Carroll MD, Kit BK, Flegal KM. Prevalence of childhood and adult obesity in the United States, 2011-2012. *JAMA.* 2014;311(8):806-814.

60. Geiss LS, Wang J, Cheng YJ, Thompson TJ, Barker L, Li Y, Albright AL, Gregg EW. Prevalence and incidence trends for diagnosed diabetes among adults aged 20 to 79 years, United States, 1980-2012. *JAMA.* 2014;312(12):1218-1226.

61. Cani PD, Amar J, Iglesias MA, Poggi M, Knauf C, Bastelica D, Neyrinck AM, Fava F, Tuohy KM, Chabo C, Waget A, Delmee E, Cousin B, Sulpice T, Chamontin B, Ferrieres J, Tanti JF, Gibson GR, Casteilla L, Delzenne NM, Alessi MC, Burcelin R. Metabolic endotoxemia initiates obesity and insulin resistance. *Diabetes.* 2007;56(7):1761-1772.

62. Johnson AR, Milner JJ, Makowski L. The inflammation highway: metabolism accelerates inflammatory traffic in obesity. *Immunological reviews.* 2012;249(1):218-238.

63. Kahn SE, Hull RL, Utzschneider KM. Mechanisms linking obesity to insulin resistance and type 2 diabetes. *Nature.* 2006;444(7121):840-846.

64. Ding S, Lund PK. Role of intestinal inflammation as an early event in obesity and insulin resistance. *Current opinion in clinical nutrition and metabolic care.* 2011;14(4):328-333.

65. de Wit NJ, Bosch-Vermeulen H, de Groot PJ, Hooiveld GJ, Bromhaar MM, Jansen J, Muller M, van der Meer R. The role of the small intestine in the development of dietary fat-induced obesity and insulin resistance in C57BL/6J mice. *BMC medical genomics.* 2008;1:14.

66. Sakar Y, Duca FA, Langelier B, Devime F, Blottiere H, Delorme C, Renault P, Covasa M. Impact of high-fat feeding on basic helix-loop-helix transcription factors controlling enteroendocrine cell differentiation. *International journal of obesity.* 2014;38(11):1440-1448.

67. Batterham RL, Cohen MA, Ellis SM, Le Roux CW, Withers DJ, Frost GS, Ghatei MA, Bloom SR. Inhibition of food intake in obese subjects by peptide YY3-36. *The New England journal of medicine.* 2003;349(10):941-948.

68. Duca FA, Sakar Y, Covasa M. Combination of obesity and high-fat feeding diminishes sensitivity to GLP-1R agonist exendin-4. *Diabetes.* 2013;62(7):2410-2415.

69. Duca FA, Zhong L, Covasa M. Reduced CCK signaling in obese-prone rats fed a high fat diet. *Hormones and behavior.* 2013;64(5):812-817.

70. Baldassano S, Amato A, Cappello F, Rappa F, Mule F. Glucagon-like peptide-2 and mouse intestinal adaptation to a high-fat diet. *The Journal of endocrinology.* 2013;217(1):11-20.

71. Holst JJ. Enteroendocrine secretion of gut hormones in diabetes, obesity and after bariatric surgery. *Current opinion in pharmacology.* 2013;13(6):983-988.

72. le Roux CW, Aylwin SJ, Batterham RL, Borg CM, Coyle F, Prasad V, Shurey S, Ghatei MA, Patel AG, Bloom SR. Gut hormone profiles following bariatric surgery favor an anorectic state, facilitate weight loss, and improve metabolic parameters. *Annals of surgery.* 2006;243(1):108-114.

73. de La Serre CB, Ellis CL, Lee J, Hartman AL, Rutledge JC, Raybould HE. Propensity to high-fat diet-induced obesity in rats is associated with changes in the gut microbiota and gut inflammation. *American journal of physiology Gastrointestinal and liver physiology.* 2010;299(2):G440-448.

74. Brun P, Castagliuolo I, Di Leo V, Buda A, Pinzani M, Palu G, Martines D. Increased intestinal permeability in obese mice: new evidence in the pathogenesis of nonalcoholic steatohepatitis. *American journal of physiology Gastrointestinal and liver physiology.* 2007;292(2):G518-525.

75. Caesar R, Reigstad CS, Backhed HK, Reinhardt C, Ketonen M, Lunden GO, Cani PD, Backhed F. Gut-derived lipopolysaccharide augments adipose macrophage accumulation but is not essential for impaired glucose or insulin tolerance in mice. *Gut.* 2012;61(12):1701-1707.

76. Ding S, Chi MM, Scull BP, Rigby R, Schwerbrock NM, Magness S, Jobin C, Lund PK. High-fat diet: bacteria interactions promote intestinal inflammation which precedes and correlates with obesity and insulin resistance in mouse. *PloS one.* 2010;5(8):e12191.

77. Lam YY, Ha CW, Campbell CR, Mitchell AJ, Dinudom A, Oscarsson J, Cook DI, Hunt NH, Caterson ID, Holmes AJ, Storlien LH. Increased gut permeability and microbiota change associate with mesenteric fat inflammation and metabolic dysfunction in diet-induced obese mice. *PloS one.* 2012;7(3):e34233.

78. Brignardello J, Morales P, Diaz E, Romero J, Brunser O, Gotteland M. Pilot study: alterations of intestinal microbiota in obese humans are not associated with colonic inflammation or disturbances of barrier function. *Alimentary pharmacology & therapeutics.* 2010;32(11-12):1307-1314.

79. Pendyala S, Neff LM, Suarez-Farinas M, Holt PR. Diet-induced weight loss reduces colorectal inflammation: implications for colorectal carcinogenesis. *The American journal of clinical nutrition.* 2011;93(2):234-242.

80. Spagnuolo MI, Cicalese MP, Caiazzo MA, Franzese A, Squeglia V, Assante LR, Valerio G, Merone R, Guarino A. Relationship between severe obesity and gut inflammation in children: what's next? *Italian journal of pediatrics.* 2010;36:66.

81. Tiihonen K, Ouwehand AC, Rautonen N. Effect of overweight on gastrointestinal microbiology and immunology: correlation with blood biomarkers. *The British journal of nutrition.* 2010;103(7):1070-1078.

82. Delzenne NM, Cani PD. Interaction between obesity and the gut microbiota: relevance in nutrition. *Annual review of nutrition.* 2011;31:15-31.

83. Ley RE, Backhed F, Turnbaugh P, Lozupone CA, Knight RD, Gordon JI. Obesity alters gut microbial ecology. *Proceedings of the National Academy of Sciences of the United States of America.* 2005;102(31):11070-11075.

84. Turnbaugh PJ, Backhed F, Fulton L, Gordon JI. Diet-induced obesity is linked to marked but reversible alterations in the mouse distal gut microbiome. *Cell host & microbe.* 2008;3(4):213-223.

85. Turnbaugh PJ, Ley RE, Mahowald MA, Magrini V, Mardis ER, Gordon JI. An obesity-associated gut microbiome with increased capacity for energy harvest. *Nature.* 2006;444(7122):1027-1031.

86. Remely M, Tesar I, Hippe B, Gnauer S, Rust P, Haslberger AG. Gut microbiota composition correlates with changes in body fat content due to weight loss. *Beneficial microbes.* 2015:1-9.

87. Zhang H, DiBaise JK, Zuccolo A, Kudrna D, Braidotti M, Yu Y, Parameswaran P, Crowell MD, Wing R, Rittmann BE, Krajmalnik-Brown R. Human gut microbiota in obesity and after gastric bypass. *Proceedings of the National Academy of Sciences of the United States of America.* 2009;106(7):2365-2370.

88. Hildebrandt MA, Hoffmann C, Sherrill-Mix SA, Keilbaugh SA, Hamady M, Chen YY, Knight R, Ahima RS, Bushman F, Wu GD. High-fat diet determines the composition of the murine gut microbiome independently of obesity. *Gastroenterology.* 2009;137(5):1716-1724 e1711-1712.

89. Backhed F, Manchester JK, Semenkovich CF, Gordon JI. Mechanisms underlying the resistance to diet-induced obesity in germ-free mice. *Proceedings of the National Academy of Sciences of the United States of America.* 2007;104(3):979-984.

90. Everard A, Belzer C, Geurts L, Ouwerkerk JP, Druart C, Bindels LB, Guiot Y, Derrien M, Muccioli GG, Delzenne NM, de Vos WM, Cani PD. Cross-talk between Akkermansia muciniphila and intestinal epithelium controls diet-induced obesity. *Proceedings of the National Academy of Sciences of the United States of America.* 2013;110(22):9066-9071.

91. Santacruz A, Collado MC, Garcia-Valdes L, Segura MT, Martin-Lagos JA, Anjos T, Marti-Romero M, Lopez RM, Florido J, Campoy C, Sanz Y. Gut microbiota composition is associated with body weight, weight gain and biochemical parameters in pregnant women. *The British journal of nutrition.* 2010;104(1):83-92.

92. Shin NR, Lee JC, Lee HY, Kim MS, Whon TW, Lee MS, Bae JW. An increase in the Akkermansia spp. population induced by metformin treatment improves glucose homeostasis in diet-induced obese mice. *Gut.* 2014;63(5):727-735.

93. Donohoe DR, Holley D, Collins LB, Montgomery SA, Whitmore AC, Hillhouse A, Curry KP, Renner SW, Greenwalt A, Ryan EP, Godfrey V, Heise MT, Threadgill DS, Han A, Swenberg JA, Threadgill DW, Bultman SJ. A gnotobiotic mouse model demonstrates that dietary fiber protects against colorectal tumorigenesis in a microbiota- and butyrate-dependent manner. *Cancer discovery.* 2014;4(12):1387-1397.

94. Reddy BS. Role of dietary fiber in colon cancer: an overview. *The American journal of medicine.* 1999;106(1A):16S-19S; discussion 50S-51S.

95. Kuo SM. The interplay between fiber and the intestinal microbiome in the inflammatory response. *Advances in nutrition.* 2013;4(1):16-28.

96. Mao J, Hu X, Xiao Y, Yang C, Ding Y, Hou N, Wang J, Cheng H, Zhang X. Overnutrition stimulates intestinal epithelium proliferation through beta-catenin signaling in obese mice. *Diabetes.* 2013;62(11):3736-3746.

97. Verdam FJ, Greve JW, Roosta S, van Eijk H, Bouvy N, Buurman WA, Rensen SS. Small intestinal alterations in severely obese hyperglycemic subjects. *The Journal of clinical endocrinology and metabolism.* 2011;96(2):E379-383.

98. Dansinger ML, Gleason JA, Griffith JL, Selker HP, Schaefer EJ. Comparison of the Atkins, Ornish, Weight Watchers, and Zone diets for weight loss and heart disease risk reduction: a randomized trial. *JAMA.* 2005;293(1):43-53.

99. Das SK, Gilhooly CH, Golden JK, Pittas AG, Fuss PJ, Cheatham RA, Tyler S, Tsay M, McCrory MA, Lichtenstein AH, Dallal GE, Dutta C, Bhapkar MV, Delany JP, Saltzman E, Roberts SB. Long-term effects of 2 energy-restricted diets differing in glycemic load on dietary adherence, body composition, and metabolism in CALERIE: a 1-y randomized controlled trial. *The American journal of clinical nutrition.* 2007;85(4):1023-1030.

100. Hursting SD, Lavigne JA, Berrigan D, Perkins SN, Barrett JC. Calorie restriction, aging, and cancer prevention: mechanisms of action and applicability to humans. *Annual review of medicine.* 2003;54:131-152.

101. Omodei D, Fontana L. Calorie restriction and prevention of age-associated chronic disease. *FEBS letters.* 2011;585(11):1537-1542.

102. Anson RM, Guo Z, de Cabo R, Iyun T, Rios M, Hagepanos A, Ingram DK, Lane MA, Mattson MP. Intermittent fasting dissociates beneficial effects of dietary restriction on glucose metabolism and neuronal resistance to injury from calorie intake. *Proceedings of the National Academy of Sciences of the United States of America.* 2003;100(10):6216-6220.

103. Varady KA, Hellerstein MK. Alternate-day fasting and chronic disease prevention: a review of human and animal trials. *The American journal of clinical nutrition.* 2007;86(1):7-13.

104. Varady KA, Roohk DJ, Bruss M, Hellerstein MK. Alternate-day fasting reduces global cell proliferation rates independently of dietary fat content in mice. *Nutrition.* 2009;25(4):486-491.

105. Varady KA, Roohk DJ, Hellerstein MK. Dose effects of modified alternate-day fasting regimens on in vivo cell proliferation and plasma insulin-like growth factor-1 in mice. *Journal of applied physiology.* 2007;103(2):547-551.

106. Varady KA, Roohk DJ, McEvoy-Hein BK, Gaylinn BD, Thorner MO, Hellerstein MK. Modified alternate-day fasting regimens reduce cell proliferation rates to a similar extent as daily calorie restriction in mice. *FASEB journal : official publication of the Federation of American Societies for Experimental Biology.* 2008;22(6):2090-2096.

107. Wan R, Camandola S, Mattson MP. Intermittent fasting and dietary supplementation with 2-deoxy-D-glucose improve functional and metabolic cardiovascular risk factors in rats. *FASEB journal : official publication of the Federation of American Societies for Experimental Biology.* 2003;17(9):1133-1134.

108. Heilbronn LK, Smith SR, Martin CK, Anton SD, Ravussin E. Alternate-day fasting in nonobese subjects: effects on body weight, body composition, and energy metabolism. *The American journal of clinical nutrition.* 2005;81(1):69-73.

109. Johnson JB, Summer W, Cutler RG, Martin B, Hyun DH, Dixit VD, Pearson M, Nassar M, Telljohann R, Maudsley S, Carlson O, John S, Laub DR, Mattson MP. Alternate day calorie restriction improves clinical findings and reduces markers of oxidative stress and inflammation in overweight adults with moderate asthma. *Free radical biology & medicine.* 2007;42(5):665-674.

110. Barnosky AR, Hoddy KK, Unterman TG, Varady KA. Intermittent fasting vs daily calorie restriction for type 2 diabetes prevention: a review of human findings. *Translational research : the journal of laboratory and clinical medicine.* 2014;164(4):302-311.

111. Halberg N, Henriksen M, Soderhamn N, Stallknecht B, Ploug T, Schjerling P, Dela F. Effect of intermittent fasting and refeeding on insulin action in healthy men. *Journal of applied physiology.* 2005;99(6):2128-2136.

112. Klempel MC, Kroeger CM, Bhutani S, Trepanowski JF, Varady KA. Intermittent fasting combined with calorie restriction is effective for weight loss and cardio-protection in obese women. *Nutrition journal.* 2012;11:98.

113. Varady KA, Bhutani S, Church EC, Klempel MC. Short-term modified alternate-day fasting: a novel dietary strategy for weight loss and cardioprotection in obese adults. *The American journal of clinical nutrition.* 2009;90(5):1138-1143.

114. Varady KA, Bhutani S, Klempel MC, Kroeger CM, Trepanowski JF, Haus JM, Hoddy KK, Calvo Y. Alternate day fasting for weight loss in normal weight and overweight subjects: a randomized controlled trial. *Nutrition journal.* 2013;12(1):146.

115. Rocha NS, Barbisan LF, de Oliveira ML, de Camargo JL. Effects of fasting and intermittent fasting on rat hepatocarcinogenesis induced by diethylnitrosamine. *Teratogenesis, carcinogenesis, and mutagenesis.* 2002;22(2):129-138.

116. Siegel I, Liu TL, Nepomuceno N, Gleicher N. Effects of short-term dietary restriction on survival of mammary ascites tumor-bearing rats. *Cancer investigation.* 1988;6(6):677-680.

117. Hsieh EA, Chai CM, Hellerstein MK. Effects of caloric restriction on cell proliferation in several tissues in mice: role of intermittent feeding. *American journal of physiology Endocrinology and metabolism.* 2005;288(5):E965-972.

118. Chaix A, Zarrinpar A, Miu P, Panda S. Time-restricted feeding is a preventative and therapeutic intervention against diverse nutritional challenges. *Cell metabolism.* 2014;20(6):991-1005.

119. Hatori M, Vollmers C, Zarrinpar A, DiTacchio L, Bushong EA, Gill S, Leblanc M, Chaix A, Joens M, Fitzpatrick JA, Ellisman MH, Panda S. Time-restricted feeding without reducing caloric intake prevents metabolic diseases in mice fed a high-fat diet. *Cell metabolism.* 2012;15(6):848-860.

120. Zarrinpar A, Chaix A, Yooseph S, Panda S. Diet and feeding pattern affect the diurnal dynamics of the gut microbiome. *Cell metabolism.* 2014;20(6):1006-1017.

121. Yilmaz OH, Katajisto P, Lamming DW, Gultekin Y, Bauer-Rowe KE, Sengupta S, Birsoy K, Dursun A, Yilmaz VO, Selig M, Nielsen GP, Mino-Kenudson M, Zukerberg LR, Bhan AK, Deshpande V, Sabatini DM. mTORC1 in the Paneth cell niche couples intestinal stem-cell function to calorie intake. *Nature.* 2012;486(7404):490-495.

122. Bortvedt SF, Lund PK. Insulin-like growth factor 1: common mediator of multiple enterotrophic hormones and growth factors. *Current opinion in gastroenterology.* 2012;28(2):89-98.

123. Han VK, D'Ercole AJ, Lund PK. Cellular localization of somatomedin (insulin-like growth factor) messenger RNA in the human fetus. *Science.* 1987;236(4798):193-197.

124. Han VK, Lund PK, Lee DC, D'Ercole AJ. Expression of somatomedin/insulin-like growth factor messenger ribonucleic acids in the human fetus: identification, characterization, and tissue distribution. *The Journal of clinical endocrinology and metabolism.* 1988;66(2):422-429.

125. Leen JL, Izzo A, Upadhyay C, Rowland KJ, Dube PE, Gu S, Heximer SP, Rhodes CJ, Storm DR, Lund PK, Brubaker PL. Mechanism of action of glucagon-like peptide-2 to increase IGF-I mRNA in intestinal subepithelial fibroblasts. *Endocrinology.* 2011;152(2):436-446.

126. Lund PK, Moats-Staats BM, Hynes MA, Simmons JG, Jansen M, D'Ercole AJ, Van Wyk JJ. Somatomedin-C/insulin-like growth factor-I and insulin-like growth factor-II mRNAs in rat fetal and adult tissues. *The Journal of biological chemistry.* 1986;261(31):14539-14544.

127. Szendroedi J, Yoshimura T, Phielix E, Koliaki C, Marcucci M, Zhang D, Jelenik T, Muller J, Herder C, Nowotny P, Shulman GI, Roden M. Role of diacylglycerol activation of PKCtheta in lipid-induced muscle insulin resistance in humans. *Proceedings of the National Academy of Sciences of the United States of America.* 2014;111(26):9597-9602.

128. Williams KL, Fuller CR, Fagin J, Lund PK. Mesenchymal IGF-I overexpression: paracrine effects in the intestine, distinct from endocrine actions. *American journal of physiology Gastrointestinal and liver physiology.* 2002;283(4):G875-885.

129. Frasca F, Pandini G, Sciacca L, Pezzino V, Squatrito S, Belfiore A, Vigneri R. The role of insulin receptors and IGF-I receptors in cancer and other diseases. *Archives of physiology and biochemistry.* 2008;114(1):23-37.

130. Belfiore A, Frasca F, Pandini G, Sciacca L, Vigneri R. Insulin receptor isoforms and insulin receptor/insulin-like growth factor receptor hybrids in physiology and disease. *Endocrine reviews.* 2009;30(6):586-623.

131. Ben Lulu S, Coran AG, Mogilner JG, Shaoul R, Shamir R, Shehadeh N, Sukhotnik I. Oral insulin stimulates intestinal epithelial cell turnover in correlation with insulin-receptor expression along the villus-crypt axis in a rat model of short bowel syndrome. *Pediatric surgery international.* 2010;26(1):37-44.

132. Sukhotnik I, Shehadeh N, Shamir R, Bejar J, Bernshteyn A, Mogilner JG. Oral insulin enhances intestinal regrowth following massive small bowel resection in rat. *Digestive diseases and sciences.* 2005;50(12):2379-2385.

133. Ben Lulu S, Coran AG, Shehadeh N, Shamir R, Mogilner JG, Sukhotnik I. Oral insulin stimulates intestinal epithelial cell turnover following massive small bowel resection in a rat and a cell culture model. *Pediatric surgery international.* 2012;28(2):179-187.

134. Hu FB, Manson JE, Liu S, Hunter D, Colditz GA, Michels KB, Speizer FE, Giovannucci E. Prospective study of adult onset diabetes mellitus (type 2) and risk of colorectal cancer in women. *Journal of the National Cancer Institute.* 1999;91(6):542-547.

135. Will JC, Galuska DA, Vinicor F, Calle EE. Colorectal cancer: another complication of diabetes mellitus? *American journal of epidemiology.* 1998;147(9):816-825.

136. Keku TO, Lund PK, Galanko J, Simmons JG, Woosley JT, Sandler RS. Insulin resistance, apoptosis, and colorectal adenoma risk. *Cancer epidemiology, biomarkers & prevention : a publication of the American Association for Cancer Research, cosponsored by the American Society of Preventive Oncology.* 2005;14(9):2076-2081.

137. Tran TT, Medline A, Bruce WR. Insulin promotion of colon tumors in rats. *Cancer epidemiology, biomarkers & prevention : a publication of the American Association for Cancer Research, cosponsored by the American Society of Preventive Oncology.* 1996;5(12):1013-1015.

138. Frasca F, Pandini G, Scalia P, Sciacca L, Mineo R, Costantino A, Goldfine ID, Belfiore A, Vigneri R. Insulin receptor isoform A, a newly recognized, high-affinity insulin-like growth factor II receptor in fetal and cancer cells. *Molecular and cellular biology.* 1999;19(5):3278-3288.

139. Andres SF, Simmons JG, Mah AT, Santoro MA, Van Landeghem L, Lund PK. Insulin receptor isoform switching in intestinal stem cells, progenitors, differentiated lineages and tumors: evidence that IR-B limits proliferation. *Journal of cell science.* 2013;126(Pt 24):5645-5656.

140. Santoro MA, Andres SF, Galanko JA, Sandler RS, Keku TO, Lund PK. Reduced insulin-like growth factor I receptor and altered insulin receptor isoform mRNAs in normal mucosa predict colorectal adenoma risk. *Cancer epidemiology, biomarkers & prevention : a publication of the American Association for Cancer Research, cosponsored by the American Society of Preventive Oncology.* 2014;23(10):2093-2100.

141. Dahly EM, Guo Z, Ney DM. Alterations in enterocyte proliferation and apoptosis accompany TPN-induced mucosal hypoplasia and IGF-I-induced hyperplasia in rats. *The Journal of nutrition.* 2002;132(7):2010-2014.

142. Dahly EM, Guo Z, Ney DM. IGF-I augments resection-induced mucosal hyperplasia by altering enterocyte kinetics. *American journal of physiology Regulatory, integrative and comparative physiology.* 2003;285(4):R800-808.

143. Knott AW, Juno RJ, Jarboe MD, Profitt SA, Erwin CR, Smith EP, Fagin JA, Warner BW. Smooth muscle overexpression of IGF-I induces a novel adaptive response to small bowel resection. *American journal of physiology Gastrointestinal and liver physiology.* 2004;287(3):G562-570.

144. Peterson CA, Gillingham MB, Mohapatra NK, Dahly EM, Adamo ML, Carey HV, Lund PK, Ney DM. Enterotrophic effect of insulin-like growth factor-I but not growth hormone and localized expression of insulin-like growth factor-I, insulin-like growth factor binding protein-3 and -5 mRNAs in jejunum of parenterally fed rats. *JPEN Journal of parenteral and enteral nutrition.* 2000;24(5):288-295.

145. Baregamian N, Song J, Jeschke MG, Evers BM, Chung DH. IGF-1 protects intestinal epithelial cells from oxidative stress-induced apoptosis. *The Journal of surgical research.* 2006;136(1):31-37.

146. Ohneda K, Ulshen MH, Fuller CR, D'Ercole AJ, Lund PK. Enhanced growth of small bowel in transgenic mice expressing human insulin-like growth factor I. *Gastroenterology.* 1997;112(2):444-454.

147. Simmons JG, Ling Y, Wilkins H, Fuller CR, D'Ercole AJ, Fagin J, Lund PK. Cell-specific effects of insulin receptor substrate-1 deficiency on normal and IGF-I-mediated colon growth. *American journal of physiology Gastrointestinal and liver physiology.* 2007;293(5):G995-1003.

148. Wilkins HR, Ohneda K, Keku TO, D'Ercole AJ, Fuller CR, Williams KL, Lund PK. Reduction of spontaneous and irradiation-induced apoptosis in small intestine of IGF-I transgenic mice. *American journal of physiology Gastrointestinal and liver physiology.* 2002;283(2):G457-464.

149. Dube PE, Forse CL, Bahrami J, Brubaker PL. The essential role of insulin-like growth factor-1 in the intestinal tropic effects of glucagon-like peptide-2 in mice. *Gastroenterology.* 2006;131(2):589-605.

150. Rowland KJ, Trivedi S, Lee D, Wan K, Kulkarni RN, Holzenberger M, Brubaker PL. Loss of glucagon-like peptide-2-induced proliferation following intestinal epithelial insulin-like growth factor-1-receptor deletion. *Gastroenterology.* 2011;141(6):2166-2175 e2167.

151. Jenkins PJ. Acromegaly and colon cancer. *Growth hormone & IGF research : official journal of the Growth Hormone Research Society and the International IGF Research Society.* 2000;10 Suppl A:S35-36.

152. Jenkins PJ, Fairclough PD, Richards T, Lowe DG, Monson J, Grossman A, Wass JA, Besser M. Acromegaly, colonic polyps and carcinoma. *Clinical endocrinology.* 1997;47(1):17-22.

153. Orme SM, McNally RJ, Cartwright RA, Belchetz PE. Mortality and cancer incidence in acromegaly: a retrospective cohort study. United Kingdom Acromegaly Study Group. *The Journal of clinical endocrinology and metabolism.* 1998;83(8):2730-2734.

154. Giovannucci E, Pollak MN, Platz EA, Willett WC, Stampfer MJ, Majeed N, Colditz GA, Speizer FE, Hankinson SE. A prospective study of plasma insulin-like growth factor-1 and binding protein-3 and risk of colorectal neoplasia in women. *Cancer epidemiology, biomarkers & prevention : a publication of the American Association for Cancer Research, cosponsored by the American Society of Preventive Oncology.* 2000;9(4):345-349.

155. Ma J, Pollak MN, Giovannucci E, Chan JM, Tao Y, Hennekens CH, Stampfer MJ. Prospective study of colorectal cancer risk in men and plasma levels of insulin-like growth factor (IGF)-I and IGF-binding protein-3. *Journal of the National Cancer Institute.* 1999;91(7):620-625.

156. Dy DY, Whitehead RH, Morris DL. SMS 201.995 inhibits in vitro and in vivo growth of human colon cancer. *Cancer research.* 1992;52(4):917-923.

157. Sakatani T, Kaneda A, Iacobuzio-Donahue CA, Carter MG, de Boom Witzel S, Okano H, Ko MS, Ohlsson R, Longo DL, Feinberg AP. Loss of imprinting of Igf2 alters intestinal maturation and tumorigenesis in mice. *Science.* 2005;307(5717):1976-1978.

158. Takano Y, Shiota G, Kawasaki H. Analysis of genomic imprinting of insulin-like growth factor 2 in colorectal cancer. *Oncology.* 2000;59(3):210-216.

159. Hassan AB, Howell JA. Insulin-like growth factor II supply modifies growth of intestinal adenoma in Apc(Min/+) mice. *Cancer research.* 2000;60(4):1070-1076.

160. Pollak M. The insulin and insulin-like growth factor receptor family in neoplasia: an update. *Nature reviews Cancer.* 2012;12(3):159-169.

161. Longo VD, Fontana L. Calorie restriction and cancer prevention: metabolic and molecular mechanisms. *Trends in pharmacological sciences.* 2010;31(2):89-98.

162. Olivo-Marston SE, Hursting SD, Perkins SN, Schetter A, Khan M, Croce C, Harris CC, Lavigne J. Effects of calorie restriction and diet-induced obesity on murine colon carcinogenesis, growth and inflammatory factors, and microRNA expression. *PloS one.* 2014;9(4):e94765.

163. Renehan AG, Frystyk J, Flyvbjerg A. Obesity and cancer risk: the role of the insulin-IGF axis. *Trends in endocrinology and metabolism: TEM.* 2006;17(8):328-336.

164. Vucenik I, Stains JP. Obesity and cancer risk: evidence, mechanisms, and recommendations. *Annals of the New York Academy of Sciences.* 2012;1271:37-43.

165. Calle EE, Kaaks R. Overweight, obesity and cancer: epidemiological evidence and proposed mechanisms. *Nature reviews Cancer.* 2004;4(8):579-591.

166. Cohen DH, LeRoith D. Obesity, type 2 diabetes, and cancer: the insulin and IGF connection. *Endocrine-related cancer.* 2012;19(5):F27-45.

167. Dunn SE, Kari FW, French J, Leininger JR, Travlos G, Wilson R, Barrett JC. Dietary restriction reduces insulin-like growth factor I levels, which modulates apoptosis, cell proliferation, and tumor progression in p53-deficient mice. *Cancer research.* 1997;57(21):4667-4672.

168. Abumrad NA, Davidson NO. Role of the gut in lipid homeostasis. *Physiological reviews.* 2012;92(3):1061-1085.

169. Drover VA, Ajmal M, Nassir F, Davidson NO, Nauli AM, Sahoo D, Tso P, Abumrad NA. CD36 deficiency impairs intestinal lipid secretion and clearance of chylomicrons from the blood. *The Journal of clinical investigation.* 2005;115(5):1290-1297.

170. Bahrami J, Yusta B, Drucker DJ. ErbB activity links the glucagon-like peptide-2 receptor to refeeding-induced adaptation in the murine small bowel. *Gastroenterology.* 2010;138(7):2447-2456.

171. Hoyt EC, Lund PK, Winesett DE, Fuller CR, Ghatei MA, Bloom SR, Ulshen MH. Effects of fasting, refeeding, and intraluminal triglyceride on proglucagon expression in jejunum and ileum. *Diabetes.* 1996;45(4):434-439.

172. Liu X, Murali SG, Holst JJ, Ney DM. Enteral nutrients potentiate the intestinotrophic action of glucagon-like peptide-2 in association with increased insulin-like growth factor-I responses in rats. *American journal of physiology Regulatory, integrative and comparative physiology.* 2008;295(6):R1794-1802.

173. Nelson DW, Murali SG, Liu X, Koopmann MC, Holst JJ, Ney DM. Insulin-like growth factor I and glucagon-like peptide-2 responses to fasting followed by controlled or ad libitum refeeding in rats. *American journal of physiology Regulatory, integrative and comparative physiology.* 2008;294(4):R1175-1184.

174. Shin ED, Estall JL, Izzo A, Drucker DJ, Brubaker PL. Mucosal adaptation to enteral nutrients is dependent on the physiologic actions of glucagon-like peptide-2 in mice. *Gastroenterology.* 2005;128(5):1340-1353.

175. Winesett DE, Ulshen MH, Hoyt EC, Mohapatra NK, Fuller CR, Lund PK. Regulation and localization of the insulin-like growth factor system in small bowel during altered nutrient status. *The American journal of physiology.* 1995;268(4 Pt 1):G631-640.

176. McLeod CJ, Wang L, Wong C, Jones DL. Stem cell dynamics in response to nutrient availability. *Current biology : CB.* 2010;20(23):2100-2105.

177. O'Brien LE, Soliman SS, Li X, Bilder D. Altered modes of stem cell division drive adaptive intestinal growth. *Cell.* 2011;147(3):603-614.

178. Scoville DH, Sato T, He XC, Li L. Current view: intestinal stem cells and signaling. *Gastroenterology.* 2008;134(3):849-864.

179. Lin SA, Barker N. Gastrointestinal stem cells in self-renewal and cancer. *Journal of gastroenterology.* 2011;46(9):1039-1055.

180. Binder H, Reuben A. Nutrient digestion and absorption. In: Boron WF BE, ed. *Medical Physiology*. Philadelphia: Saunders; 2003:947-974.

181. Bjerknes M, Cheng H. The stem-cell zone of the small intestinal epithelium. III. Evidence from columnar, enteroendocrine, and mucous cells in the adult mouse. *The American journal of anatomy.* 1981;160(1):77-91.

182. Sei Y, Lu X, Liou A, Zhao X, Wank SA. A stem cell marker-expressing subset of enteroendocrine cells resides at the crypt base in the small intestine. *American journal of physiology Gastrointestinal and liver physiology.* 2011;300(2):G345-356.

183. Lalles JP, Orozco-Solis R, Bolanos-Jimenez F, de Coppet P, Le Drean G, Segain JP. Perinatal undernutrition alters intestinal alkaline phosphatase and its main transcription factors KLF4 and Cdx1 in adult offspring fed a high-fat diet. *The Journal of nutritional biochemistry.* 2012;23(11):1490-1497.

184. May R, Riehl TE, Hunt C, Sureban SM, Anant S, Houchen CW. Identification of a novel putative gastrointestinal stem cell and adenoma stem cell marker, doublecortin and CaM kinase-like-1, following radiation injury and in adenomatous polyposis coli/multiple intestinal neoplasia mice. *Stem cells.* 2008;26(3):630-637.

185. Furuyama K, Kawaguchi Y, Akiyama H, Horiguchi M, Kodama S, Kuhara T, Hosokawa S, Elbahrawy A, Soeda T, Koizumi M, Masui T, Kawaguchi M, Takaori K, Doi R, Nishi E, Kakinoki R, Deng JM, Behringer RR, Nakamura T, Uemoto S. Continuous cell supply from a Sox9-expressing progenitor zone in adult liver, exocrine pancreas and intestine. *Nature genetics.* 2011;43(1):34-41.

186. Algire C, Amrein L, Zakikhani M, Panasci L, Pollak M. Metformin blocks the stimulative effect of a high-energy diet on colon carcinoma growth in vivo and is associated with reduced expression of fatty acid synthase. *Endocrine-related cancer.* 2010;17(2):351-360.

187. Gniuli D, Calcagno A, Dalla Libera L, Calvani R, Leccesi L, Caristo ME, Vettor R, Castagneto M, Ghirlanda G, Mingrone G. High-fat feeding stimulates endocrine, glucose-dependent insulinotropic polypeptide (GIP)-expressing cell hyperplasia in the duodenum of Wistar rats. *Diabetologia.* 2010;53(10):2233-2240.

188. Hyland NP, Pittman QJ, Sharkey KA. Peptide YY containing enteroendocrine cells and peripheral tissue sensitivity to PYY and PYY(3-36) are maintained in diet-induced obese and diet-resistant rats. *Peptides.* 2007;28(6):1185-1190.

189. Benzler J, Andrews ZB, Pracht C, Stohr S, Shepherd PR, Grattan DR, Tups A. Hypothalamic WNT signalling is impaired during obesity and reinstated by leptin treatment in male mice. *Endocrinology.* 2013;154(12):4737-4745.

190. Chen JR, Lazarenko OP, Wu X, Tong Y, Blackburn ML, Shankar K, Badger TM, Ronis MJ. Obesity reduces bone density associated with activation of PPARgamma and suppression of Wnt/beta-catenin in rapidly growing male rats. *PloS one.* 2010;5(10):e13704.

191. Dearth RK, Cui X, Kim HJ, Kuiatse I, Lawrence NA, Zhang X, Divisova J, Britton OL, Mohsin S, Allred DC, Hadsell DL, Lee AV. Mammary tumorigenesis and metastasis caused by overexpression of insulin receptor substrate 1 (IRS-1) or IRS-2. *Molecular and cellular biology.* 2006;26(24):9302-9314.

192. Ghosh MC, Gorantla V, Makena PS, Luellen C, Sinclair SE, Schwingshackl A, Waters CM. Insulin-like growth factor-I stimulates differentiation of ATII cells to ATI-like cells through activation of Wnt5a. *American journal of physiology Lung cellular and molecular physiology.* 2013;305(3):L222-228.

193. Sastre-Perona A, Santisteban P. Wnt-independent role of betacatenin in thyroid cell proliferation and differentiation. *Molecular endocrinology.* 2014:me20131377.

194. Srivenugopal K, Singh SP, Yuan XH, Ehmann S, Snyder AK. Differential removal of insulin-like growth factor binding proteins in rat serum by solvent extraction procedures. *Experientia.* 1994;50(5):451-455.

195. Dehmer JJ, Garrison AP, Speck KE, Dekaney CM, Van Landeghem L, Sun X, Henning SJ, Helmrath MA. Expansion of intestinal epithelial stem cells during murine development. *PloS one.* 2011;6(11):e27070.

196. Dekaney CM, Fong JJ, Rigby RJ, Lund PK, Henning SJ, Helmrath MA. Expansion of intestinal stem cells associated with long-term adaptation following ileocecal resection in mice. *American journal of physiology Gastrointestinal and liver physiology.* 2007;293(5):G1013-1022.

197. Gillingham MB, Kritsch KR, Murali SG, Lund PK, Ney DM. Resection upregulates the IGF-I system of parenterally fed rats with jejunocolic anastomosis. *American journal of physiology Gastrointestinal and liver physiology.* 2001;281(5):G1158-1168.

198. Colman RJ, Beasley TM, Kemnitz JW, Johnson SC, Weindruch R, Anderson RM. Caloric restriction reduces age-related and all-cause mortality in rhesus monkeys. *Nature communications.* 2014;5:3557.

199. Mattison JA, Roth GS, Beasley TM, Tilmont EM, Handy AM, Herbert RL, Longo DL, Allison DB, Young JE, Bryant M, Barnard D, Ward WF, Qi W, Ingram DK, de Cabo R. Impact of caloric restriction on health and survival in rhesus monkeys from the NIA study. *Nature.* 2012;489(7415):318-321.

200. Varady KA. Intermittent versus daily calorie restriction: which diet regimen is more effective for weight loss? *Obesity reviews : an official journal of the International Association for the Study of Obesity.* 2011;12(7):e593-601.

201. Varady KA, Allister CA, Roohk DJ, Hellerstein MK. Improvements in body fat distribution and circulating adiponectin by alternate-day fasting versus calorie restriction. *The Journal of nutritional biochemistry.* 2010;21(3):188-195.

202. Klurfeld DM, Weber MM, Kritchevsky D. Inhibition of chemically induced mammary and colon tumor promotion by caloric restriction in rats fed increased dietary fat. *Cancer research.* 1987;47(11):2759-2762.

203. Kumar SP, Roy SJ, Tokumo K, Reddy BS. Effect of different levels of calorie restriction on azoxymethane-induced colon carcinogenesis in male F344 rats. *Cancer research.* 1990;50(18):5761-5766.

204. Pollard M, Luckert PH, Pan GY. Inhibition of intestinal tumorigenesis in methylazoxymethanol-treated rats by dietary restriction. *Cancer treatment reports.* 1984;68(2):405-408.

205. Raju J, Bird RP. Energy restriction reduces the number of advanced aberrant crypt foci and attenuates the expression of colonic transforming growth factor beta and cyclooxygenase isoforms in Zucker obese (fa/fa) rats. *Cancer research.* 2003;63(20):6595-6601.

206. Reddy BS, Wang CX, Maruyama H. Effect of restricted caloric intake on azoxymethane-induced colon tumor incidence in male F344 rats. *Cancer research.* 1987;47(5):1226-1228.

207. Steinbach G, Heymsfield S, Olansen NE, Tighe A, Holt PR. Effect of caloric restriction on colonic proliferation in obese persons: implications for colon cancer prevention. *Cancer research.* 1994;54(5):1194-1197.

208. Steinbach G, Kumar SP, Reddy BS, Lipkin M, Holt PR. Effects of caloric restriction and dietary fat on epithelial cell proliferation in rat colon. *Cancer research.* 1993;53(12):2745-2749.

209. Mah AT, Van Landeghem L, Gavin HE, Magness ST, Lund PK. Impact of diet-induced obesity on intestinal stem cells: hyperproliferation but impaired intrinsic function that requires insulin/IGF1. *Endocrinology.* 2014;155(9):3302-3314.

210. Dunel-Erb S, Chevalier C, Laurent P, Bach A, Decrock F, Le Maho Y. Restoration of the jejunal mucosa in rats refed after prolonged fasting. *Comparative biochemistry and physiology Part A, Molecular & integrative physiology.* 2001;129(4):933-947.

211. Habold C, Chevalier C, Dunel-Erb S, Foltzer-Jourdainne C, Le Maho Y, Lignot JH. Effects of fasting and refeeding on jejunal morphology and cellular activity in rats in relation to depletion of body stores. *Scandinavian journal of gastroenterology.* 2004;39(6):531-539.

212. Hagemann RF, Stragand JJ. Fasting and refeeding: cell kinetic response of jejunum, ileum and colon. *Cell and tissue kinetics.* 1977;10(1):3-14.

213. Bi P, Shan T, Liu W, Yue F, Yang X, Liang XR, Wang J, Li J, Carlesso N, Liu X, Kuang S. Inhibition of Notch signaling promotes browning of white adipose tissue and ameliorates obesity. *Nature medicine.* 2014;20(8):911-918.

214. Yu M, Jiang M, Yang C, Wu Y, Liu Y, Cui Y, Huang G. Maternal high-fat diet affects Msi/Notch/Hes signaling in neural stem cells of offspring mice. *The Journal of nutritional biochemistry.* 2014;25(2):227-231.

215. Gracz AD, Williamson IA, Roche KC, Johnston MJ, Wang F, Wang Y, Attayek PJ, Balowski J, Liu XF, Laurenza RJ, Gaynor LT, Sims CE, Galanko JA, Li L, Allbritton NL, Magness ST. A high-throughput platform for stem cell niche co-cultures and downstream gene expression analysis. *Nature cell biology.* 2015.

216. Andres SF, Santoro MA, Mah AT, Keku JA, Bortvedt AE, Blue RE, Lund PK. Deletion of intestinal epithelial insulin receptor attenuates high-fat diet-induced elevations in cholesterol and stem, enteroendocrine, and Paneth cell mRNAs. *American journal of physiology Gastrointestinal and liver physiology.* 2015;308(2):G100-111.

217. Hodin CM, Verdam FJ, Grootjans J, Rensen SS, Verheyen FK, Dejong CH, Buurman WA, Greve JW, Lenaerts K. Reduced Paneth cell antimicrobial protein levels correlate with activation of the unfolded protein response in the gut of obese individuals. *The Journal of pathology.* 2011;225(2):276-284.

218. Hernandez V, Clofent J. Intestinal cancer in inflammatory bowel disease: natural history and surveillance guidelines. *Annals of gastroenterology : quarterly publication of the Hellenic Society of Gastroenterology.* 2012;25(3):193-200.

219. Hamilton KE, Simmons JG, Ding S, Van Landeghem L, Lund PK. Cytokine induction of tumor necrosis factor receptor 2 is mediated by STAT3 in colon cancer cells. *Molecular cancer research : MCR.* 2011;9(12):1718-1731.

220. Drew JE. Molecular mechanisms linking adipokines to obesity-related colon cancer: focus on leptin. *The Proceedings of the Nutrition Society.* 2012;71(1):175-180.

221. Fenton JI, Hord NG, Lavigne JA, Perkins SN, Hursting SD. Leptin, insulin-like growth factor-1, and insulin-like growth factor-2 are mitogens in ApcMin/+ but not Apc+/+ colonic epithelial cell lines. *Cancer epidemiology, biomarkers & prevention : a publication of the American Association for Cancer Research, cosponsored by the American Society of Preventive Oncology.* 2005;14(7):1646-1652.

222. Fenton JI, Hursting SD, Perkins SN, Hord NG. Interleukin-6 production induced by leptin treatment promotes cell proliferation in an Apc (Min/+) colon epithelial cell line. *Carcinogenesis.* 2006;27(7):1507-1515.

223. Kawasaki N, Asada R, Saito A, Kanemoto S, Imaizumi K. Obesity-induced endoplasmic reticulum stress causes chronic inflammation in adipose tissue. *Scientific reports.* 2012;2:799.

224. Heijmans J, van Lidth de Jeude JF, Koo BK, Rosekrans SL, Wielenga MC, van de Wetering M, Ferrante M, Lee AS, Onderwater JJ, Paton JC, Paton AW, Mommaas AM, Kodach LL, Hardwick JC, Hommes DW, Clevers H, Muncan V, van den Brink GR. ER stress causes rapid loss of intestinal epithelial stemness through activation of the unfolded protein response. *Cell reports.* 2013;3(4):1128-1139.

225. Niederreiter L, Fritz TM, Adolph TE, Krismer AM, Offner FA, Tschurtschenthaler M, Flak MB, Hosomi S, Tomczak MF, Kaneider NC, Sarcevic E, Kempster SL, Raine T, Esser D, Rosenstiel P, Kohno K, Iwawaki T, Tilg H, Blumberg RS, Kaser A. ER stress transcription factor Xbp1 suppresses intestinal tumorigenesis and directs intestinal stem cells. *The Journal of experimental medicine.* 2013;210(10):2041-2056.

226. Kaser A, Lee AH, Franke A, Glickman JN, Zeissig S, Tilg H, Nieuwenhuis EE, Higgins DE, Schreiber S, Glimcher LH, Blumberg RS. XBP1 links ER stress to intestinal inflammation and confers genetic risk for human inflammatory bowel disease. *Cell.* 2008;134(5):743-756.

227. Hursting SD, Smith SM, Lashinger LM, Harvey AE, Perkins SN. Calories and carcinogenesis: lessons learned from 30 years of calorie restriction research. *Carcinogenesis.* 2010;31(1):83-89.

228. Barker N, Ridgway RA, van Es JH, van de Wetering M, Begthel H, van den Born M, Danenberg E, Clarke AR, Sansom OJ, Clevers H. Crypt stem cells as the cells-of-origin of intestinal cancer. *Nature.* 2009;457(7229):608-611.

229. Powell AE, Vlacich G, Zhao ZY, McKinley ET, Washington MK, Manning HC, Coffey RJ. Inducible loss of one Apc allele in Lrig1-expressing progenitor cells results in multiple distal colonic tumors with features of familial adenomatous polyposis. *American journal of physiology Gastrointestinal and liver physiology.* 2014;307(1):G16-23.

230. Ramalingam S, Daughtridge GW, Johnston MJ, Gracz AD, Magness ST. Distinct levels of Sox9 expression mark colon epithelial stem cells that form colonoids in culture. *American journal of physiology Gastrointestinal and liver physiology.* 2012;302(1):G10-20.

231. Backhed F, Ding H, Wang T, Hooper LV, Koh GY, Nagy A, Semenkovich CF, Gordon JI. The gut microbiota as an environmental factor that regulates fat storage. *Proceedings of the National Academy of Sciences of the United States of America.* 2004;101(44):15718-15723.

232. Karlsson F, Tremaroli V, Nielsen J, Backhed F. Assessing the human gut microbiota in metabolic diseases. *Diabetes.* 2013;62(10):3341-3349.

233. Sommer F, Backhed F. The gut microbiota--masters of host development and physiology. *Nature reviews Microbiology.* 2013;11(4):227-238.

234. Wichmann A, Allahyar A, Greiner TU, Plovier H, Lunden GO, Larsson T, Drucker DJ, Delzenne NM, Cani PD, Backhed F. Microbial modulation of energy availability in the colon regulates intestinal transit. *Cell host & microbe.* 2013;14(5):582-590.

235. Tremaroli V, Backhed F. Functional interactions between the gut microbiota and host metabolism. *Nature.* 2012;489(7415):242-249.

236. Nigro G, Rossi R, Commere PH, Jay P, Sansonetti PJ. The cytosolic bacterial peptidoglycan sensor Nod2 affords stem cell protection and links microbes to gut epithelial regeneration. *Cell host & microbe.* 2014;15(6):792-798.

237. Abreu MT, Thomas LS, Arnold ET, Lukasek K, Michelsen KS, Arditi M. TLR signaling at the intestinal epithelial interface. *Journal of endotoxin research.* 2003;9(5):322-330.

238. Hisamatsu T, Suzuki M, Podolsky DK. Interferon-gamma augments CARD4/NOD1 gene and protein expression through interferon regulatory factor-1 in intestinal epithelial cells. *The Journal of biological chemistry.* 2003;278(35):32962-32968.

239. Ogura Y, Lala S, Xin W, Smith E, Dowds TA, Chen FF, Zimmermann E, Tretiakova M, Cho JH, Hart J, Greenson JK, Keshav S, Nunez G. Expression of NOD2 in Paneth cells: a possible link to Crohn's ileitis. *Gut.* 2003;52(11):1591-1597.

240. Bevins CL, Salzman NH. Paneth cells, antimicrobial peptides and maintenance of intestinal homeostasis. *Nature reviews Microbiology.* 2011;9(5):356-368.

241. Chausse B, Solon C, Caldeira da Silva CC, Masselli Dos Reis IG, Manchado-Gobatto FB, Gobatto CA, Velloso LA, Kowaltowski AJ. Intermittent fasting induces hypothalamic modifications resulting in low feeding efficiency, low body mass and overeating. *Endocrinology.* 2014;155(7):2456-2466.

242. Crawford PA, Crowley JR, Sambandam N, Muegge BD, Costello EK, Hamady M, Knight R, Gordon JI. Regulation of myocardial ketone body metabolism by the gut microbiota during nutrient deprivation.

Proceedings of the National Academy of Sciences of the United States of America. 2009;106(27):11276-11281.

243. De Filippo C, Cavalieri D, Di Paola M, Ramazzotti M, Poullet JB, Massart S, Collini S, Pieraccini G, Lionetti P. Impact of diet in shaping gut microbiota revealed by a comparative study in children from Europe and rural Africa. *Proceedings of the National Academy of Sciences of the United States of America.* 2010;107(33):14691-14696.

244. Flint HJ, Scott KP, Duncan SH, Louis P, Forano E. Microbial degradation of complex carbohydrates in the gut. *Gut microbes.* 2012;3(4):289-306.

245. Martens EC, Chiang HC, Gordon JI. Mucosal glycan foraging enhances fitness and transmission of a saccharolytic human gut bacterial symbiont. *Cell host & microbe.* 2008;4(5):447-457.

246. Crittenden R, Laitila A, Forssell P, Matto J, Saarela M, Mattila-Sandholm T, Myllarinen P. Adhesion of bifidobacteria to granular starch and its implications in probiotic technologies. *Applied and environmental microbiology.* 2001;67(8):3469-3475.

247. Bultman SJ. Emerging roles of the microbiome in cancer. *Carcinogenesis.* 2014;35(2):249-255.

248. De Vadder F, Kovatcheva-Datchary P, Goncalves D, Vinera J, Zitoun C, Duchampt A, Backhed F, Mithieux G. Microbiota-generated metabolites promote metabolic benefits via gut-brain neural circuits. *Cell.* 2014;156(1-2):84-96.

249. Mithieux G, Gautier-Stein A. Intestinal glucose metabolism revisited. *Diabetes research and clinical practice.* 2014;105(3):295-301.

250. Okada T, Fukuda S, Hase K, Nishiumi S, Izumi Y, Yoshida M, Hagiwara T, Kawashima R, Yamazaki M, Oshio T, Otsubo T, Inagaki-Ohara K, Kakimoto K, Higuchi K, Kawamura YI, Ohno H, Dohi T. Microbiota-derived lactate accelerates colon epithelial cell turnover in starvation-refed mice. *Nature communications.* 2013;4:1654.